Studies on Physiological Roles of the Extracellular Matrix Protein Polydom in Lymphatic Vessel Development

細胞外マトリックス蛋白質 polydom の

リンパ管発生における生理機能解析

A Doctoral Dissertation Presented to Osaka University

2017

Nanami Morooka

Contents

Non-standard Abbreviations and Acronyms - 5

Introduction - 6

Extracellular Matrix - 6

What Was Known about Polydom/Svep1 - 8

Lymphatic Vascular System - 10

Material and Methods - 18

Results - 26

Polydom Shows Characteristic Distribution in Lymphatic Vessels - - - - - - - - - - - - - - - - - 26

Polydom Localizes around Lymphatic Vessels through Embryonic Development - - - - - 30

Polydom Is Produced by Mesenchymal Cells - 32

Targeted Disruption of the *Polydom* Gene in Mice Causes Severe Edema - - - - - - - - - - 34

Polydom Deficient Mice Show the Defect in Lymphatic and Venous Vascular Formation
in Some Tissues - 37

Polydom Deficient Mice Exhibit Aberrant Lymphatic Vessel Formation
and Dysfunction of Fluid Drainage - 40

The Expression of Transcriptional Factor Foxc2 is Reduced in *polydom*$^{-/-}$ Mice - - - - - - 44

Phenotypes in *Polydom*$^{-/-}$ Mice Resemble Those in *Foxc2*$^{-/-}$ Mice - - - - - - - - - - - - - - - 46

Polydom–Integrin α9β1 Interaction Is Not Necessary
for Lymphatic Vessel Remodeling - 48

Ang-2 Binds to Polydom and Potentiates Foxc2 Expression in LECs - - - - - - - - - - - - - 51

Tie Receptor Expression Is Decreased in *polydom*$^{-/-}$ Mice - 53

Discussion ---------- 54

Polydom Upregulates Remodeling Factor Foxc2 ---------- 54

Polydom Regulates Foxc2 via Ang-2 Mediated Signaling ---------- 55

Schematic Model for Lymphatic Remodeling ---------- 58

Mechanism of Polydom Expression and Deposition ---------- 62

LEC Migration in Lymphatic Vessel Remodeling ---------- 62

ECM Function in Lymphatic Vascular Development ---------- 63

Conclusion ---------- 65

References ---------- 66

List of Publications ---------- 73

Acknowledgements ---------- 74

Non-standard Abbreviations and Acronyms

ADAMTS	a disintegrin and metalloproteinase with thrombospondin motifs
Ang	Angiopoietin
BSA	bovine serum albumin
CCBE1	collagen and calcium binding EGF domains 1
CCP	complement control protein
COUP-TFII	chicken ovalbumin upstream promoter transcription factor
CLEC	C-type lectin-like receptor
DAB	3,3'-Diaminobenzidine
ECM	extracellular matrix
EGF	epidermal growth factor
EIIIA	extra type-III repeat A
EMILIN	elastic microfibril-associated protein
FN	fibronectin
Foxc2	forkhead box protein c2
GAG	glycosaminoglycans
HDLEC	human dermal lymphatic endothelial cell
Itga9	integrin α9
LEC	lymphatic endothelial cell
LYVE-1	lymphatic vessel hyaluronan receptor-1
MACS	magnetic-activated cell sorting
NFAT	nuclear factor of activated T cells
NP-40	Nonidet P-40
Nrp	Neuropilin
PB	phosphate buffer
PBS-T	PBS containing Triton X-100
PB-T	PB containing Triton X-100
PDGF	platelet-derived growth factor receptor
PFA	paraformaldehyde
Prox1	prospero-related homeodomain transcription factor
pTD	primordial thoracic duct
SMA	smooth muscle actin
SMC	smooth muscle cell
Sox18	Sry-related Hmg-box transcription factor
TM	Tamoxifen
VEGF	vascular endothelial growth factor
VEGFR	vascular endothelial growth factor receptor
VWA	von Willebrand factor A domain

Introduction

Extracellular Matrix

Multicellular Organism Is Comprised of Cells and Extracellular Matrix

Multicellular organism is formed of many types of tissues, in which cells are assembled and bound together. Cells are bound directly to one another by cell-cell junctions, but tissues are not made up solely of cells. An essential part of the cell assembly is played by extracellular matrix (ECM). It fills extracellular space and helps hold cells and tissue together or forms a supporting framework. In addition, it provides an organized environment within which migratory cells can move and interact with one another in orderly ways. Thus, evolution of ECM proteins was a key in the transition to multicellularity, the arrangement of cells into tissue layers, and the elaboration of novel structures during vertebrate evolution.

In vertebrates, the major tissue types are nerve, muscle, blood, lymphoid, epithelial, and connective tissues. Among these, connective tissue and epithelial tissue represent two extremes of organization (Figure 1A) (Alberts, 2002). In connective tissue, ECM is plentiful and rich in fibrous polymers such as collagen, and cells are sparsely distributed within it (Figure 1B). ECM, rather than cells, bears most of the mechanical stress in tissues. In epithelial tissue, by contrast, cells are tightly bound together into sheets called epithelia. ECM is scanty, consisting mainly of a thin mat called the basement membrane, which underlies the epithelium (Figure 1C). Cells are attached to each other by cell-cell adhesions, which bear most of the mechanical stress.

ECM Is Not Just a Scaffold but Regulates Cell Behaviors

ECM plays an important role for resisting two major physical pressures in tissues, compressive forces and tensile forces. In connective tissues, proteoglycan molecules, which polysaccharide chains called “glycosaminoglycans (GAGs)” are covalently linked to core protein, form a highly hydrated, gel-like “ground substance”. Polysaccharide gels resist compressive forces on ECM, while permitting the rapid diffusion of nutrients, metabolites, and hormones because they are porous. In contrast to proteoglycans/GAGs, fibrous proteins, including collagen, elastin, fibronectin (FN), and laminin, have both structural and adhesive functions. Collagen fibrils form structures that resist tensile forces, and

rubberlike elastin fibers give it resilience.

Thus, vertebrate ECM was thought to serve mainly as a relatively inert scaffold to provide strength and space-filling functions in tissues. But now it is clear that ECM has a far more active and complex role in regulating behavior of cells that it contacts. They are able to determine cell polarity, influence cell metabolism, organize the proteins in adjacent plasma membranes, promote cell survival, proliferation, or differentiation, and serve as specific highways for cell migration.

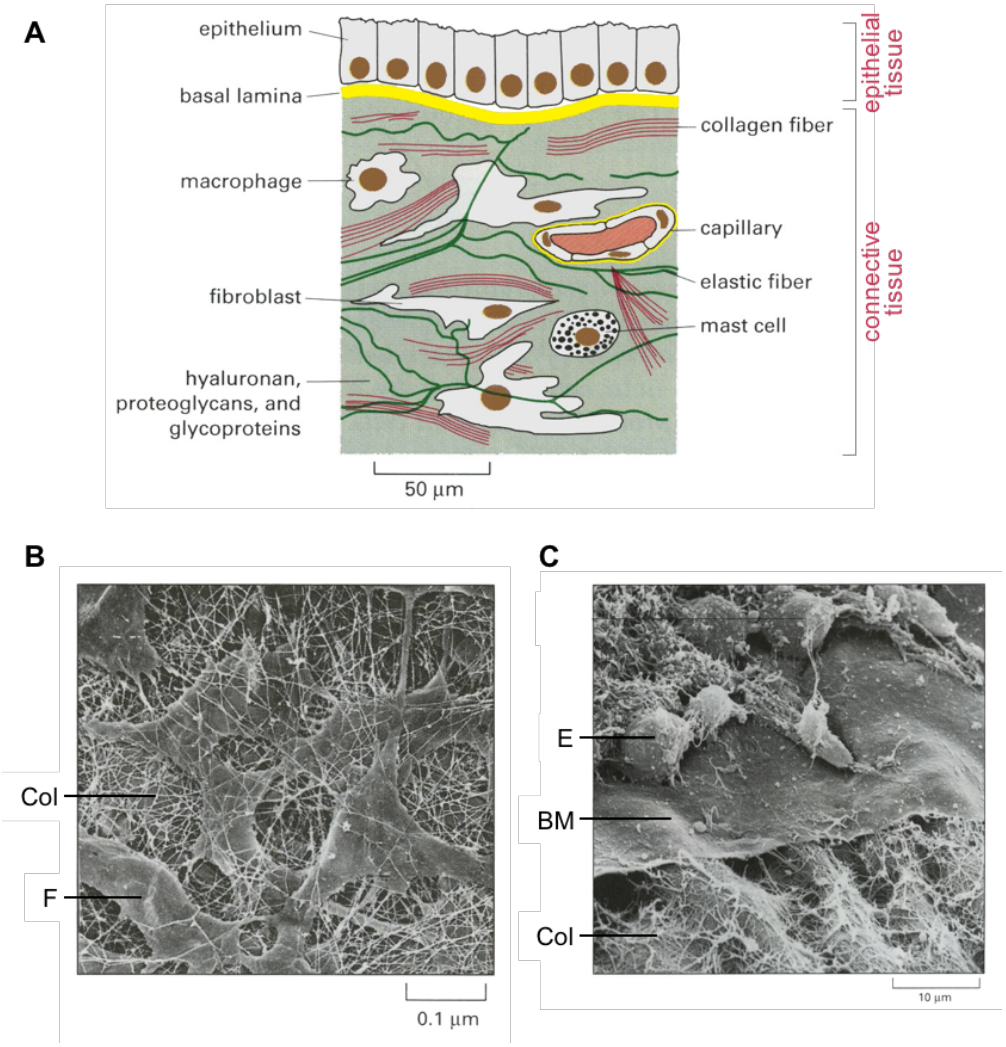

Figure 1. Two main ways in which animal cells are bound together. (**A**) In epithelial tissue, cells (epithelium) are tightly bound together on the basement membrane (basal lamina). In connective tissue, a space is filled with ECMs and variety of cells are distributed within it. The predominant cell type is the fibroblast, which secretes abundant ECM. (**B**) Fibroblasts in connective tissue of a rat cornea. The scanning electron micrograph image shows the ECM surrounding the fibroblasts (F) is composed largely of collagen fibrils (Col). (**C**) The basement membrane in the cornea of a chick embryo. The scanning electron micrograph shows the epithelial cells (E) rest on the basement membrane (BM). A network of collagen fibrils (Col) in the underlying connective tissue interact with the lower surface of the BM. (**A**–**C** are cited from Molecular Biology of the Cell, Fourth Edition, Garland Science, with minor modifications.)

Molecular Characteristics and Entire List of ECM Proteins

ECM is, by its very nature, insoluble and is frequently cross-linked. ECM proteins tend to be large and typically contain repeats of a characteristic set of domains (laminin globular domain, FN type 3 repeat, von Willebrand factor A domain (VWA), immunoglobulin domain, epidermal growth factor (EGF)-like domain, collagen prodomains, etc.), often encoded in the genome as separate exonic units (Hynes and Naba, 2012). ECM domains confer myriad functions including ECM assembly, cell adhesion, binding to growth factors, and also signaling into cells. Cell behaviors described above are reflected in these domain motif functions.

Although biochemistry of ECM is challenging because of its size and the insolubility, availability of complete genome sequences coupled with our accumulated knowledge about ECM proteins now makes it possible to come up with a reasonably complete list of ECM proteins (Manabe et al., 2008; Naba et al., 2012). Our group proposed that the term ‘‘matrixome’’ be used for the subset of the proteome that constitutes the customized microenvironments (Manabe et al., 2008). It comprises almost 300 proteins (1%–1.5% of the mammalian proteome), including 43 collagen subunits, three dozens or so proteoglycans, and around 200 glycoproteins (Hynes and Naba, 2012). One third of the ECM genes have yet to be identified. Previously, we encountered polydom in our *in silico* screening for functionally unknown ECM proteins (Sato-Nishiuchi et al., 2012).

What Was Known about Polydom/Svep1

Molecular Characteristics of Polydom

Polydom/Svep1 (hereafter referred to as polydom) is a large ECM protein over 300 kDa containing an array of complement control protein (CCP) domains along with a VWA, a pentraxin domain, and multiple EGF-like domains (Figure 2) (Gilges et al., 2000). Polydom is found in the cnidarian (*Hydractinia*) genome and its domain architecture of the N-terminal half is highly conserved in both vertebrates and invertebrates (Schwarz et al., 2008). Polydom was originally identified in murine bone marrow stromal cells as a protein containing EGF-like domains that share strong similarities with those in the Notch family proteins. The human orthologue of polydom, named SEL-OB (selectin-like osteoblast derived) or SVEP1 (sushi, VWA, EGF, and pentraxin), was reported

as a protein expressed on the surface of osteogenic cells (Shur et al., 2006). Polydom was detected in a variety of tissues, including the stomach, intestine, and lungs, where it was predominantly detected in the mesenchymal ECM, and also detected in the kidneys, liver, nerve fiber bundles, and choroid plexus (Sato-Nishiuchi et al., 2012). Recently, we identified polydom as a high affinity ligand for integrin α9β1, having higher affinity than other known ligands such as tenascin-C, osteopontin and FN (Sato-Nishiuchi et al., 2012).

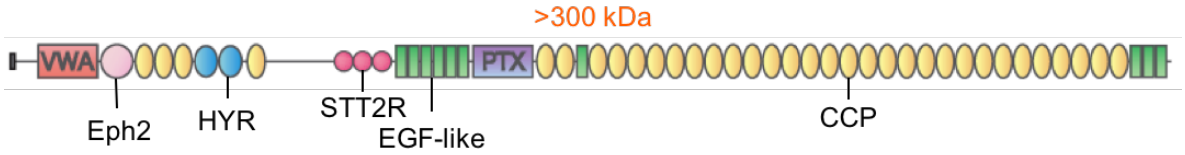

Figure 2. Domain structure of polydom. The protein is drawn to scale. EGF, EGF-like domain; CCP, complement control protein; Eph2, ephrin-2; HYR, hyalin repeat; PTX, pentraxin; STT2R, similar to thyroglobulin type 2 repeats; VWA, von Willebrand factor type A.

Integrin α9β1 Is Key Factor for Lymphatic Valve Development

Several lines of evidence indicate that integrin α9β1 is involved in lymphangiogenesis. Integrin α9 is predominantly expressed in lymphatic valves. *Itga9* deficiency in mice leads to the defects in the formation of luminal valves in collecting lymphatic vessels and early postnatal death from chylothorax between 6 and 12 days of age (Bazigou et al., 2009; Huang et al., 2000). The ligand for integrin α9β1 that functions in lymphangiogenesis remains to be defined, because gene knockout of known integrin α9β1 ligands like osteopontin and tenascin-C do not cause any defects in lymphatic vessels (Forsberg et al., 1996; Fukamauchi et al., 1996; Liaw et al., 1998). I hypothesized that polydom might play a role in lymphatic development as an integrin α9β1 ligand.

Lymphatic Vascular System

Functions of Lymphatic Vasculature System

The main function of the lymphatic vasculature is to collect the protein-rich tissue fluid extravasated from blood vessels and return it back to the blood circulation (Figure 3) (Alitalo et al., 2005; Sevick-Muraca et al., 2014). Lymphatic vessels are also required for lipid absorption as well as immune cell trafficking and surveillance. Defects in lymphatic function lead to lymph accumulation in tissues known as lymphedema and compromises immune function (Alitalo, 2011; Schulte-Merker et al., 2011). Aberrant lymphatic growth is also associated with pathological conditions, including cancer metastasis and chronic inflammation.

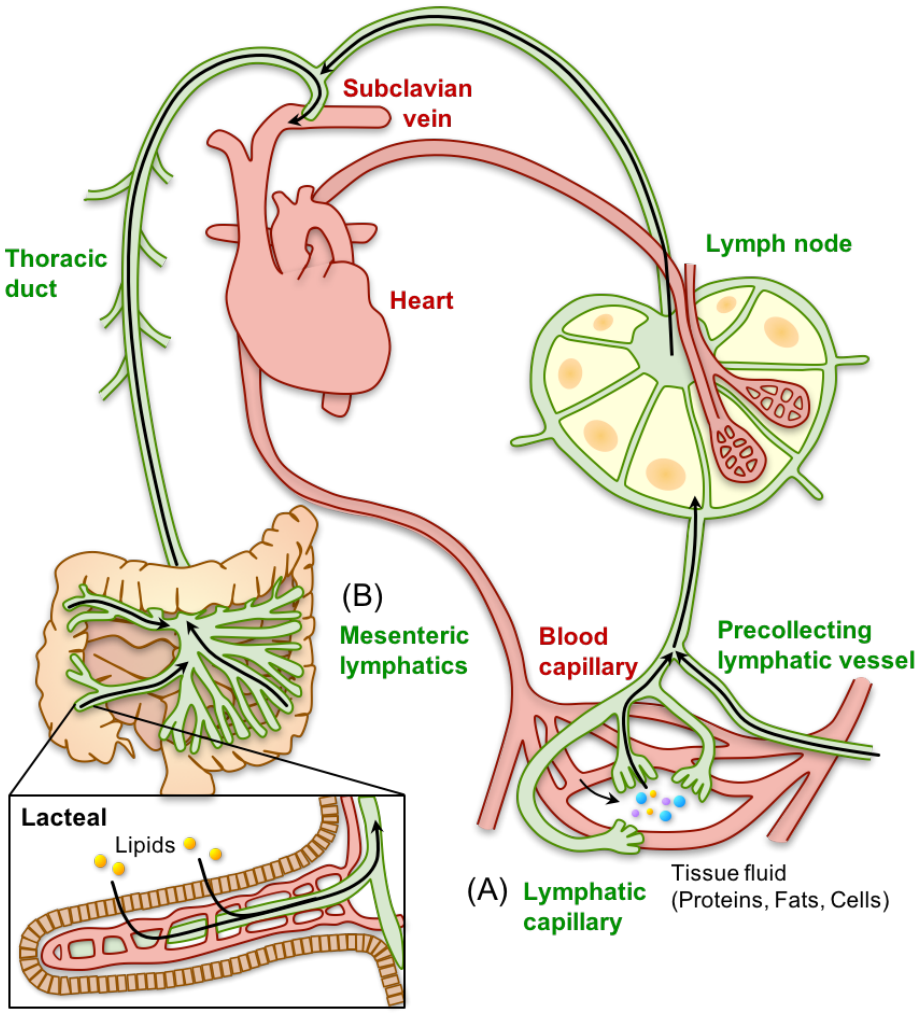

Figure 3. Routes of lymphatic fluid. (**A**) Interstitial fluid uptake into the lymphatic capillary plexus through collecting lymphatic vessels, and eventually into the thoracic duct that drains into the subclavian vein (*arrows*). (**B**) Oral gavage of hydrophobic lipids results in uptake through the lacteals into the mesenteric lymphatics that eventually drain into the thoracic duct. (Figure is cited from Sevick-Muraca et al., 2014, with some modifications.)

Evolution of Lymphatic System

The lymphatic vascular system is a characteristic feature of higher vertebrates, whose complex cardiovascular system and large body size require the presence of a secondary vascular system for the maintenance of fluid balance, whereas most invertebrates have an open vascular system that ensures circulation of immune cells and interstitial fluid throughout the body. Specialized lymph hearts first appeared in amphibians and reptiles (Kampmeier, 1969); later, lymph nodes appeared in birds, and the final refinement of the lymphatic vasculature occurred in mammals (Witte et al., 2001). Recent reports have also demonstrated that the zebrafish has a well-defined lymphatic vascular system that shares many of the morphological, molecular, and functional characteristics of the lymphatic vessels found in other vertebrates (Kuchler et al., 2006; Yaniv et al., 2006).

Morphology of Lymphatic Vessel

Blood vessels form a closed circulatory system, whereas lymphatic vessels form a one-way conduit for tissue fluid and leukocytes. The lymphatic vasculature is blind ending: its small capillaries funnel first into precollecting and larger collecting vessels and then into the thoracic duct or the right lymphatic trunk, which drains lymph into the subclavian veins (Figure 3) (Jeltsch et al., 2003). Lymphatic capillaries are thin-walled vessels of approximately 30-80 μm in diameter, composed of a single layer of oak-leaf-shaped lymphatic endothelial cells (LECs) (Figure 4) (Coso et al., 2014; Schulte-Merker et al., 2011). These LECs have discontinuous “button-like” junctions, allowing fluid and certain leukocytes to enter into the vessel lumen through flap-like openings (Baluk et al., 2007). Anchoring filaments attach LECs to collagen fibers and regulate the flap-like opening into the lymphatic vessel lumen. In contrast to blood capillaries, lymphatic capillaries lack pericytes, which are connective tissue cells surrounding vascular walls. Lymphatic capillaries have a discontinuous basement membrane containing portals for cells, such as dendritic cells, that can migrate into the vessel lumens. Collecting lymphatic vessels have continuous “zipper-like” junctions, and they are covered with basement membrane and pericytes/smooth muscle cells (SMCs) (Figure 4). Collecting lymphatic vessels contain intraluminal valves, which consist of two semilunar leaflets, covered by a specialized endothelium attached to the core of ECM. The intrinsic contractility of SMCs, the

contraction of surrounding skeletal muscles, and arterial pulsations are necessary for lymph propulsion, whereas the valves prevent lymph backflow.

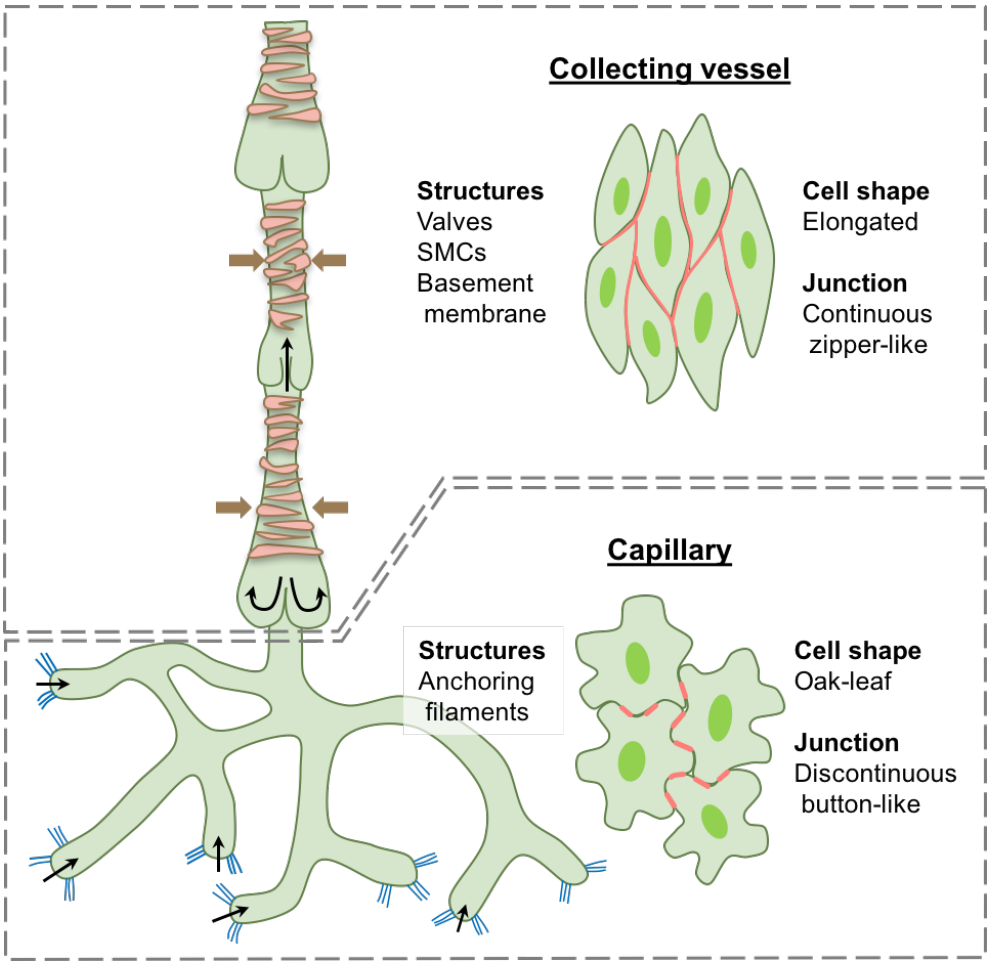

Figure 4. Organization and function of lymphatic system. In lymphatic capillary, anchoring filaments attach LECs to the ECM and prevent vessel collapse under conditions of increased interstitial pressure. Oak leaf shaped LECs of lymphatic capillaries, which have discontinuous button-like cell junction, direct fluid entry to the junction-free region. In collecting vessels, coordinated opening and closure of lymphatic valves is important for efficient lymph transport. SMCs covering each lymphangion possess intrinsic contractile activity. Basement membrane supports LECs to prevent lymph leakage. LECs in collecting vessels have conventional, continuous, zipper-like junctions, and are elongated to the direction of the flow. (Figure is cited from Coso et al., 2014 and Schlute-Merker et al., 2011, with some modifications.)

Molecular Mechanisms in Lymphatic Vascular Development

Lymphatic vascular development requires trans differentiation of venous endothelial cells toward the lymphatic endothelial phenotype, formation of primordial lymphatic vascular structures, separation of blood and lymphatic vasculature, sprouting of lymphatic vessels to form primitive capillary plexus, and lymphatic vascular remodeling and maturation.

Specification of LEC from Venous Endothelial Cells

Differentiation of LECs in mice starts around E9.5 in a subset of endothelial cells of cardinal vein via upregulation of prospero-related homeodomain transcription factor (Prox1), a master regulator of LECs (Figure 5A, B) (Aspelund et al., 2016; Wigle and Oliver, 1999). Prox1 downregulates blood markers and upregulates vascular endothelial growth factor receptor (VEGFR)-3. Prior to Prox1 upregulation, Sry-related Hmg-box transcription factor (Sox18) is expressed in cardinal vein endothelial cells. Sox18 binds to Prox1 promoter and initiates LEC differentiation program upstream of Prox1 (Francois et al., 2008). The orphan nuclear receptor chicken ovalbumin upstream promoter transcription factor (COUP-TFII), which has an earlier developmental role as a venous identity factor, is also required for initiation of Prox1 expression (Srinivasan et al., 2010).

Formation of Primordial Lymphatic Vascular Structure

During E12.5, LEC progenitors bud and migrate from the cardinal vein (Figure 5C). They form two primordial lymphatic structures: the dorsal peripheral longitudinal lymphatic vessel and the ventral primordial thoracic duct (pTD, also commonly called “jugular lymph sacs” in earlier publications) (Figure 5D) (Hagerling et al., 2013; Oliver, 2004; Tammela and Alitalo, 2010). Vascular endothelial growth factor (VEGF)-C, which is provided by the lateral mesoderm, acts as a morphogen to activate VEGFR-3 signaling in LECs, then drives LECs out of the cardinal vein (Figure 5C) (Karkkainen et al., 2004; Zhang et al., 2010). Collagen and calcium binding EGF domains 1 (CCBE1) (Bos et al., 2011) is essential for activation of VEGF-C by enhancing proteolytic processing of VEGF-C via the metalloprotease ADAMTS3 (a disintegrin and metalloproteinase with thrombospondin motifs 3) (Jeltsch et al., 2014; Roukens et al., 2015). Neuropilin (Nrp)-2 is a non-signaling co-receptor for VEGFR-3 that is highly expressed in lymphatic capillaries (Yuan et al., 2002). Nrp2 is important for capillary sprouting but dispensable for the formation of lymph sacs (Xu et al., 2010; Yuan et al., 2002).

Separation of Venous and Lymphatic Vasculatures

During the course of development, communication between the lymphatics and veins are lost, except the small apertures at the subclavian veins. This connection is protected by the lymphovenous valve, which is important for preventing the backflow of blood into the thoracic duct (Figure 5D’’)

(Hagerling et al., 2013; Srinivasan and Oliver, 2011; Yang and Oliver, 2014). Platelets are important for keeping both vascular systems apart. Podoplanin expressed on LECs activates the platelet receptor CLEC-2 (C-type lectin-like receptor 2) and triggers the Syk-, Slp76-, and PLC-γ2-dependent signaling cascade leading to the aggregation of platelets at site of connection then "seal off" lymphatic vessels from the vein (Figure 5D') (Abtahian et al., 2003; Bertozzi et al., 2010; Ichise et al., 2009; Suzuki-Inoue et al., 2010; Uhrin et al., 2010).

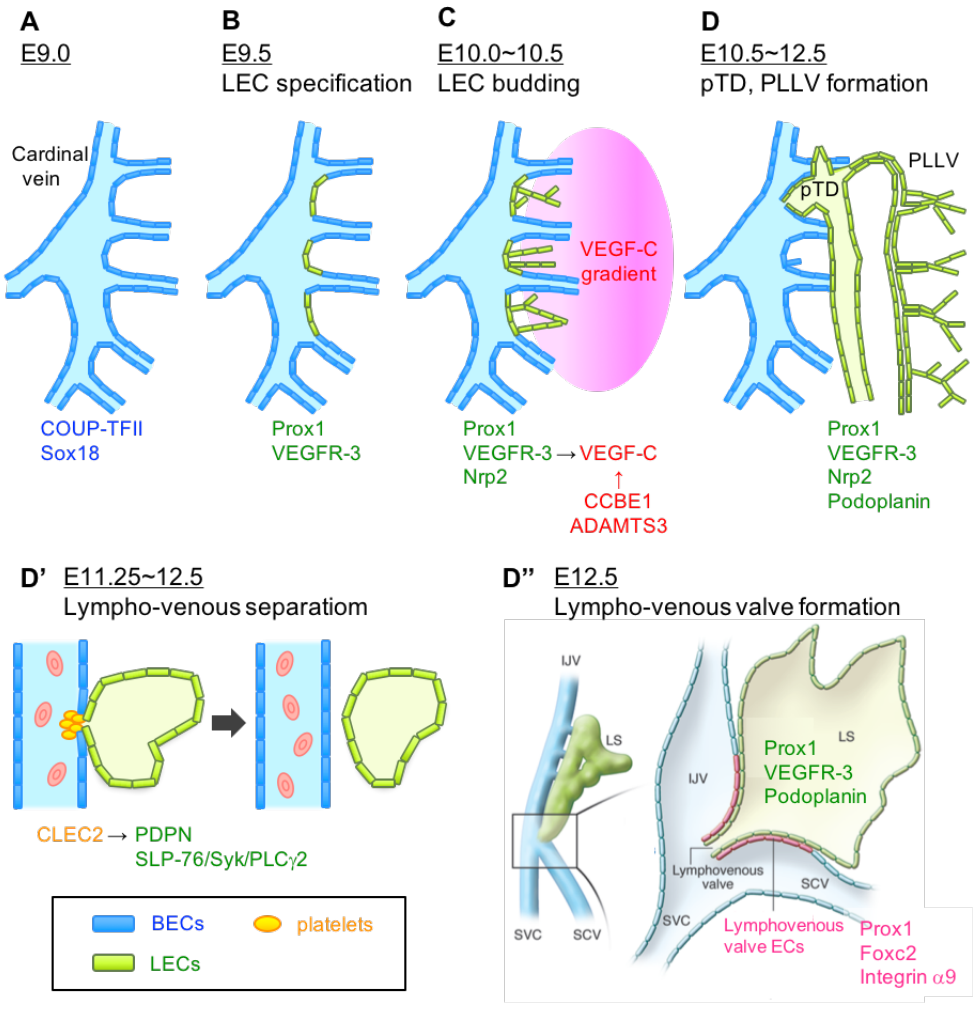

Figure 5. Early development of lymphatic vascular tree. (**A**) The cardinal vein at E9.0. (**B**) Specification of LECs at E9.5, identified by Prox1 expression in the cardinal vein. (**C**) Budding of VEGFR-3$^+$ LECs from the cardinal vein in accordance with VEGF-C gradient at E10.0 to E10.5. (**D**) Formation of the pTD and primordial longitudinal lymphatic vessel (PLLV) between E10.5 and E12.5. (**D'**) Separation of lymphatic vessels from the cardinal veins. Podoplanin$^+$ LECs bind and activate CLEC-2$^+$ platelets aggregation, leading to separation of lymphatic vessels from vein. (**D"**) Schematic representation of the lymphovenous valves. Each of the valve's two leaflets has two layers of Prox1$^+$ endothelial cells: an inner Prox1$^+$Podoplanin$^+$ layer continuous with the pTD and an outer Prox1$^+$Podoplanin$^-$ layer continuous with the veins. IJV, internal jugular vein; LS, lymph sac; SCV, subclavian veins; SVC, superior vena cava. (**A**–**D** are cited from Aspelund et al., 2016 with some modifications. **D"** is cited from Yang & Oliver, 2014 with minor modifications.)

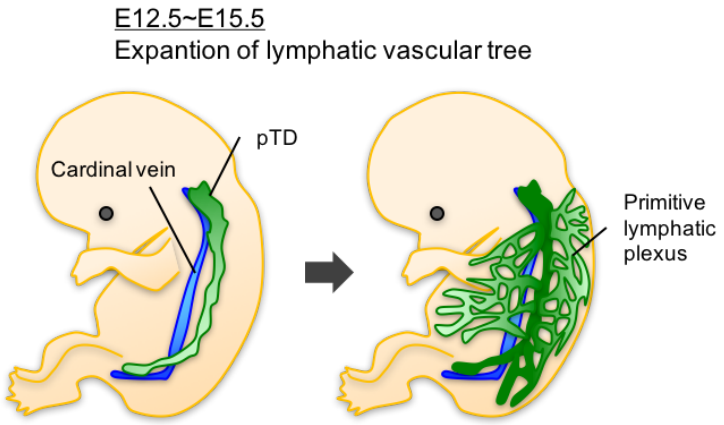

Figure 6. Expansion of lymphatic vascular tree. Lymphatic vessels further spread throughout the body to form primitive lymphatic plexus by E15.5.

Remodeling and Maturation of Lymphatic Vessels

Lymphatic vessels further sprout from primordial lymphatic structures to form the lymphatic network throughout the body (Figure 6). The lymphatic network is initially established as the primitive lymphatic plexus, and then remodeled into a hierarchical vascular network composed of lymphatic capillaries and collecting vessels. This process requires sprouting of new capillaries from pre-existing vasculature and formation of collecting vessels via fusion and pruning of primary plexus (Figure 7). Environmental cues as well as intrinsic genetic program involving gene products such as ephrin-B2, angiopoietin-2 (Ang-2), Tie1, and forkhead box protein c2 (Foxc2) play important roles in the remodeling processes (Dellinger et al., 2008; Gale et al., 2002; Makinen et al., 2005; Norrmen et al., 2009; Petrova et al., 2004). Deficiency of these molecules in mice does not affect the initial lymphatic plexus, but leads to defective remodeling and failure of collecting lymphatic vessels and lymphatic valves. These mutant mice also display defective sprouting of lymphatic capillaries with ectopic SMCs coverage. The lymphatic maturation defects during late gestation and postnatal period lead to lymphatic dysfunction and impaired postnatal survival.

Formation of Lymphatic Valves

After formation of collecting vessels, lymphatic valves start to develop by specification of valve-forming cells during E16.5. These cells express high levels of the transcription factors Prox1 and Foxc2 (Norrmen et al., 2009). Downstream of Prox1 and Foxc2, together with a response to oscillatory shear stress, connexin37, connexin43 and calcineurin/NFAT (nuclear factor of activated T cells) regulate the formation of a ring-like valve area (Norrmen et al., 2009; Sabine et al., 2012). Following specification, valve cells delaminated from the vessel wall extend into the lumen and mature into V-shaped leaflets capable of preventing lymph backflow. The axonal guidance genes semaphorin 3A and its receptors Nrp1 and plexinA1 are also required for lymphatic valve formation (Bouvree et al., 2012; Jurisic et al., 2012).

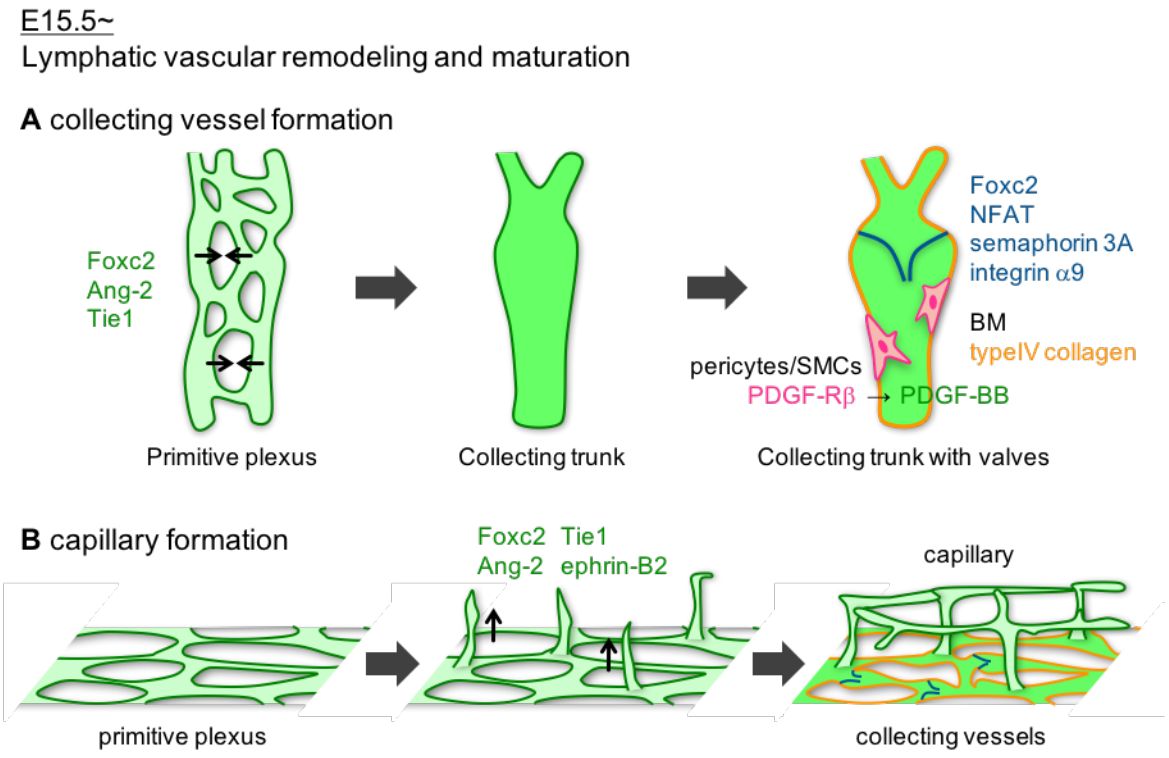

Figure 7. Remodeling and maturation of lymphatic vascular tree. (**A**) Collecting vessel formation. Primitive lymphatic plexus is fused or pruned, and remodeled into collecting trunk at E15.5 to E16.5. After formation of collecting trunk, lymphatic valves develop from Foxc2^{+} valve-forming cells. Recruitment of pericytes/SMCs and deposition of basement membrane (BM) starts from E17. (**B**) Capillary formation. Secondary sprouts emerge from primitive plexus to form lymphatic capillaries.

ECM in Lymphatic Vessel Formation, Maintenance and Function

Several ECM structures interact with lymphatic vessels, such as basement membranes, core matrix in luminal valves, and anchoring filaments (Figure 4). Basement membrane proteins are deposited on the abluminal (basal) surface of collecting vessels. Basement membrane provides structural support for LECs and interacts with mural cells, and is likely to contribute to the barrier function to both soluble molecules and migrating cells. In the luminal valve leaflets, specialized endothelium is anchored to the ECM core (Bazigou et al., 2009; Lauweryns and Boussauw, 1973). Valve development is accompanied by deposition of ECM proteins, such as laminin α5 and type IV collagen, and increased expression of integrin α9 (Bazigou et al., 2009). Anchoring filaments attach LECs to the mesenchymal ECM and, in so doing, prevent the collapse of the lymphatic capillaries and drive lymph within the vessels (Gerli et al., 1990; Leak and Burke, 1968; Solito et al., 1997). Fibrillin and the elastic microfibril-associated protein (EMILIN1) are reported as the components of the anchoring filaments in lymphatic vessels (Danussi et al., 2008; Gerli et al., 2000; Vainionpaa et al., 2007).

Although these ECM structures are involved in maintenance or stabilization of lymphatic vessels, the roles of ECM proteins in lymphatic development are largely unknown. Here we show that the ECM protein polydom is required for the lymphatic development by generating polydom-deficient mice. *Polydom*$^{-/-}$ mice showed severe edema from the mid-gestation stage and died immediately after birth. In *Polydom*$^{-/-}$ embryos, the primitive lymphatic plexus was developed, but the subsequent remodeling was impaired. I explored the mechanism underlying the phenotype of *Polydom*$^{-/-}$ mice by focusing on a panel of transcription factors and growth factors involved in lymphangiogenesis.

Material and Methods

Mouse Strains

To generate *Polydom*$^{-/-}$ mice, we constructed a targeting vector containing a single loxP site upstream of exon 2 followed by a PGK promoter-driven neomycin-resistance (*PGK-neo*) cassette flanked by two FRT sequences at the 5′ and 3′ ends, respectively, and another loxP site in the downstream of these sequences (Figure 18A). The construct was flanked by 4.4-kb upstream and 4.6-kb downstream *Polydom* genomic sequences. The targeting vector was introduced into C57BL/6N-background mouse embryonic stem cells to induce homologous recombination. Mice derived from the recombinant embryonic stem cell clone containing the *neo* allele were crossed with a transgenic line, B6.Cg-Tg(CAG-cre)CZ-MO20sb (RIKEN BRC) (Matsumura et al., 2004), to excise exon 2 and the *PGK-neo* cassette. Excision of exon 2 was verified by Southern blotting. Genomic DNA was isolated from the embryonic liver using DNAzol® Reagent (Invitrogen) and digested with BamHI and XhoI for detection with a 5′ probe and SpeI for detection with a 3′ probe. Antisense probes labeled with digoxigenin (DIG) were prepared using a PCR DIG Probe Synthesis Kit (Roche) with the following primers: 5′-probe-F, 5′-TGGTTGTACTGGGTAGCTGA-3′; 5′-probe-R, 5′-CGTCTGGCATTTTTCTCCTG-3′; 3′-probe-F, 5′-TCTCGCCAGAATGTTTCCAG-3′; 3′-probe-R, 5′-TAAGGTTAGCTAGGAACCCC-3′. Genotyping was performed by PCR using tail DNA with the following three primers: 5′-TGACACTGGAGCTCCTGTGCCTTTG-3′ (F1); 5′-GATCCATGAGATGAATTGAGGTGTGTTT-3′ (F2); and 5′-CCTGTTGGGACTGATGTTCTTATGACA-3′ (R1); 5′-GTTTCACTGGTTATGCGGCGG-3′ (Cre-F); 5′-TTCCAGGGCGCGAGTTGATAG-3′ (Cre-R). The wild-type allele gave a 243-bp band, while the flox allele and the mutant allele gave a 360-bp and a 559-bp band, respectively. *Polydom*$^{+/+}$ littermate embryos of *Polydom*$^{-/-}$ embryos were used as controls in this study.

A *Polydom-lacZ* knock-in mouse line (*Polydom*^{lacZ}), B6N(Cg)-Svep1$^{tm1b(EUCOMM)Hmgu}$/J, was obtained from The Jackson Laboratory (Skarnes et al., 2011). To generate mice containing the *flox* allele, mice containing the *neo* allele were crossed with a transgenic line, C57BL/6-Tg(CAG-flpe)36Ito/ItoRbrc (RIKEN BRC) (Kanki et al., 2006), to excise the *PGK-neo*

cassette. For endothelial cell-specific polydom deletion, mice containing the *flox* allele were bred with another mouse strain, B6.Cg-Tg(Tek-cre)1Ywa/J, in which Cre recombinase was uniformly expressed in endothelial cells under control of a *Tie2* promoter (The Jackson Laboratory) (Kisanuki et al., 2001). For inducible polydom deletion, mice containing the *flox* allele (*Polydom*$^{fl/fl}$) were crossed with a CAGGCre-ER^{TM} (hemizygous allele) transgenic line, B6.Cg-Tg(CAG-cre/Esr1*)5Amc/J (The Jackson Laboratory) (Hayashi and McMahon, 2002). Tamoxifen (TM) in sunflower oil was administered via intraperitoneal injection (5 mg/40 g) to females at E15.5 (Murtomaki et al., 2014; Srinivasan et al., 2010). *Polydom*$^{fl/fl}$ littermate embryos of *Polydom*$^{fl/fl}$;CreER^{TM} embryos were used as controls.

Itga9$^{-/-}$ mice were generated using the same strategy of *Polydom*$^{-/-}$ mice. A targeting vector was designed to excise the second exon of the *Itga9* gene. The construct was flanked by 5.1-kb upstream and 4.4-kb downstream *Itga9* genomic sequences. Genotyping was performed by PCR using tail DNA with the following three primers: 5′-ACTTAGGACAGCCTCATCACTTGC-3′ (a9F1); 5′-TCAGAAAGGGCAGGAATCTGGAGGC-3′ (a9F2); and 5′-CTACCTTCCATACACAGCAAGATC-3′ (a9R1). The wild-type allele gave a 304-bp band (a9F1 and a9R1 primer set), while the mutant allele gave a 376-bp band (a9F2 and a9R1 primer set). *Itga9*$^{+/+}$ littermate embryos of *Itga9*$^{-/-}$ embryos were used as controls.

All mouse experiments were approved by the Experimental Animal Committee of the Institute for Protein Research, Osaka University, and were performed in compliance with the institutional guidelines.

Antibodies and Reagents

Rabbit anti-N-terminal region of mouse polydom (Sato-Nishiuchi et al., 2012) and rabbit anti-human plasma FN (8209 and 8259) (Manabe et al., 1997) were raised in our laboratory. Rat anti-mouse laminin α1 (5B7-H1), rat anti-mouse laminin α2 (4H8-2), rat anti-mouse laminin α3 (M35-N3-B9), rat anti-mouse laminin α4 (M49-N7-F3), rat anti-mouse laminin α5 (M5N8-C8), and rabbit anti-mouse nidogen2 were raised in our laboratory (Manabe et al., 2008). Rabbit anti-mouse fibrillin-1 (pAb 9543) and Rabbit anti-mouse fibrillin-2 (pAb 0868) were kindly provided by Prof. Lynn Sakai (Shriners Hospital for Children) (Charbonneau et al., 2003). Rabbit anti-human type IV

collagen was purchased from Rockland. Rabbit anti-human EMILIN1 was obtained from Proteintech. Goat anti-mouse VEGFR-3, lymphatic vessel hyaluronan receptor (LYVE)-1, rat anti-mouse LYVE-1, goat anti-mouse EphB4, goat anti-mouse ephrin-B2, sheep anti-mouse Foxc2, sheep anti-human FOXC2, goat anti-mouse integrin α9, goat anti-human Tie1, and goat anti-mouse/rat Tie2 were purchased from R&D Systems. Rabbit anti-mouse Prox1 and LYVE-1, and hamster anti-mouse podoplanin were obtained from AngioBio. Rat anti-mouse PECAM-1 was purchased from BD Pharmingen. Mouse anti-rat neurofilament (2H3) was obtained from Developmental Studies Hybridoma Bank. Cy3-conjugated mouse anti-human α-smooth muscle actin (αSMA) (clone 1A4) was purchased from Sigma. Rat anti-mouse nidogen1 and goat anti-human Connexin 40 was obtained from Santa Cruz Biotechnology. Mouse anti-human COUP-TFII was purchased from Perseus Proteomics. Rat anti-mouse perlecan and rabbit anti-human SP-C was obtained from Millipore. Rat anti-mouse VE-cadherin was purchased from Abcam. Rat anti-mouse CD45 and F4/80 were obtained from Molecular Probes. Alexa Fluor™-conjugated secondary antibodies were purchased from Invitrogen. HRP-conjugated secondary antibody was obtained from Jackson Immune Research. EnVision+ System-HRP Labeled Polymer Anti-Rabbit was purchased from Dako. Goat anti-rat IgG Microbeads, anti-rabbit IgG Microbeads, and the LS column for the magnetic-activated cell sorting (MACS) System were purchased from Miltenyi Biotec. Collagenase type II, collagenase type IV, and deoxyribonuclease I were obtained from Worthington. Type I collagen (Cellmatrix type I-A and type I-C) was purchased from Nitta gelatin. Recombinant human Ang-1 and Ang-2 were purchased from R&D Systems.

Quantitative RT-PCR

Total RNA was isolated using an RNeasy Mini Kit (Qiagen), in accordance with the corresponding manufacturer's instructions. For investigation of mRNA expression, single-stranded cDNA was transcribed from total RNA using a SuperScript III™ First-Strand Synthesis System for RT-PCR and random hexamers (Invitrogen). The primers used for quantitative RT-PCR are shown in Table 1. PCR was performed with Power SYBR® Green PCR Master Mix (Applied Biosystems) and analyzed using an ABI PRISM® 7000 Sequence Detection System (Applied Biosystems).

Table 1. Oligonucleotide Primers for Quantitative RT-PCR

Name	Sequence
mSvep1_exon2_qPCR_F	GAGACCCCAGACCTATTGC
mSvep1_exon2_qPCR_R	ATATTCCCCTGCCAAATCCC
mSvep1_exon6to7_qPCR_F	TCCGACAGCCCAAACACGGC
mSvep1_exon6to7_qPCR_R	GGCGTTCTACACACCGGGGC
mFoxc2_qPCR_F	GCAACCCAACAGCAAACTTTC
mFoxc2_qPCR_R	GACGGCGTAGCTCGATAGG
mPdgfb_qPCR_F	CTGAGGAACTGTATGAAATGCTG
mPdgfb_qPCR_R	ATGAGCTTTCCAACTCGACTC
mAng2_qPCR_F	CGCTACGTGCTTAAGATCCAG
mAng2_qPCR_R	CATTGTCCGAATCCTTTGTGC
mTie1_qPCR_F	GCCAGGATGTGTCAAGGATT
mTie1_qPCR_R	TCTACAACCTGCTGTGCCTG
mTie2_qPCR_F	GAGCTAGAGTCAACACCAAGG
mTie2_qPCR_R	TTTGCCCTGAACCTTATACCG
mActb_qPCR_F	TGGATCGGTGGCTCCATCCTGG
mActb_qPCR_R	GCAGCTCAGTAACAGTCCGCCTAGA

Immunohistochemistry

Whole-mount staining of embryonic skin, mesentery, and heart was performed in accordance with the methods of Hirashima et al. (Hirashima et al., 2008) with some modifications. Briefly, embryonic tissues were dissected and fixed with 4% paraformaldehyde (PFA) in PBS overnight at 4°C. The fixed tissues were washed three times in PBS containing 0.2% Triton X-100 (PBS-T) for 30 min at 4°C, blocked in PBS-T containing 1% bovine serum albumin (BSA) for 1 h at 4°C, and incubated with primary antibodies for 1–4 days at 4°C. After six washes in PBS-T for 30 min at 4°C, the bound antibodies were visualized with Alexa Fluor™-conjugated secondary antibodies overnight at 4°C. After another six washes in PBS-T for 30 min at 4°C, the tissues were flat-mounted on glass slides with Mount-quick (Daido Sangyo). The immunostained tissues were analyzed with an LSM5 PASCAL (Zeiss) or Fluoview FV1200 (Olympus) confocal microscope.

Whole embryonic skin was stained for β-galactosidase activity according to Yamauchi et al. (Yamauchi et al., 1999) with some modifications. Briefly, samples were fixed with 1% PFA and 0.02%

Nonidet P-40 (NP-40) in 0.2 mol/L phosphate buffer (PB) for 30 min at 4°C. After washing in PB, the skin was dissected and re-fixed with 1% PFA and 0.02% NP-40 in PB for 30 min at 4°C. The fixed samples were washed in PB and incubated overnight at 37°C in staining solution (5 mmol/L potassium ferricyanide, 5 mmol/L potassium ferrocyanide, 2 mmol/L $MgCl_2$, 0.5% X-gal, 0.02% NP-40 in PB). The samples were rinsed twice in PB, postfixed with 4% PFA overnight at 4°C, and immunostained for VEGFR-3 using the following steps. The tissues were dehydrated with methanol, and incubated with 30% H_2O_2:DMSO:methanol (1:1:4) for >5 h at 4°C to inactivate endogenous peroxidase. After rehydration, the samples were washed three times with PB containing 0.2% Triton X-100 (PB-T), blocked with PB-T containing 1% BSA for 1 h at 4°C, and stained with primary antibodies for 3 days at 4°C. After three washes in PB-T for 30 min at 4°C, the bound antibodies were visualized with HRP-conjugated secondary antibodies and 3,3'-Diaminobenzidine (DAB) buffer tablets (Merck Millipore).

For immunostaining of cryosections, mouse embryos were embedded in OCT compound (Sakura Finetek). Sections at 10-μm thickness were fixed in ice-cold acetone or 4% PFA, and incubated with 0.3% H_2O_2 to inactivate endogenous peroxidase. After washing in PBS, the sections were blocked with 3% BSA in PBS for 1 h at room temperature, and incubated with primary antibodies overnight at 4°C. The sections were washed in PBS, and the bound antibodies were visualized with EnVision+ System-HRP Labeled Polymer or Alexa Fluor-conjugated secondary antibodies. Finally, the sections were counterstained with Mayer's hematoxylin (for DAB staining) or Hoechst 33342 (for immunofluorescence staining) and mounted with Mount-quick (Daido Sangyo) or FluorSave™ Reagent (Calbiochem).

Lymphangiography

Indian ink was intradermally injected into the footpad of the hindlimb of newborn mice delivered by Caesarean section to visualize functional lymphatic vessels, or the buccal region and hindlimb of E15.5 mice for observation of the facial lymphatic plexus and retroperitoneum collecting vessels. The lymphatic flow carrying Indian ink in the embryos was analyzed with an Olympus SZX12 stereomicroscope.

Isolation of LECs from Dermal Cells

LECs were isolated from dermal cells using the method of Kazenwadel et al. (Kazenwadel et al., 2012) with some modifications. Mouse embryonic skin was dissected and digested with PBS containing 1% FBS, 2.5 mg/ml collagenase type II and type IV, and 1 mg/ml deoxyribonuclease I for 30 min at 37°C. The digested skin was hemolyzed with distilled water and filtered through a 40-μm cell strainer. Cell fractionation was carried out using a MACS System (Miltenyi Biotec). Briefly, cells were centrifuged at 400×*g* for 5 min and suspended at approximately 1×10^8 cells/ml in 1% FBS in PBS containing anti-F4/80 and anti-CD45 antibodies (1:100). The cells were incubated for 30 min at 4°C, washed with 10 ml of MACS buffer (2 mmol/L EDTA, 1% FBS in PBS), centrifuged as described above, and resuspended at 1×10^8 cells/ml in MACS buffer. F4/80(+)/CD45(+) cells were separated using goat anti-rat IgG Microbeads (200 μl beads/1×10^8 cells) and a MACS LS column according to the manufacturer's instructions. F4/80(−)/CD45(−) cells were collected and the entire process was repeated to ensure maximal depletion of hematopoietic cells. F4/80(−)/CD45(−) cells were centrifuged at 400×*g* for 5 min and resuspended at approximately 1×10^8 cells/ml in 1% FBS in PBS with an anti-LYVE-1 antibody (1:200). LYVE-1(+) LECs were separated using goat anti-rabbit IgG Microbeads and a MACS LS column. F4/80(−)/CD45(−)/LYVE-1(−) cells were centrifuged at 400×*g* for 5 min and resuspended at approximately 1×10^8 cells/ml in 1% FBS in PBS containing an anti-CD31 antibody (1:100). CD31(+) blood vascular endothelial cells were purified using goat anti-rat IgG Microbeads and a MACS LS column according to the manufacturer's instructions. The fractionated cells were subjected to RNA isolation.

cDNA Cloning and Construction of Expression Vectors

The expression vector for recombinant polydom with an N-terminal FLAG tag and a C-terminal His_6 tag was constructed as described previously (Sato-Nishiuchi et al., 2012). A cDNA encoding human VEGF-C (proVEGF-C) was obtained by RT-PCR using human fetal liver total RNA (Clontech). The signal sequence of proVEGF-C was substituted with the Ig κ-chain signal sequence of the pSecTag2A mammalian expression vector (Thermo Fisher Scientific) and a His_6 tag by extension PCR,

with an NheI site at the 5' end and a NotI site at the 3' end. The PCR products were digested with NheI/NotI and inserted into the corresponding restriction sites of the pSecTag2A vector.

Expression and Purification of Recombinant Proteins

All recombinant proteins were produced using a FreeStyle 293 Expression System (Thermo Fisher Scientific). For purification of recombinant polydom, conditioned media were applied to anti-FLAG M2-agarose (Sigma), and the bound proteins were eluted with 100 μg/ml FLAG peptide (Sigma) (Sato-Nishiuchi et al., 2012). Recombinant truncated integrin α9β1 was purified as described (Sato-Nishiuchi et al., 2012). For purification of recombinant human proVEGF-C, conditioned media were subjected to affinity chromatography using Ni-NTA agarose (Qiagen). The bound proteins were eluted with 200 mmol/L imidazole, and dialyzed against PBS.

Solid-phase Binding Assay

Microtiter plates (Maxisorp; Nunc) were coated with 5 μg/ml integrin α9β1, type I collagen, proVEGF-C, Ang-1, or Ang-2 overnight at 4°C, and then blocked with 1% BSA for 1 h at room temperature. After washing with TBS containing 0.1% BSA and 0.02% Tween-20 (Buffer W) or Buffer W containing 1 mmol/L $MnCl_2$ (for binding to integrin α9β1 only), recombinant polydom (5 μg/ml) was allowed to bind to the microtiter plates and incubated for 3 h at room temperature. After three washes, the bound polydom was quantified. Briefly, the wells were incubated with an anti-polydom antibody for 1 h at room temperature, washed three times, and incubated with an HRP-conjugated anti-rabbit IgG antibody for 40 min. After three washes, the bound polydom was quantified by measuring the absorbance at 490 nm after incubation with *o*-phenylenediamine.

Cell Culture

Human dermal lymphatic endothelial cells (HDLECs; PromoCell) were plated on type I-C collagen-coated dishes in EBM-MV2 medium supplemented with EGM-MV2 (Promocell) and grown at 37°C in a humidified atmosphere containing 5% CO_2. Freshly isolated LECs were seeded on type

I-C collagen-coated wells at a density of 1.2×10^4 cells per 0.4 ml in Lab-Tek™ II Chamber Slide System 8 wells (Nunc) and cultured for 3 days. Cells were starved with EBM-MV2 for 1 h and overlaid with 0.2 ml of EBM-MV2 containing recombinant human Ang-1 or Ang-2. After incubation at 37°C in a humidified atmosphere containing 5% CO_2 for 12 h, the cells were fixed with 4% PFA in PBS and washed in PBS-T for 30 min. The staining procedure was the same as the protocol for embryonic section staining. Nuclear FOXC2 intensities were analyzed using ImageJ software.

Statistical Analysis

The cell alignment in E18.5 mesenteric lymphatic vessels and the signal intensity of Tie1 and Tie2 in E16.5 skin were analyzed using ImageJ. All data were presented as means ± SEM. The statistical significance of differences between paired samples was determined by Student's *t*-test. Data were considered statistically significant at $P<0.05$.

Results

Polydom Shows Characteristic Distribution in Lymphatic Vessels

To identify extracellular environment around lymphatic vessels, I set out to survey comprehensively the expression profiles of ECM proteins in mouse embryos. First, I studied the distribution of basement membrane proteins around lymphatic vessels. In embryonic skin at E18.5, laminin α4, β1, β2, and γ1 chains were co-localized with VEGFR-3 positive collecting lymphatic trunks (Figure 8). All skin lymphatic vessels lacked laminin α1, α2, α3, β3, γ2, γ3 chains (Figure 8 and the image-based database "Mouse Basement Membrane Bodymap"; http://dbarchive.biosciencedbc.jp/archive/matrixome/bm/home.html). Other basement membrane components, such as perlecan, nidogen1, 2, and type IV collagen, were found around lymphatic endothelium (Figure 8). The expression profile of basement membrane proteins in luminal valve regions was different from that in lymphangion (Figure 8 and summarized in Table 2). Laminin α5 and β2 were predominantly detected in the luminal valve region. Continuous expression of basement membrane proteins was not detected in lymphatic plexus at E15.5 (Figure 8).

Table 2. Summary of the distribution of ECM proteins in lymphatic vessels. Results obtained from in vivo immunofluorescence staining are indicated. Labeling in white, yellow and orange denotes negative, positive and highly positive results, respectively.

skin	lymphatic trunk	lymphatic valve
laminin α1	−	−
laminin α2	−	−
laminin α3	−	−
laminin α4	+	+
laminin α5	−	++
laminin β1	+	+
laminin β2	+	++
laminin γ1	+	+
collagen-IV	+	+
perlecan	+	+
nidogen1	+	+
nidogen2	+	+
fibrillin1	−	−
fibrillin2	−	−
FN	−	−
EMILIN1	−	+
polydom	+	++

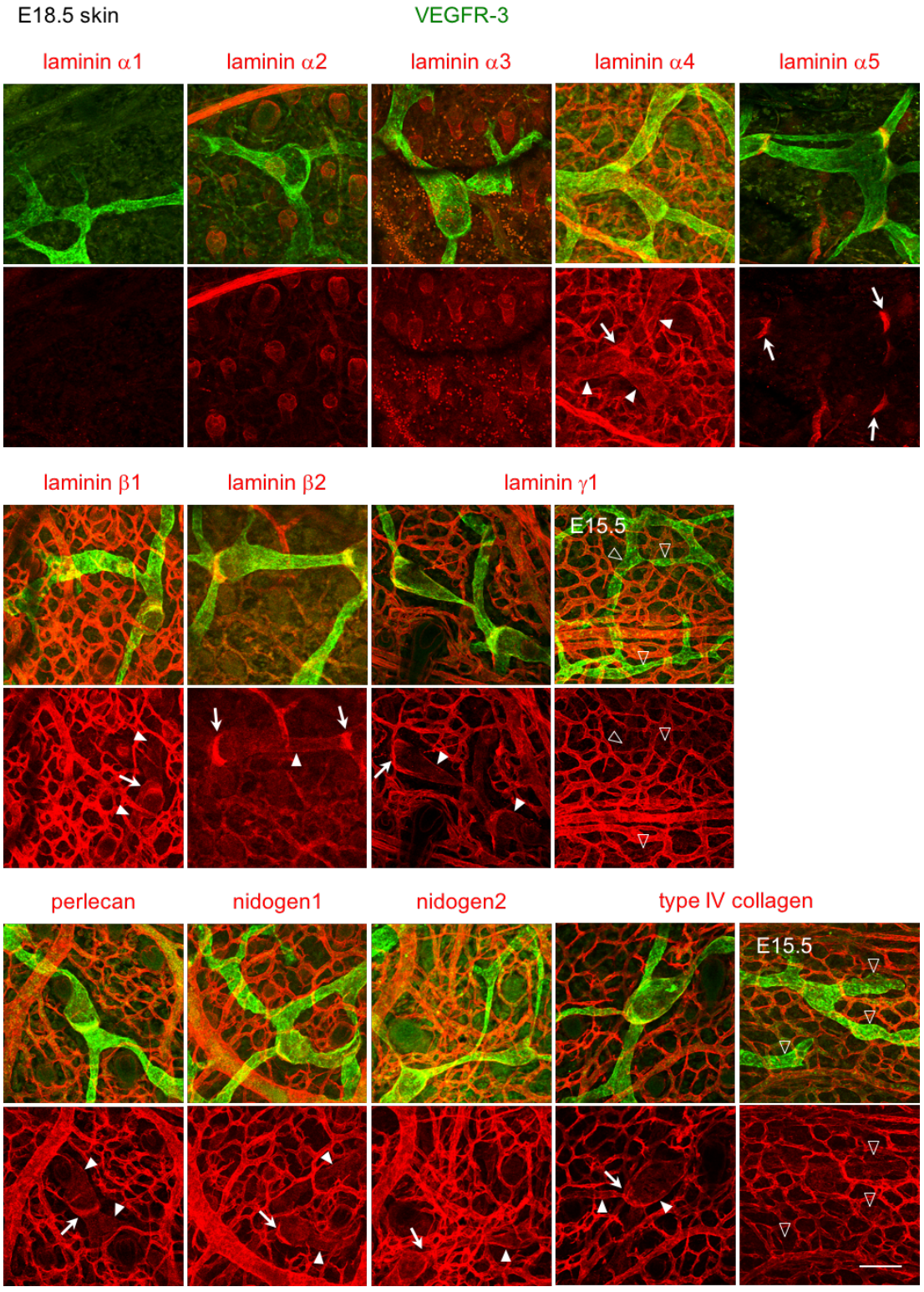

Figure 8. Distribution of basement membrane proteins in embryonic skin. Whole-mount immunofluorescence staining for laminin α1-5, β1-2, γ1, perlecan, nidogen1 and 2, and type IV collagen with VEGFR-3 in wild-type skin at E18.5 (laminin γ1 and type IV collagen also examined at E15.5). *Solid arrowheads*, lymphatic trunk; *open arrowheads*, primitive lymphatic plexus; *arrows*, valves. Bar, 100 μm.

Mesenchymal ECM proteins, such as fibrillin, EMILIN-1 and FN, have been reported to associate with lymphatic vessels. Fibrillin has been known as a component of anchoring filaments. In our experiments, Fibrillin-1 and -2 were deposited in lower dermis, but anchoring filaments around lymphatic capillaries were not detected with fibrillin-1 or -2 at E18.5 (Figure 9). Although FN-EIIIA (extra type-III repeat A) expression was reported on the free edge of the valve leaflets during embryonic development (Bazigou et al., 2009), accumulation of FN was detected at neither valve region nor other region of lymphatic vessels (Figure 9). EMILIN1, whose upregulation correlates with the initiation of valve leaflet development and becomes evident according to valve maturation (Danussi et al., 2013), was stained weak in lymphatic valves at E18.5 (Figure 9).

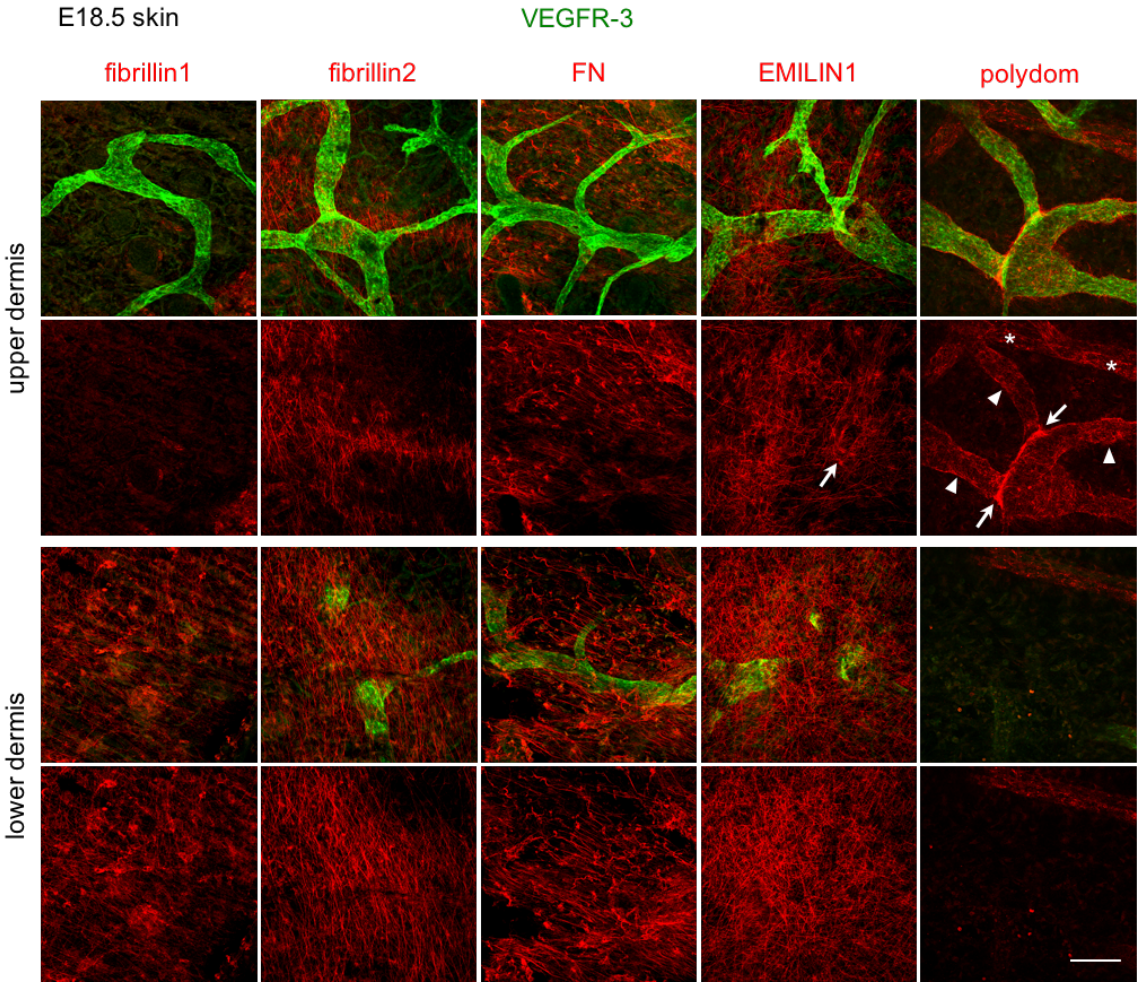

Figure 9. Distribution of mesenchymal ECM proteins in embryonic skin. Whole-mount immunofluorescence staining for fibrillin1 and 2, FN, EMILIN1, and polydom with VEGFR-3 in wild-type skin at E18.5. First and second rows show upper dermis where lymphatic vessels mainly exist, and third and fourth rows show lower dermis. *Solid arrowheads*, lymphatic trunk; *arrows*, valves; *asterisks*, non-lymphatic vessel staining. Bar, 100 μm.

In contrast to other mesenchymal ECM proteins, polydom was specifically expressed along lymphatic vessels and also concentrated in valves (Figure 9). Polydom was accumulated in the abluminal (basal) surface of the lymphatic vessels (Figure 10) and the outer side of basement membrane (Figure 11). Polydom was detected at other tubular structures in skin (asterisk in Figure 9). Double immunofluorescence staining with neurofilament and PECAM-1 showed that polydom was also localized at perineurium and around arteries but not around veins (Figure 12). Taken together, polydom is localized around lymphatic vessels, peripheral nerve, and artery.

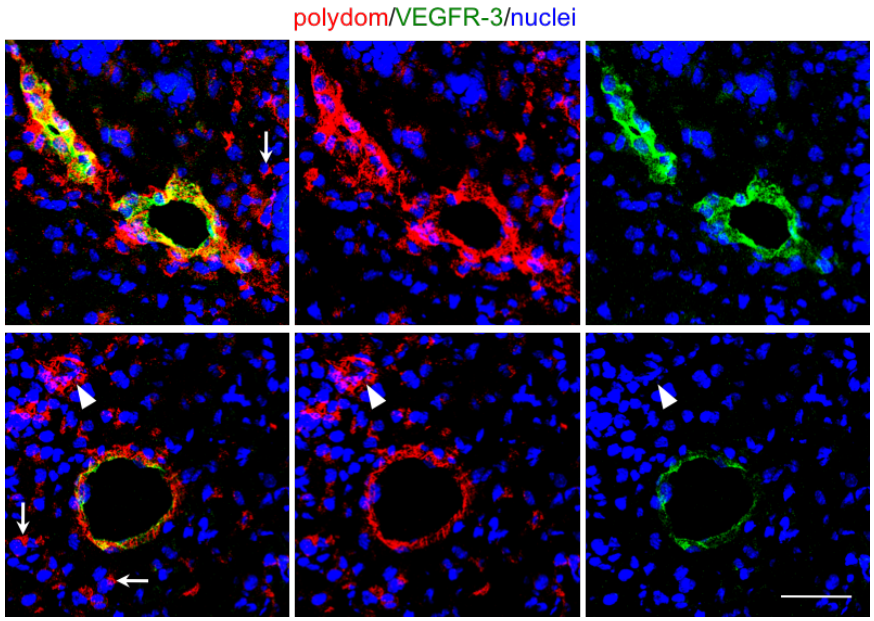

Figure 10. Polydom is deposited outside of lymphatic tubes. Immunofluorescence staining for polydom (red) and VEGFR-3 (green) in cross-sections of the wild-type skin at E18.5. Nuclei were stained with Hoechst 33342 (blue). Bar, 50 μm. Note that polydom is deposited to surround VEGFR-3^{+} lymphatic vessels. *Arrows*, polydom-expressing cells; *arrowheads*, non-lymphatic vessel staining.

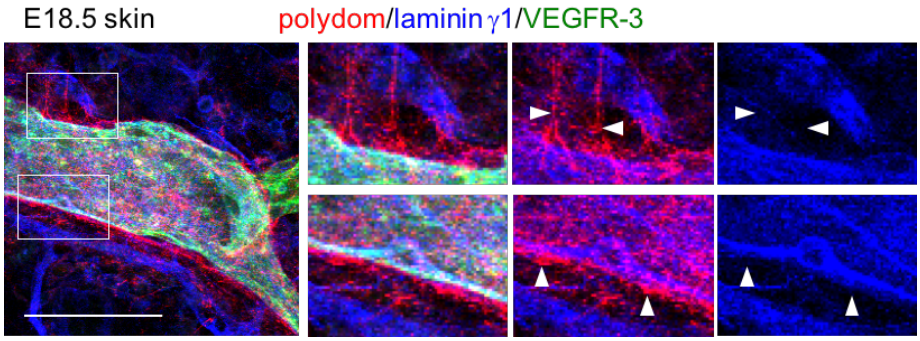

Figure 11. Polydom accumulated outside of basement membrane of lymphatic vessels. Whole-mount immunofluorescence staining for polydom (red), laminin γ1 (blue), and VEGFR-3 (green) in wild-type skin at E18.5. *Arrowheads* indicate polydom fibrils outside the laminin γ1^{+} lymphatic basement membrane. Boxed areas are enlarged on the right. Bar, 100 μm.

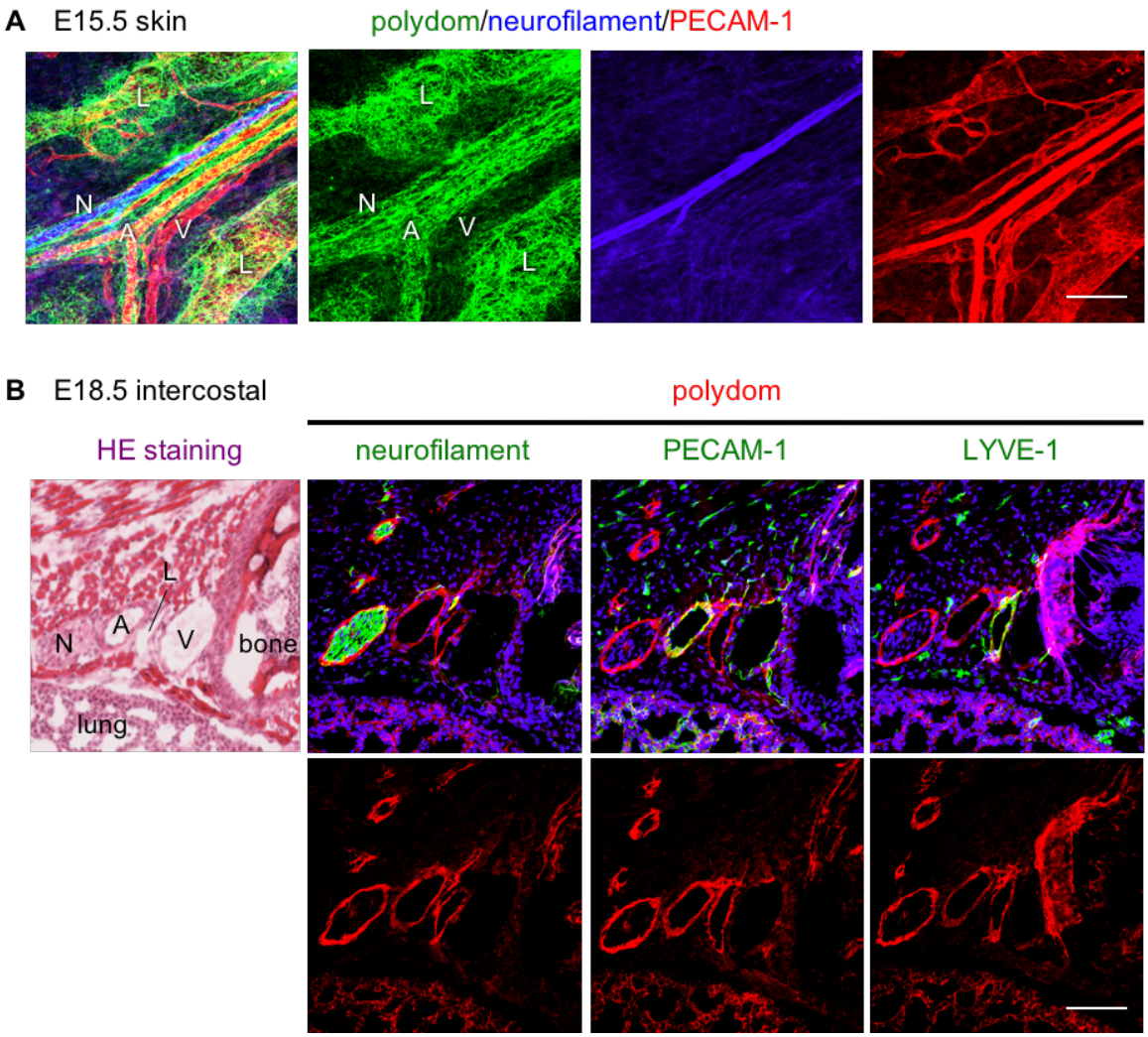

Figure 12. Polydom is localized not only at lymphatic vessels but also at arteries and nerves. (**A**) Whole-mount immunofluorescence staining for polydom (green), neurofilament (as nerve marker, blue), and PECAM-1 (as vascular marker, red) in wild-type skin at E15.5. (**B**) H&E staining in cross-section of the wild-type intercostal region at E18.5 and immunofluorescence staining of serial sections for neurofilament (green in *left*), PECMA-1 (green in *middle*), and LYVE-1 (green in *right*) with polydom (red). Nuclei were stained with Hoechst 33342 (blue). A, artery; L, lymphatic vessel; N, nerve; V, vein. Bars, 100 μm.

Polydom Localizes around Lymphatic Vessels through Embryonic Development

Previous studies showed that polydom is a high affinity ligand for integrin α9β1 (Sato-Nishiuchi et al., 2012), a cell adhesion receptor involved in lymphangiogenesis. To gain further insight into the role of polydom in lymphatic development, I analyzed its expression at different embryonic stages. In E12.5 embryos, polydom was expressed around pTD (Figure 13). Whole-mount immunofluorescence

staining of the skin and the mesentery revealed that polydom was deposited in a fibrillar pattern around lymphatic plexus at E15.5 and around collecting lymphatic vessels at E18.5 (Figure 14A–H). In addition, polydom was strongly detected at lymphatic valves (Figure 14E–H). Polydom continues to be expressed until postnatal period (at least postnatal day 21, P21, Figure 15). These results indicate that polydom directly associates with lymphatic vessels throughout lymphatic development.

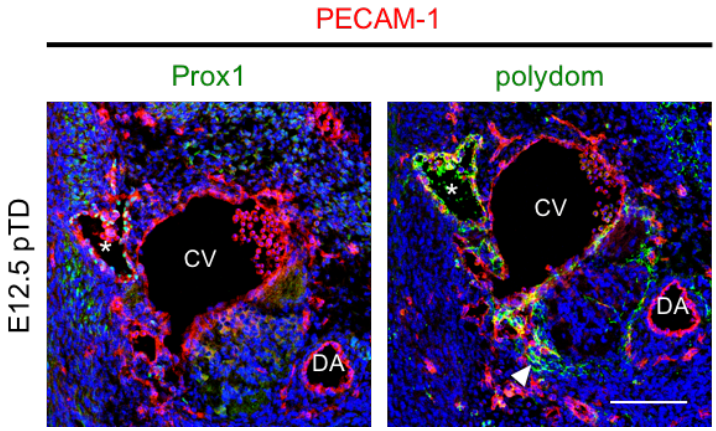

Figure 13. Polydom is expressed in the pTD at E12.5. Immunofluorescence staining of transverse sections of the E12.5 cervical region for PECAM-1 (red) and Prox1 (green in *left*) or polydom (green in *right*). Nuclei were stained with Hoechst 33342 (blue). Polydom is localized around the pTD (*asterisks*) at E12.5. CV, cardinal vein; DA, dorsal aorta; *arrowhead*, perineurium. Bar, 100 μm.

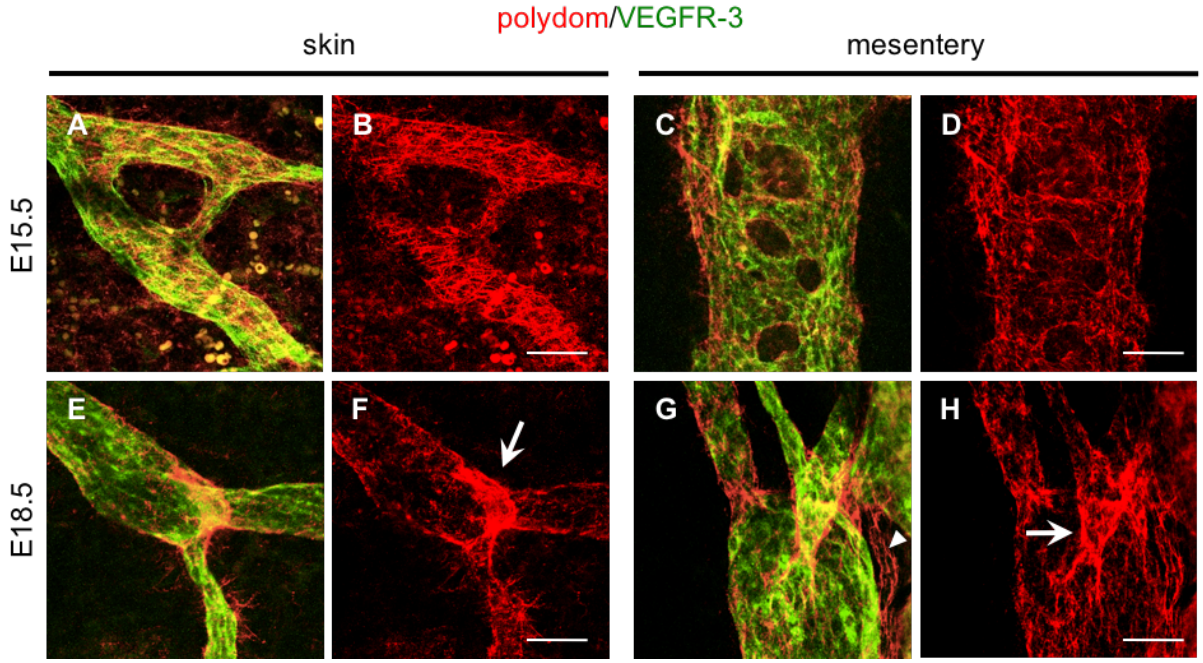

Figure 14. Polydom is expressed in lymphatic vessels throughout its embryonic development. (**A**–**H**) Whole-mount immunofluorescence staining for polydom (red) and VEGFR-3 (green) in the wild-type skin and mesentery at E15.5 and E18.5. Note that polydom is deposited in fibrils around the primitive lymphatic plexus (**A**–**D**) and collecting lymphatic vessels (**E**–**H**). Polydom is prominently detected at luminal valves (*arrows* in **F** and **H**). *Arrowhead* in (**G**) indicates perineurial expression of polydom. Bars, 50 μm.

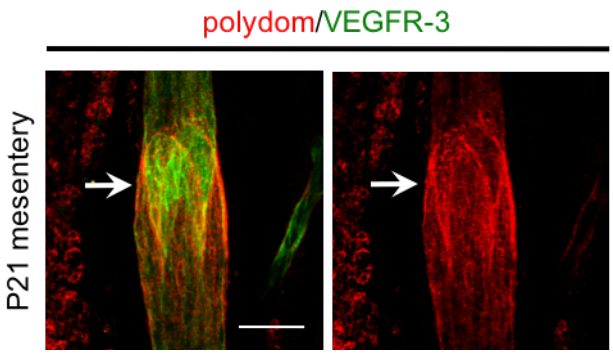

Figure 15. Polydom is expressed in postnatal lymphatic vessels. Whole-mount immunofluorescence staining for polydom (red) and VEGFR-3 (green) in the wild-type mesentery at P21. Polydom is prominently detected at luminal valves (*arrows*). Bar, 50 μm.

Polydom Is Produced by Mesenchymal Cells

To examine whether polydom is produced and deposited by LECs, I visualized the polydom-expressing cells using the mutant mouse strain B6N(Cg)-Svep1$^{tm1b(EUCOMM)Hmgu}$/J, which carries a *lacZ* reporter downstream of the first exon of *polydom*. Contrary to our expectation, expression of the *lacZ* reporter was not detected on lymphatic vessels, but in cells scattered in the dermis (Figure 16), which suggests that polydom is expressed in mesenchymal cells, but not in LECs.

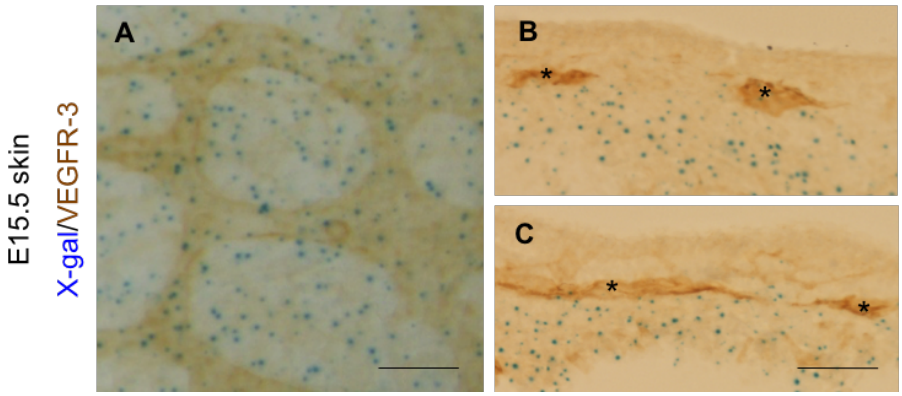

Figure 16. Polydom is expressed in scattered cells in dermis. Double-staining of X-gal$^+$ polydom-expressing cells (blue) and VEGFR-3$^+$ lymphatic vessels (brown) in whole-mount *Polydom*$^{lacZ/+}$ skin (**A**) and its sections (**B**, **C**) at E15.5. X-gal$^+$ polydom-expressing cells are scattered in the mesenchyme beneath VEGFR-3$^+$ lymphatic vessels (*asterisks*). Bars, 100 μm.

To corroborate this observation, I serially fractionated cells from skin of E15.5 embryos into blood cells, LECs, blood vascular endothelial cells, and flow-through cells (referred to as "Others" in Figure 17B) and compared expression levels of *polydom* mRNA in the fractionated cells (Figure 17A). *Polydom* expression was predominantly detected in the flow-through cells, but not in LECs, blood vascular endothelial cells nor blood cells (Figure 17B). Furthermore, fractionation of cells that

expressed platelet-derived growth factor receptor (PDGF)-α, a marker for mesenchymal stem cells, revealed that *Polydom* was strongly expressed in PDGFR-α^+ cells (Figure 17C). *Polydom* was also expressed in PDGFR-β^+ cells, which include pericytes and mesenchymal cells (Figure 17D). These results were consistent with the localized lacZ activity in the mesenchymal cells of the *Polydom-lacZ* reporter mice. I also examined the conditional knockout mice in which polydom expression was disrupted in endothelial cells by the expression of Cre recombinase under control of a *Tie2* promoter. These mice were viable and fertile with no symptoms of edema (*Polydom*$^{fl/fl}$ (control), *n*=6; *Polydom*$^{fl/fl}$;*Tie2-Cre*, *n*=11), which confirms that LECs are not the major source of polydom.

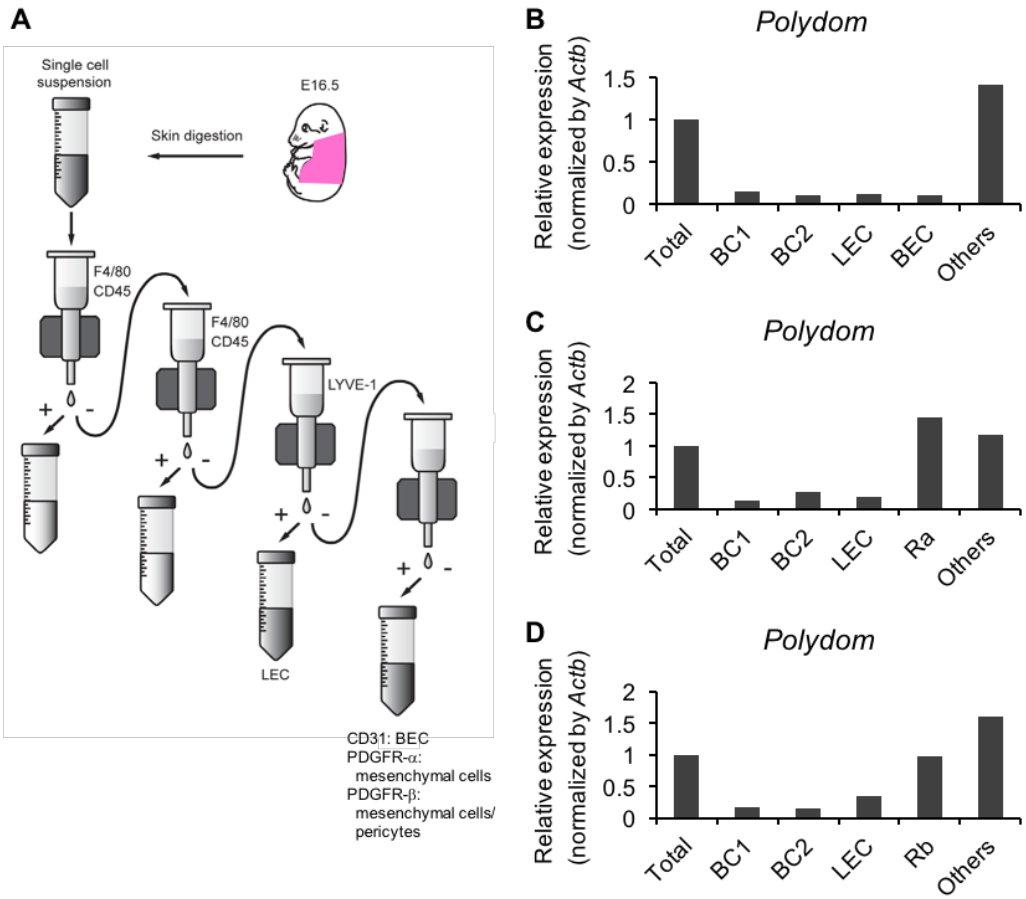

Figure 17. Polydom is secreted from mesenchymal cells. (**A**) Schematic illustration of embryonic dermal cell isolation. (**B–D**) Expression levels of *Polydom* transcripts determined by quantitative RT-PCR in cells fractionated from the wild-type skin at E15.5. BC1 and BC2, first and second (respectively) batches of CD45(+)F4/80(+) blood cells; LEC, CD45(−)F4/80(−)LYVE-1(+) lymphatic endothelial cells; BEC, CD45(−)F4/80(−)LYVE-1(−)CD31(+) blood vascular endothelial cells; Ra, CD45(−)F4/80(−)LYVE-1(−)PDGFR-α(+) mesenchymal cells; Rb, CD45(−)F4/80(−)LYVE-1(−)PDGFR-β(+) pericytes/mesenchymal cells; Others, CD45(−)F4/80(−)LYVE-1(−)CD31(−) cells. Unfractionated cells are labeled as "Total". *Actb* was used as a control. Data are representative of three and two independent experiments, respectively. (**A** is cited from Kazenwadel et al., 2012, with some modifications).

Targeted Disruption of the *Polydom* Gene in Mice Causes Severe Edema

To clarify the physiological roles of polydom, we generated polydom deficient mice. A targeting vector was designed to excise the second exon of the *Polydom* gene, thereby resulting in an aberrant termination of polydom protein translation (Figure 18A). The targeted *Polydom* gene was confirmed by Southern blotting (Figure 18B) and genomic PCR (Figure 18C). RT-PCR analysis showed that the exon2 was deleted but subsequent exons were transcribed in the targeted allele (Figure 18D). Immunohistochemical staining with anti-polydom antibody failed to detect polydom protein in *Polydom*$^{-/-}$ mice (Figure 18E), which confirmed that excising exon2 resulted in loss of the functional protein.

Polydom$^{-/-}$ embryos were born at a nearly Mendelian frequency at E18.5, although no homozygotes survived to day 7 after birth (Figure 18F). Further examination showed that *Polydom*$^{-/-}$ mice die immediately after birth: *Polydom*$^{-/-}$ embryos obtained by Caesarian section at E18.5 were alive but cyanotic and died within 30 minutes after birth (Figure 18G). *Polydom*$^{-/-}$ pups exhibited severe edema with excessive fluid accumulation in the thoracic and abdominal cavities and in the subcutaneous space (Figure 18H). The hydrostatic as well as histological examination of the lung of *Polydom*$^{-/-}$ pups indicated that the excessive accumulation of pleural fluid caused the alveolar airspace unable to inflate, thereby resulting in respiratory failure (Figure 19). These results point to the role for polydom in fluid homeostasis.

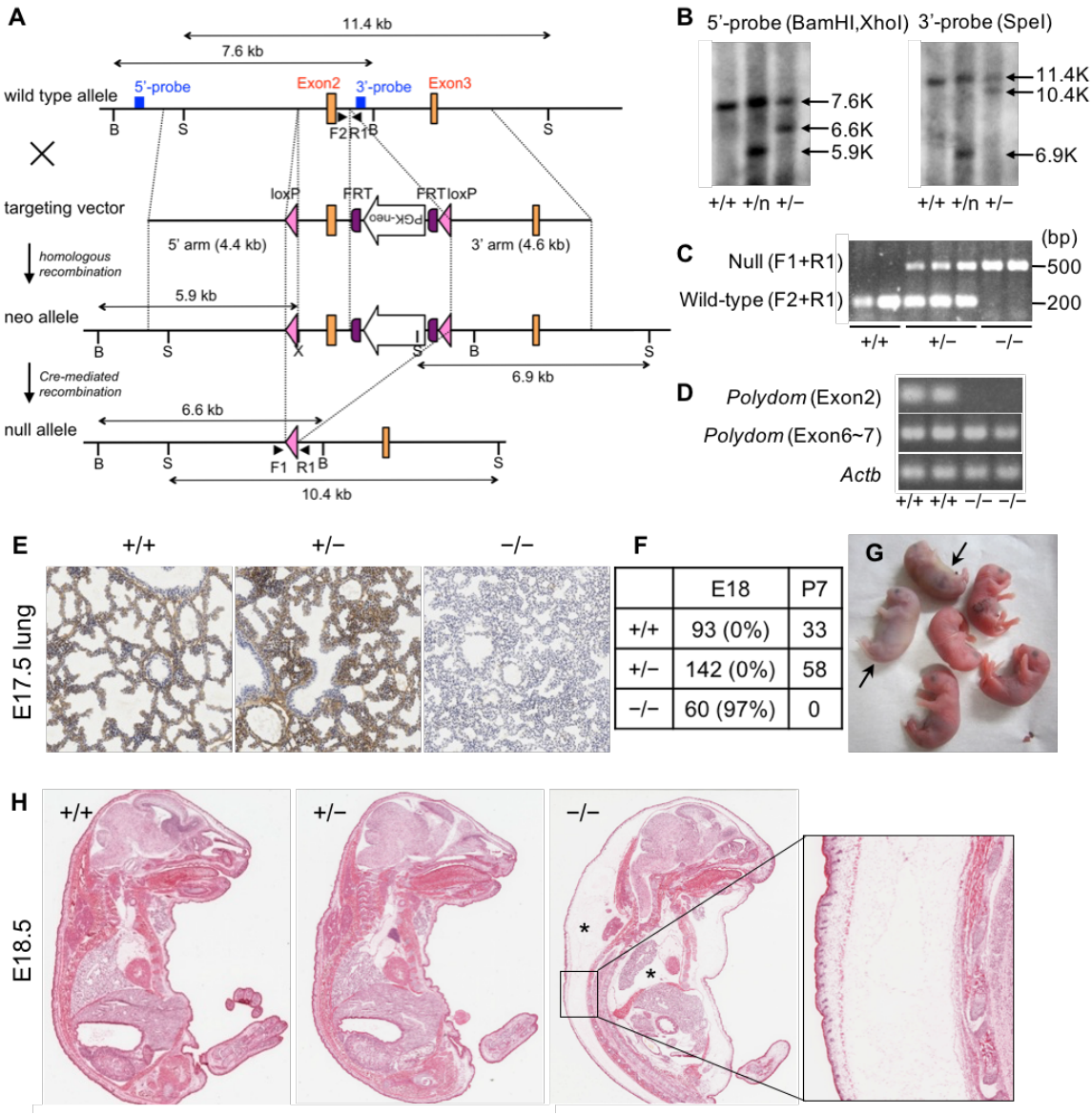

Figure 18. Targeted disruption of the *Polydom* gene causes severe edema. (**A**) Schematic representation of the gene targeting by homologous recombination. The targeting vector was designed to excise exon2 of *Polydom*. The floxed targeted exon and the FRT-*PGK*-*neo*-FRT cassette were removed by Cre-mediated recombination. Probes used for Southern blot analysis are shown as *blue boxes* (5′-flanking and 3′-flanking). Primers used for PCR genotyping are shown by *black arrowheads* (F1, F2, and R1). B, BamHI; S, SpeI; X, XhoI. (**B**) Southern blot analysis. Genomic DNA was digested with BamHI and XhoI for the 5′-probe or SpeI for the 3′-probe. The 5′-probe detected 7.6-kb, 6.6-kb, and 5.9-kb fragments corresponding to the wild-type (+), null (−), and *neo* (n) alleles, respectively. The 3′-probe detected 11.4-kb, 10.4-kb, and 6.9-kb fragments corresponding to the wild-type (+), null (−), and *neo* (n) alleles, respectively. (**C**) PCR genotyping with the F1, F2, and R1 primers. (**D**) RT-PCR analysis for *Polydom* transcripts in the E11.5 whole body. *Actb* was detected as a control. (**E**) Immunohistochemical staining of the E17.5 lung using an anti-polydom antibody. The specificity of the antibody used is confirmed by its negative reactivity toward the lung of *Polydom*$^{-/-}$ mice. (**F**) Genotypes of embryos obtained by intercrossing of heterozygotes. Numbers in parentheses, percentages of edema incidence. (**G**) Newborn pups obtained by caesarean section at E18.5. *Arrows*, *Polydom*$^{-/-}$ pups, which exhibited cyanosis and died within 30 min after birth. (**H**) H&E staining of sagittal sections of E18.5 embryos. Heterozygous mice (+/−) show no gross phenotypic abnormalities, while polydom-null mice (−/−) develop severe edema in the skin and thoracic cavity (*asterisks*). The *boxed region* is magnified on the right.

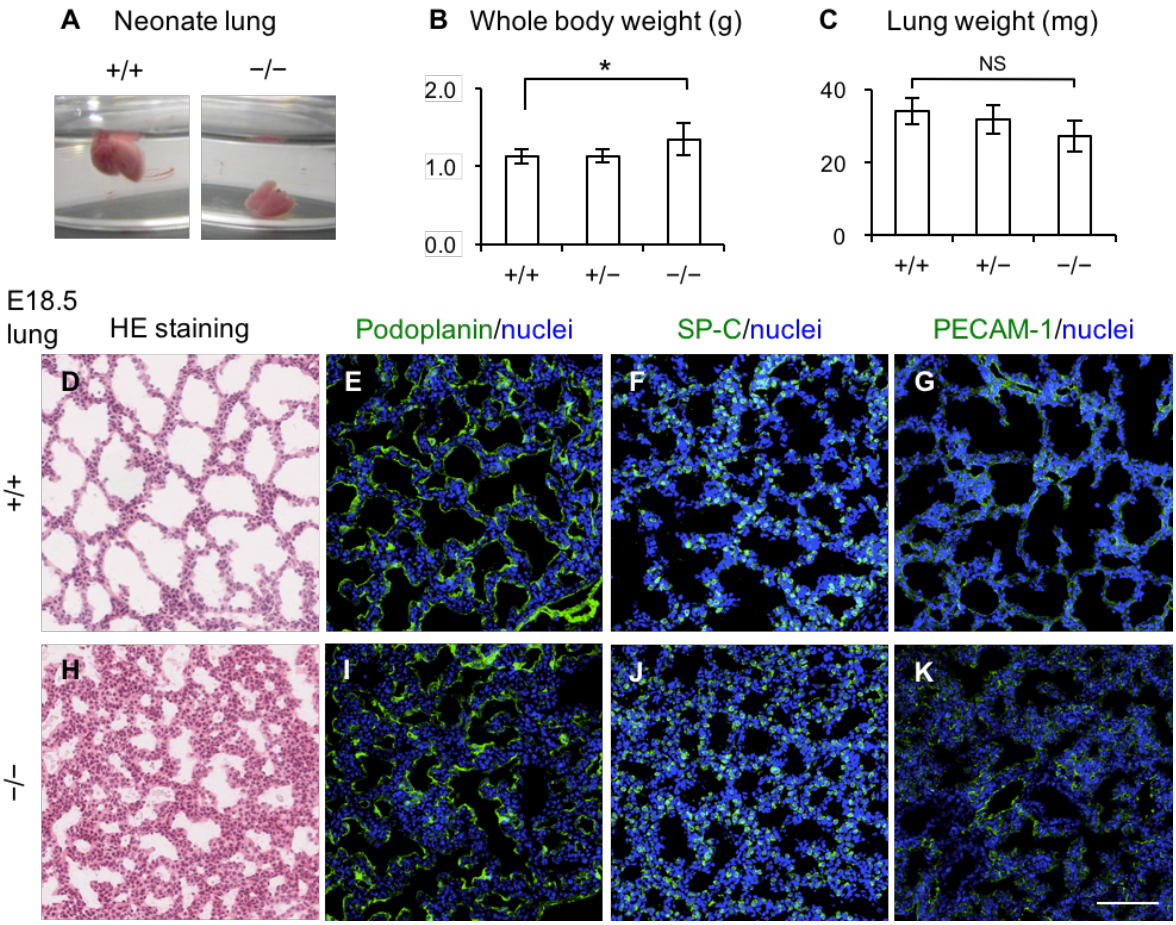

Figure 19. Loss of polydom does not affect the development of lung cell types, but results in failure of lung inflation. (**A**) Flotation of *Polydom*$^{-/-}$ neonate lungs (right) in saline compared with those from control littermates (left). (**B**, **C**) Weights of the whole body (**B**) and lungs (**C**) for wild-type (+/+), heterozygous (+/−), and homozygous (−/−) mice. Data are means ± SEM (n=10 for wild-type pups; n=15 for heterozygous pups; n=8 for homozygous pups). *P<0.001; NS, not significant. (**D**, **H**) H&E staining of lung sections at E18.5 showing thickened walls with a smaller alveolar space in *Polydom*$^{-/-}$ mice. (**E**–**G** and **I**–**K**) Immunofluorescence staining of lung sections at E18.5 for Podoplanin as a type I epithelial cell marker (**B**, **F**), SP-C as a type II epithelial cell marker (**C**, **G**), and PECAM-1 as a blood capillary marker (**D**, **H**). Nuclei were stained with Hoechst 33342 (blue). Note that the differentiation of lung epithelial cells and formation of blood capillaries are comparable between wild-type and *Polydom*$^{-/-}$ lungs. Bar, 100 µm.

Polydom Deficient Mice Show the Defect in Lymphatic and Venous Vascular Formation in Some Tissues

The edema observed in *Polydom*$^{-/-}$ embryos suggested a dysfunction of the cardiovascular or lymphatic system. To clarify whether the edema was caused from the failure of vascular development, I performed immunofluorescence staining of *Polydom*$^{-/-}$ embryos. In the wild-type intercostal region, one nerve bundle and three vessels (an artery, a lymphatic vessel and a vein) were arranged in order next to each bone (Figure 20A). In *Polydom*$^{-/-}$ embryos, however, there was only one vessel remained next to each bone (Figure 20B). Arterial and venous marker staining revealed that the remaining vessels were ephrin-B2^{+}EphB4^{-} arteries, suggesting that lymphatic vessels and veins were absent in *Polydom*$^{-/-}$ intercostal region (Figure 20C–F).

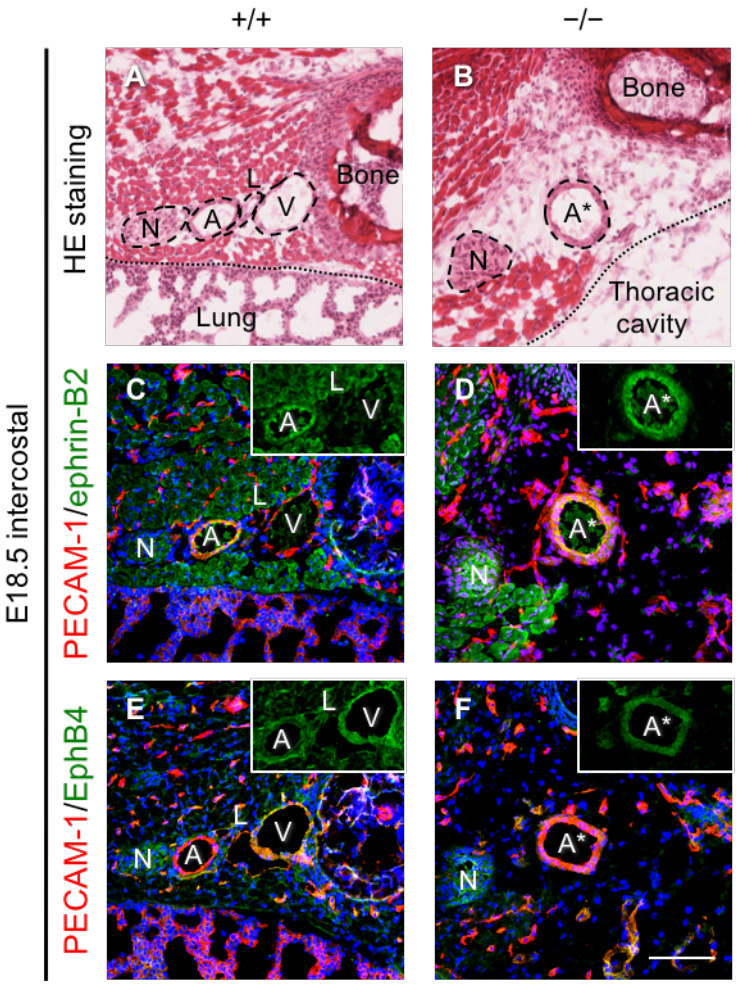

Figure 20. Arterio-venos characterization of intercostal vessels in wild-type and *Polydom*$^{-/-}$ embryos. (**A**, **B**) H&E staining in cross-sections of the intercostal region of wild-type (+/+) (**A**) and *Polydom*$^{-/-}$ embryos (**B**) at E18.5. (**C**–**F**) Immunofluorescence staining of serial sections for ephrin-B2 as arterial marker (green in **C** and **D**) and EphB4 as venous marker (green in **E** and **F**) with PECMA-1 (red) in wild-type (+/+) (**C**, **E**) and *Polydom*$^{-/-}$ embryos (**D**, **F**) at E18.5. Nuclei were stained with Hoechst 33342 (blue). Insets show green channel only of vascular area. A, artery; A*, artery-like vessel; L, lymphatic vessel; N, nerve; V, vein. Bar, 100 μm.

I further characterized the vessels using basement membrane and SMC markers. *Polydom*$^{-/-}$ intercostal vessels were covered with thick layer of SMCs similar to wild-type arteries (Figure 21C, D). In wild-type, laminin α4 was expressed around both arteries and veins, whereas laminin α5 was expressed around arteries (Figure 21E**,** G). In *Polydom*$^{-/-}$ mice, laminin α4 expression was comparable to that in wild-type blood vessels, but laminin α5 expression was weaker than that in wild-type arteries (Figure 21E–H). These results suggest that the intercostal vessels are impaired in *Polydom*$^{-/-}$ embryos and develop only artery-like vessels. I also examined various organs, and found that some organs such as skin lacked vein-like structures, but other organs, such as heart and mesentery, showed normal development of artery and vein (Figure 22).

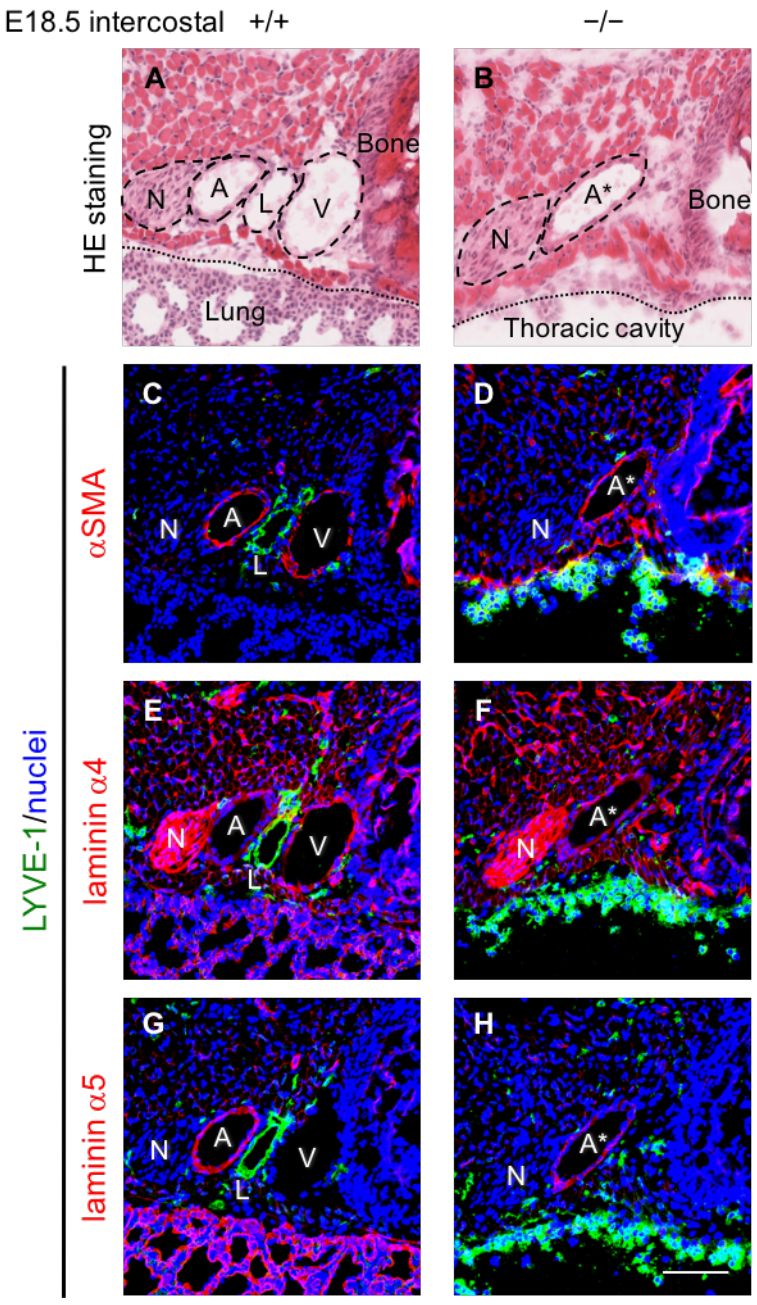

Figure 21. Laminins and αSMA expressions in wild-type and *Polydom*$^{-/-}$ intercostal vessels. (**A**, **B**) H&E staining in cross-sections of intercostal region of wild-type (+/+) (**A**) and *Polydom*$^{-/-}$ embryos (**B**) at E18.5. (**C**–**H**) Immunofluorescence staining of serial sections for αSMA (red in **C** and **D**), laminin α4 (red in **E** and **F**), and laminin α5 (red in **G** and **H**), with LYVE-1 (green) in wild-type (+/+) (**C**, **E** and **G**) and *Polydom*$^{-/-}$ embryos (**D**, **F** and **H**) at E18.5. Nuclei were stained with Hoechst 33342 (blue). A, artery; A*, artery-like vessel; L, lymphatic vessel; N, nerve; V, vein. Bar, 100 μm.

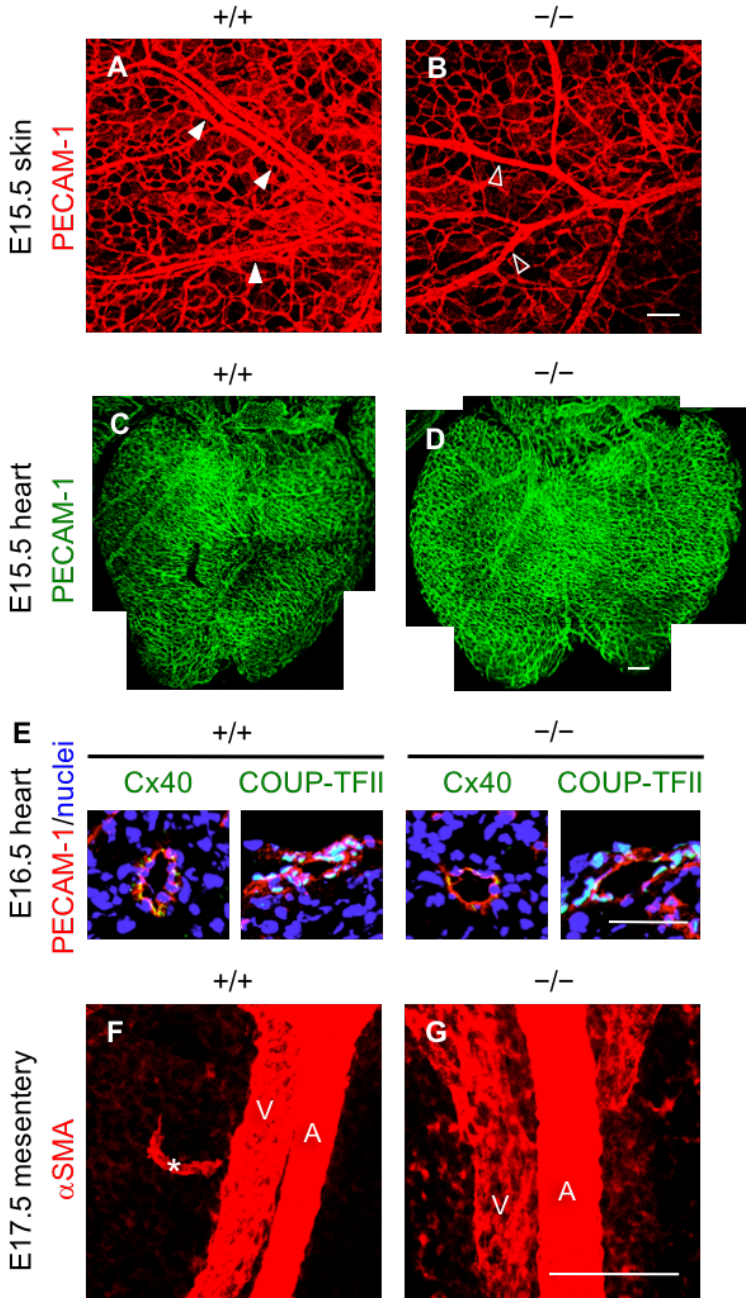

Figure 22. Vascular development is not significantly impaired in *Polydom*$^{-/-}$ embryos. (**A**, **B**) Whole-mount immunofluorescence staining for PECAM-1 in the skin of E15.5 wild-type (+/+) or *Polydom*$^{-/-}$ embryos. Alignment of larger-diameter vessels in wild-type (+/+) skin (*closed arrowheads*) is not detected in the *Polydom*$^{-/-}$ skin (*open arrowheads*). Bar, 100 µm. (**C**, **D**) Whole-mount immunofluorescence staining for PECAM-1 in the heart of E15.5 wild-type (+/+) or *Polydom*$^{-/-}$ embryos. Bar, 100 µm. Data were obtained by Mr. Yuta Totani. (**E**) Immunofluorescence staining of E16.5 heart sections for Connexin 40 as an arterial marker (green in *left panels*) and COUP-TFII as a venous marker (green in *right panels*) with PECAM-1 (red). Nuclei were stained with Hoechst 33342 (blue). Note that differentiation of arteries and veins in the heart occurs comparably between wild-type and *Polydom*$^{-/-}$ embryos. Bar, 50 µm. Data were obtained by Mr. Yuta Totani. (**F**, **G**) Whole-mount immunofluorescence staining for αSMA in the mesentery of E17.5 wild-type (+/+) or *Polydom*$^{-/-}$ embryos. A, artery; V, vein; *asterisk*, pericyte recruitment on collecting lymphatic vessel. Bar, 100 µm.

Polydom Deficient Mice Exhibit Aberrant Lymphatic Vessel Formation and Dysfunction of Fluid Drainage

Next, I examined the defects in lymphatic development in detail. No apparent defects were observed for Prox1^{+} pTD formation at E12.5 (Figure 23), which suggests that the specification of LECs and the formation of the first lymphatic structures were not affected by disruption of *Polydom*.

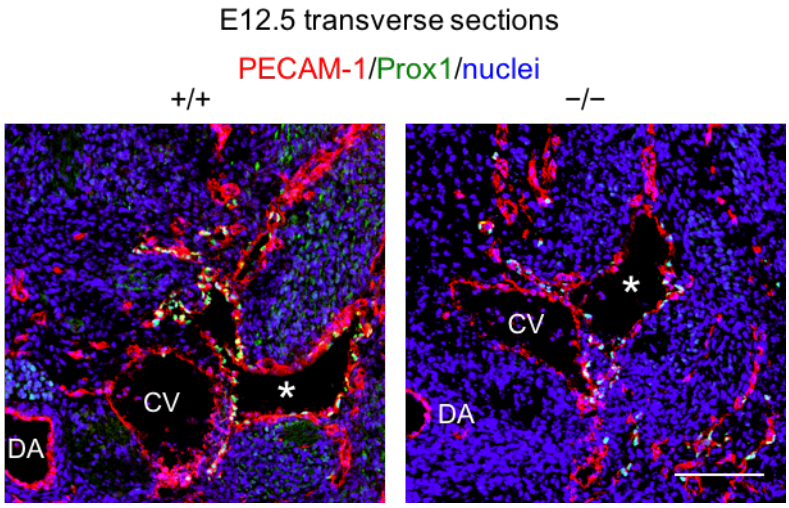

Figure 23. LEC specification and pTD formation are not impaired in *Polydom*$^{-/-}$ embryos. Immunofluorescence staining of transverse sections of the cervical region of E12.5 wild-type (+/+) or *Polydom*$^{-/-}$ embryos for PECAM-1 (red) and Prox1 (green). Nuclei were stained with Hoechst 33342 (blue). Prox1^{+} pTD (*asterisk*) was formed in all *Polydom*$^{-/-}$ embryos examined. CV, cardinal vein; DA, dorsal aorta. Bar, 100 μm.

Primitive lymphatic plexus was formed in the *Polydom*$^{-/-}$ embryos at E15.5, but the vascular patterning was impaired (Figure 24A, B and I): VEGFR-3^{+} lymphatic vessels in the skin of mutant mice were heterogeneous in size and were bumpy, whereas skin of wild-type littermates showed uniformly sized lymphatic plexus. At E18.5, lymphatic vessels gave rise to secondary sprouts that invaded into upper dermal layers in wild-type (Figure 24E, J). In *Polydom*$^{-/-}$ mice, sprouting appeared to initiate, but LECs failed to elongate and yielded rounded bumps, which suggests that migration of LECs was impaired in *Polydom*$^{-/-}$ mice (Figure 24F, J).

In the mesentery, loss of polydom resulted in a failure of collecting lymphatic vessel formation. In wild-type, primitive lymphatic plexus was remodeled to form lymphatic trunks with luminal valves

that were detected as laminin $\alpha5^{+}$ structures (Figure 24C, G and K). However, the lymphatic vessels in *Polydom*$^{-/-}$ mice remained highly branched and did not develop luminal valves (Figure 24D, H and K).

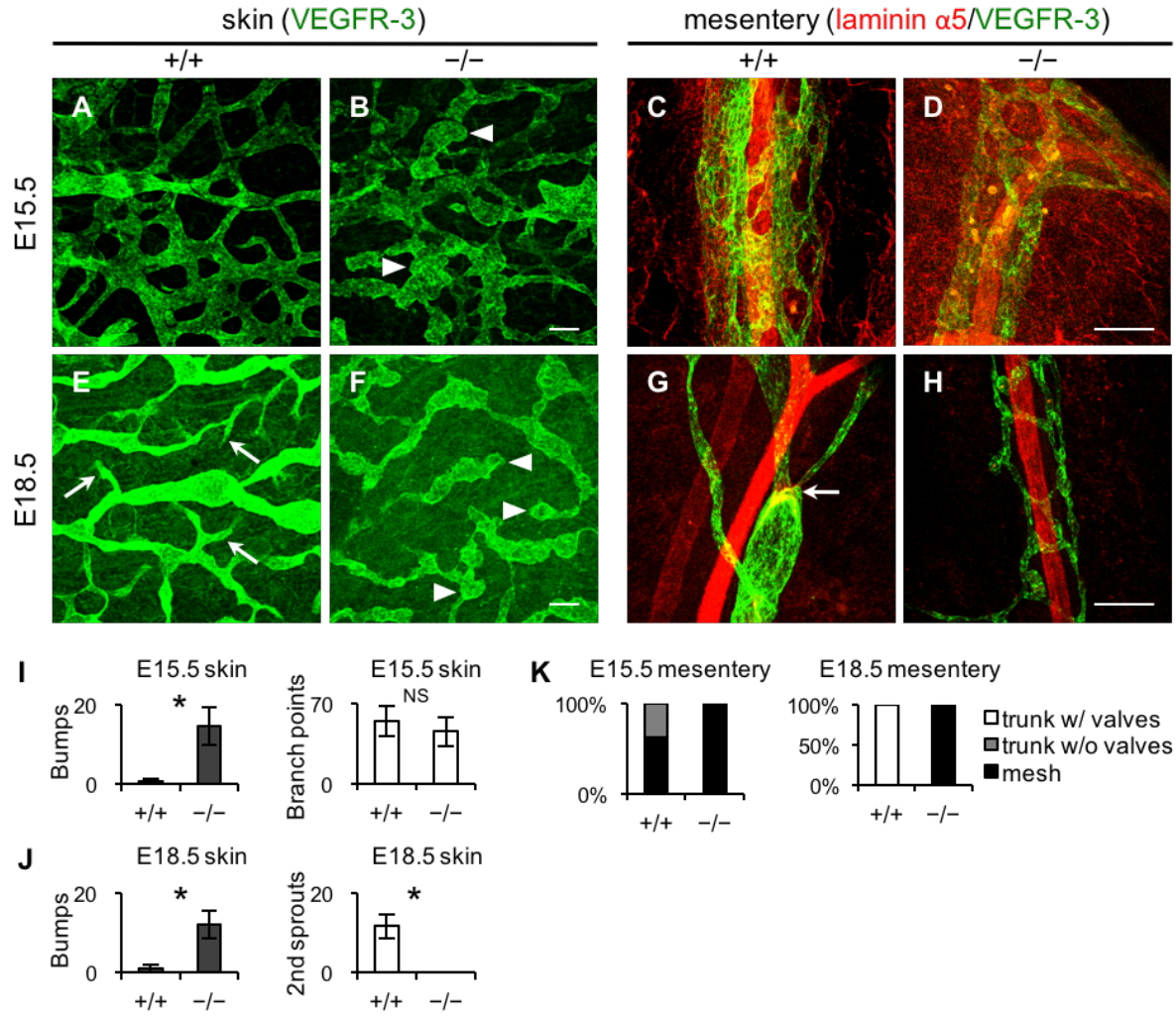

Figure 24. Aberrant lymphatic vessel formation in polydom-deficient skin and mesentery. (**A**–**H**) Whole-mount immunofluorescence staining for VEGFR-3 (green) and laminin α5 (red) in E15.5 and E18.5 *Polydom*$^{-/-}$ or wild-type (+/+) embryos. VEGFR-3^{+} lymphatic vessels show a meshwork with uniform-sized lumens in wild-type skin, but with uneven-sized lumens in *Polydom*$^{-/-}$ skin (*arrowheads* in **B** and **F**). Lymphatic sprouts at E18.5 (*arrows* in **E**) are only detected in the wild-type skin. Mesenteric lymphatic vessels at E15.5 in *Polydom*$^{-/-}$ mice are comparable to those in wild-type mice, but fail to form the lymphatic trunks and laminin $\alpha5^{+}$ lymphatic valves (*arrow* in **G**) at E18.5 (quantified in **K**). (**I**, **J**) Quantification of bumps and branch points in E15.5 skin (upper panels) and second sprouts and bumps in E18.5 skin (lower panel). Data are means ± SEM (*n*=5 embryos each for E15.5; *n*=4 embryos each for E18.5). The differences between wild-type (+/+) and homozygous (−/−) are statistically significant (**P*<0.001) except for the number of branch points in E15.5 skin (NS, not significant). Bars, 100 μm.

I also observed aberrant remodeling of lymphatic capillaries in the intestines and the hearts of *Polydom*$^{-/-}$ embryos. In the intestine, mesenteric lymphatic vessels are first organized into lymphatic plexus in the intestinal wall then sprout into villi to form lacteals (Kim et al., 2007). Similarly to the skin, lymphatic plexus emerged in the intestinal wall but lacteals could not migrate into the villi in *Polydom*$^{-/-}$ mice (Figure 25A, B and C). In heart, lymphatic vessels extended more than half of the region in wild-type (Figure 25D) (Klotz et al., 2015). On the other hand, in *Polydom*$^{-/-}$ mice, extra-cardiac LECs was found to migrate into the ventricular surface but the vessels failed to extend towards the apex of the heart (Figure 25E). These results indicated that polydom deficient mice have multiple defects in lymphatic vessel remodeling.

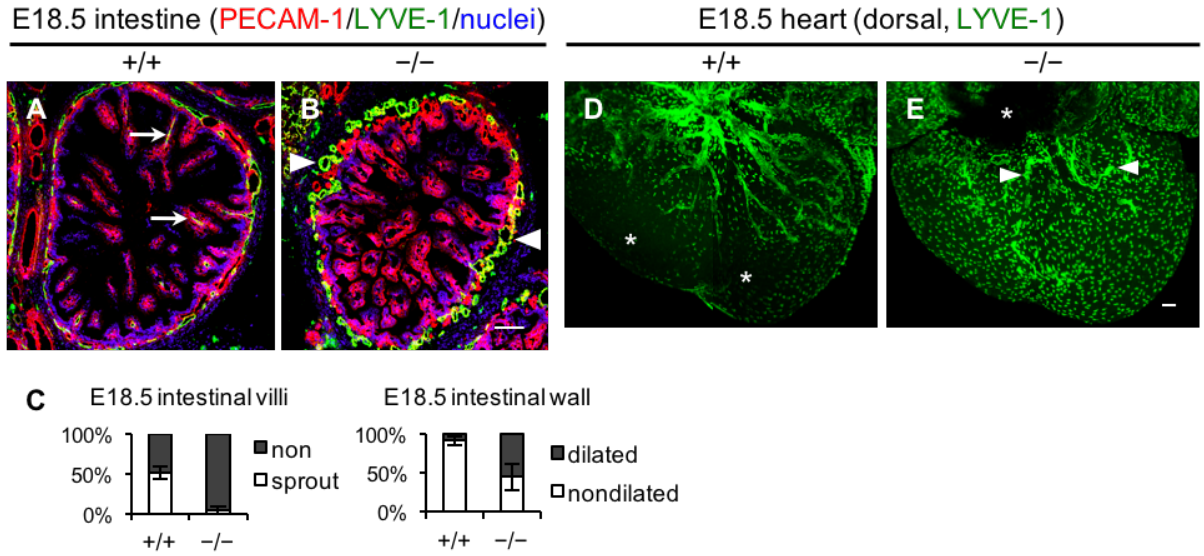

Figure 25. Aberrant lymphatic vessel formation in polydom-deficient intestine and heart. (**A**, **B**) Immunofluorescence staining for LYVE-1 (green) and PECAM-1 (red) in cross-sections of the intestine of wild-type (+/+) or *Polydom*$^{-/-}$ embryos at E18.5. Nuclei were stained with Hoechst 33342 (blue). *Arrowheads* in **B** indicate dilated lymphatic vessels. Central lacteals are absent from the villi in *Polydom*$^{-/-}$ mice, whereas lacteals extend to the tip of villus in wild-type mice (*arrows* in **A**). (**C**) Quantification of sprouts into villi and dilated lymphatic vessels in the intestine. Data are means ± SEM (wild-type (+/+), *n*=5 panels from 2 embryos; homozygous (−/−), *n*=6 panels from 3 embryos). The number of villi with lymphatic sprouts as well as that of nondilated lymphatic vessels around intestinal wall is significantly reduced in homozygous embryos (P<0.001). (**D**, **E**) Whole-mount immunofluorescence staining for LYVE-1 (green) in E18.5 hearts of wild-type (+/+) or *Polydom*$^{-/-}$ embryos. *Asterisks*, staining nonuniformity. LYVE-1^{+} coronary lymphatic vessels fail to extend toward the apex of the heart in all *Polydom*$^{-/-}$ mice examined (*arrowheads*). Bars, 100 μm.

To determine whether the morphological defects seen in lymphatic vessels lead to impaired lymphatic drainage, I assessed lymphatic function by intradermal injection of Indian ink. Ink uptake was not observed in *Polydom*$^{-/-}$ mice, indicative of the failure of the lymphatic flow (Figure 26). Consistent with the impaired lymphatic drainage, immunofluorescence staining of VE-cadherin showed that LECs in *Polydom*$^{-/-}$ embryos had cuboidal shapes and did not align longitudinally, whereas LECs in wild-type embryos elongated to the direction of lymphatic flow (Figure 27) (Sabine et al., 2012). These results indicated that polydom affects remodeling of lymphatic vessels, including sprouting of new capillaries and formation of collecting lymphatic vessels.

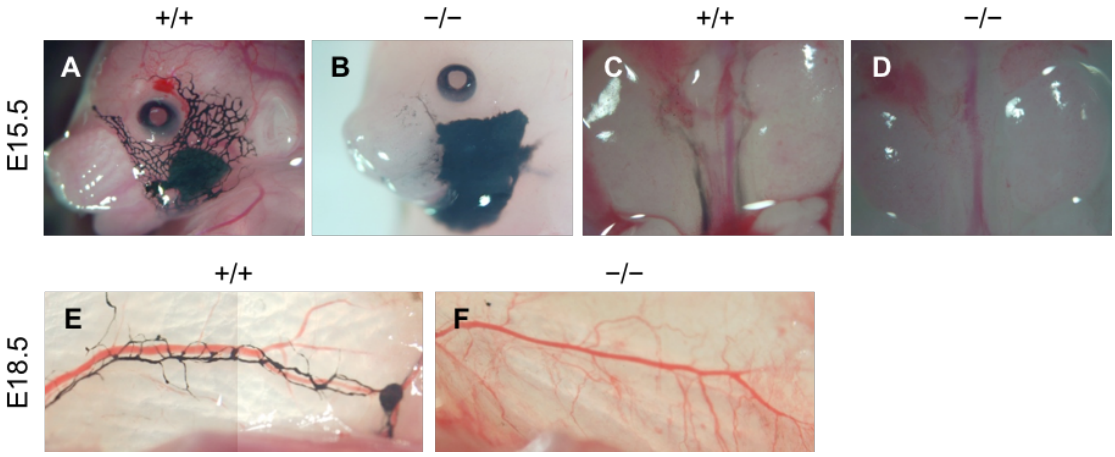

Figure 26. Dysfunction of fluid drainage in polydom-deficient mice. Lymphangiography was performed with Indian ink injected into the buccal region (**A**, **B**) or the hindlimb footpad (**C**–**F**) at E15.5 or E18.5. (**A**–**D**) The buccal lymphatic capillaries and retroperitoneal collecting lymphatic vessels are filled with ink in wild-type (+/+) embryos, but not in *Polydom*$^{-/-}$ embryos at E15.5. (**E**, **F**) The collecting lymphatic vessels and lymph nodes in ventral skin uptake ink in wild-type (+/+) embryos but not in *Polydom*$^{-/-}$ embryos at E18.5.

Figure 27. Aberrant LEC orientation in polydom-deficient mice. (**A**, **B**) Whole-mount immunofluorescence staining for Prox1 (red) and VE-cadherin (green) in the E18.5 mesentery. (**C**) Quantification of the cell alignment in E18.5 mesenteric lymphatic vessels. The rotation angle of Prox1^{+} cells relative to the longitudinal axis of the vessels was analyzed. Data are means ± SEM (wild-type (+/+), *n*=11 panels in 3 embryos; homozygous (−/−), *n*=13 panels in 3 embryos). **P*<0.001. Bars, 100 μm.

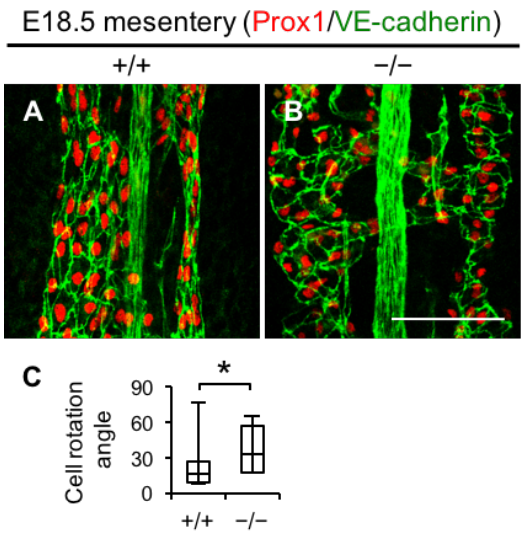

The Expression of Transcriptional Factor Foxc2 is Reduced in *polydom*$^{-/-}$ Mice

To explore the mechanism by which polydom depletion causes lymphatic defects, I compared expression of lymphatic markers in mesenteric lymphatic vessels between wild-type and *Polydom*$^{-/-}$ mice. Prox1, a master regulator of lymphatic development, was expressed uniformly in wild-type LECs at E16.5 (Figure 28A), and then downregulated at E18.5, except in the valve region, at a time when the primitive lymphatic plexus was remodeled into collecting vessels (Figure 28C). In *Polydom*$^{-/-}$ mice, Prox1 expression remained high in LECs at E18.5 (Figure 28B, D). Foxc2, which controls lymphatic vascular maturation, was widely expressed at E16.5 in wild-type mice, but thereafter restricted in the valve region (Figure 28E, G). However, Foxc2 expression was significantly lower in *Polydom*$^{-/-}$ mice at both E16.5 and E18.5 than in wild-type mice (Figure 28F, H). Quantification of Foxc2^{+} cells within the Prox1^{+} cell population showed that approximately 40% of Prox1^{+} cells were Foxc2^{+} in wild-type mice but less than 5% were Foxc2^{+} in *Polydom*$^{-/-}$ mice (Figure 28Q). LYVE-1 expression was high at E16.5 and then decreased at E18.5 in wild-type mice, whereas in *Polydom*$^{-/-}$ lymphatic vessels, it remained high at E18.5 (Figure 28I–L). No significant difference was detected in podoplanin expression between wild-type and *Polydom*$^{-/-}$ mice (Figure 28M–P). These results indicate that expression of Foxc2–but not other lymphatic markers–is reduced in *Polydom*$^{-/-}$ mice. To corroborate this observation, I examined expression of *Foxc2* transcripts in LECs isolated from *Polydom*$^{-/-}$ mouse skin, using RT-PCR. The results showed that Foxc2 expression was reduced by ~60% at E15.5 and ~80% at E18.5 in skin LECs from *Polydom*$^{-/-}$ embryos (Figure 28R), which confirms the involvement of polydom in regulating transcription of the Foxc2 gene.

Figure 28. Expression of lymphatic endothelial markers. Whole-mount immunofluorescence staining for Prox1 (**A**–**D**), Foxc2 (**E**–**H**), LYVE-1 (**I**–**L**), and Podoplanin (**M**–**P**) in *Polydom*$^{-/-}$ or wild-type (+/+) embryos at E16.5 and E18.5. Foxc2 expression is reduced in *Polydom*$^{-/-}$ mesenteric lymphatic vessels from E16.5 to E18.5 (*arrowheads* in **F** and **H**). *Asterisks* indicate arterial expression of Foxc2. Mesenteric lymphatic vessels fail to downregulate Prox1 and LYVE-1 expression at E18.5 in the absence of polydom (**D**, **L**). Bars, 100 μm. (**Q**) Numbers of Prox1^{+} cells and percentages of Foxc2^{+} cells within Prox1^{+} cells from whole-mount staining of the mesentery. Data are means ± SEM (*n*=10 panels each for E16.5; *n*=13 panels each for E18.5). (**R**) Quantitative RT-PCR analysis for *Foxc2* expression in LECs isolated from the *Polydom*$^{-/-}$ or wild-type (+/+) skin. *Actb* was used as a control. Data shows the means ± SEM of three independent experiments. **P*<0.05; ***P*<0.001.

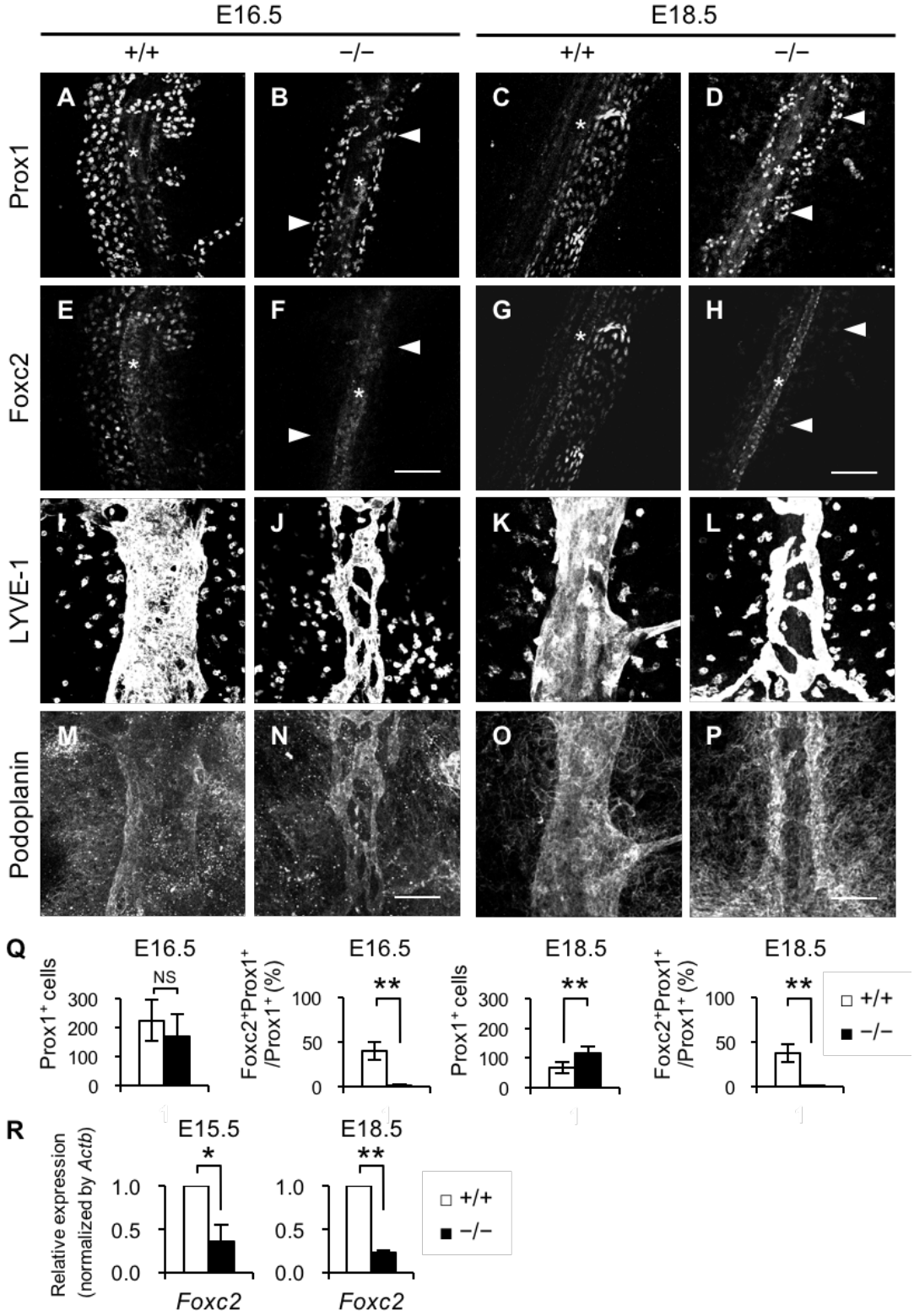
E16.5
E18.5
+/+
−/−
Prox1
Foxc2
LYVE-1
Podoplanin
A
B
C
D
E
F
G
H
I
J
K
L
M
N
O
P
Q
Prox1+ cells
NS
Foxc2+Prox1+ /Prox1+ (%)
**
R
Relative expression (normalized by Actb)
E15.5
*
Foxc2
□ +/+
■ −/−

Phenotypes in *Polydom*$^{-/-}$ Mice Resemble Those in *Foxc2*$^{-/-}$ Mice

Lymphatic defects in *Polydom*$^{-/-}$ embryos are considered to be caused by reduction of Foxc2. Therefore, I next compared the phenotype of *Polydom*$^{-/-}$ mice and that of *Foxc2*$^{-/-}$ mice (Norrmen et al., 2009; Petrova et al., 2004). Petrova et al. showed that all dermal lymphatic capillaries associated with αSMA^{+} periendothelial cells in *Foxc2*$^{-/-}$ mice, whereas normal lymphatic vessels lacked mural pericytes/SMCs (Petrova et al., 2004). Consistent with the observation, *Polydom*$^{-/-}$ mice showed recruitment of αSMA^{+} pericytes/SMCs to dermal lymphatic capillaries (Figure 29A), but the number of abnormal recruitment site was quite a few (less than five sites in whole backskin at E18.5). Pericytes/SMC recruitment to vascular vessels depends on the signaling through PDGF-B and PDGFR-β (Hellstrom et al., 1999; Lindahl, 1997). In *Foxc2*$^{-/-}$ embryonic skin, the percentage of *Pdgfb* positive lymphatic capillaries was significantly higher than that in wild-type (Petrova et al., 2004). On the contrary, *Pdgfb* expression was decreased in *Polydom*$^{-/-}$ skin LECs (Figure 29B), consistent with the infrequent pericytes/SMCs recruitment in *Polydom*$^{-/-}$ mice. The lymphatic capillaries in *Foxc2*$^{-/-}$ embryos were surrounded by a thick layer of the basement membrane protein type IV collagen (Petrova et al., 2004). Increased deposition of type IV collagen around the lymphatic capillaries was observed in *Polydom*$^{-/-}$ embryos, whereas deposition around collecting trunk was comparable between wild-type and *Polydom*$^{-/-}$ embryos (Figure 29C–J). *Ang2* expression in LECs is also induced in *Foxc2*$^{-/-}$ lymphatic LECs (Dellinger et al., 2008). In agreement with Foxc2 downregulation in *Polydom*$^{-/-}$ LECs, higher levels of *Ang2* expression was observed in *Polydom*$^{-/-}$ LECs (Figure 29B). Taken together, these results support the possibility that polydom regulates Foxc2 expression.

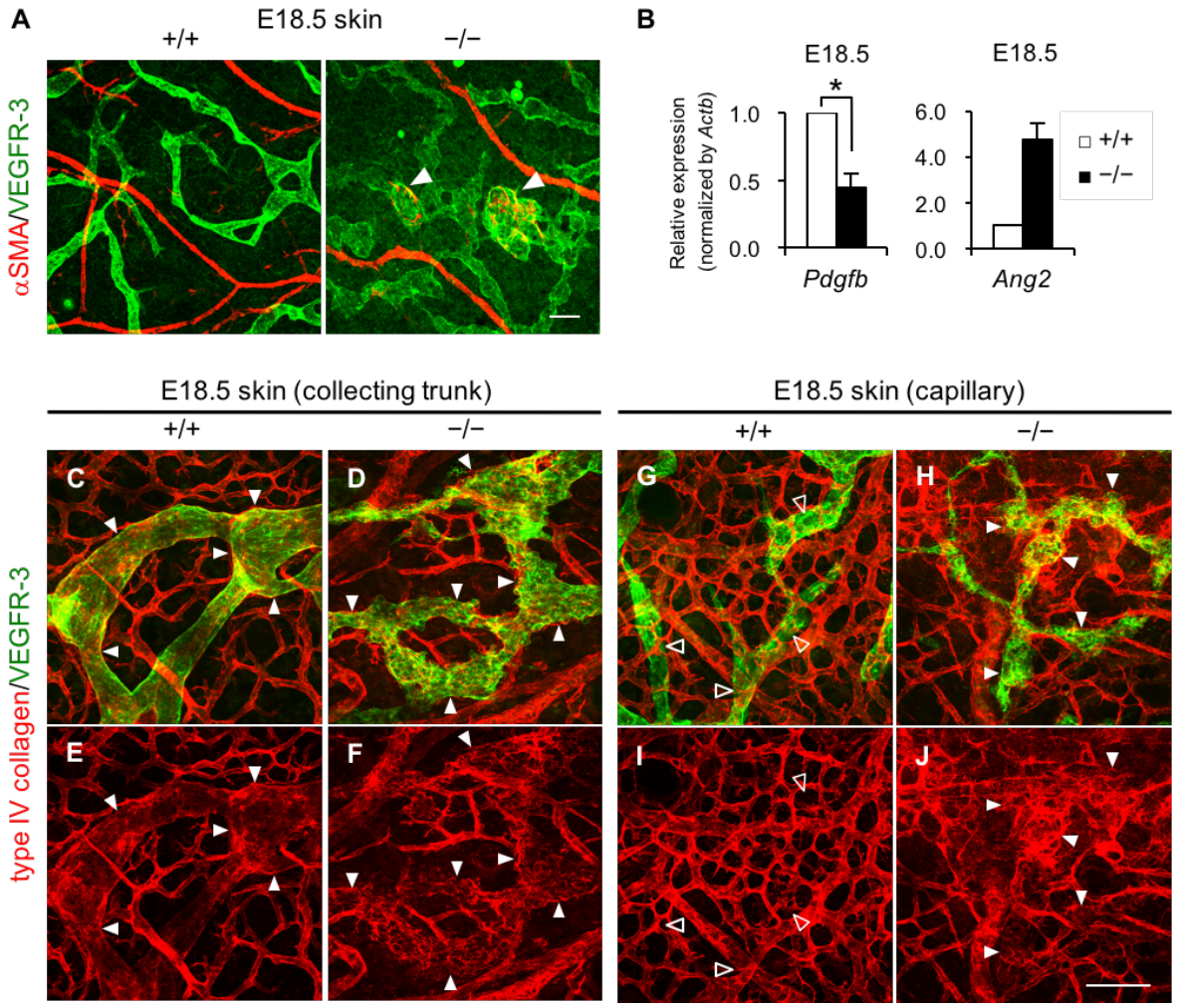

Figure 29. Abnormal pericyte recruitment and type IV collagen accumulation onto *Polydom*$^{-/-}$ lymphatic capillaries. (**A**) Whole-mount immunofluorescence staining for αSMA (red) and VEGFR-3 (green) in *Polydom*$^{-/-}$ or wild-type (+/+) skin at E18.5. Note that abnormal recruitment of pericytes/SMCs are detected in *Polydom*$^{-/-}$ lymphatic capillaries (*Solid arrowheads*). (**B**) Quantitative RT-PCR analysis for *PDGF-B* (*Pdgfb*) and *Ang-2* (*Ang2*) expression in LECs isolated from the *Polydom*$^{-/-}$ or wild-type (+/+) skin at E18.5. *Actb* was used as a control. Data shows the means ± SEM of three independent experiments. **P*<0.05. (**C**–**J**) Whole-mount immunofluorescence staining for type IV collagen (red) and VEGFR-3 (green) in *Polydom*$^{-/-}$ or wild-type (+/+) skin at E18.5. *Solid arrowheads* and *open arrowheads* indicate positive and negative staining for type IV collagen on lymphatic vessels, respectively. Bars, 100 μm.

Polydom–Integrin α9β1 Interaction Is Not Necessary for Lymphatic Vessel Remodeling

Loss-of-function studies suggest that polydom positively regulates Foxc2 expression in LECs. It remains to be elucidated how polydom upregulates Foxc2 expression in LECs. Because polydom is a high-affinity ligand for integrin α9β1 (Sato-Nishiuchi et al., 2012), I hypothesized that its interaction with integrin α9β1 may lead to upregulation of Foxc2 expression. First, I examined the localization of polydom and integrin α9β1 in wild-type mice. In mesenteric collecting lymphatic vessels, integrin α9β1 was strongly expressed in luminal valves and co-localized with polydom, whereas its expression in lymphangion was weak (Figure 30).

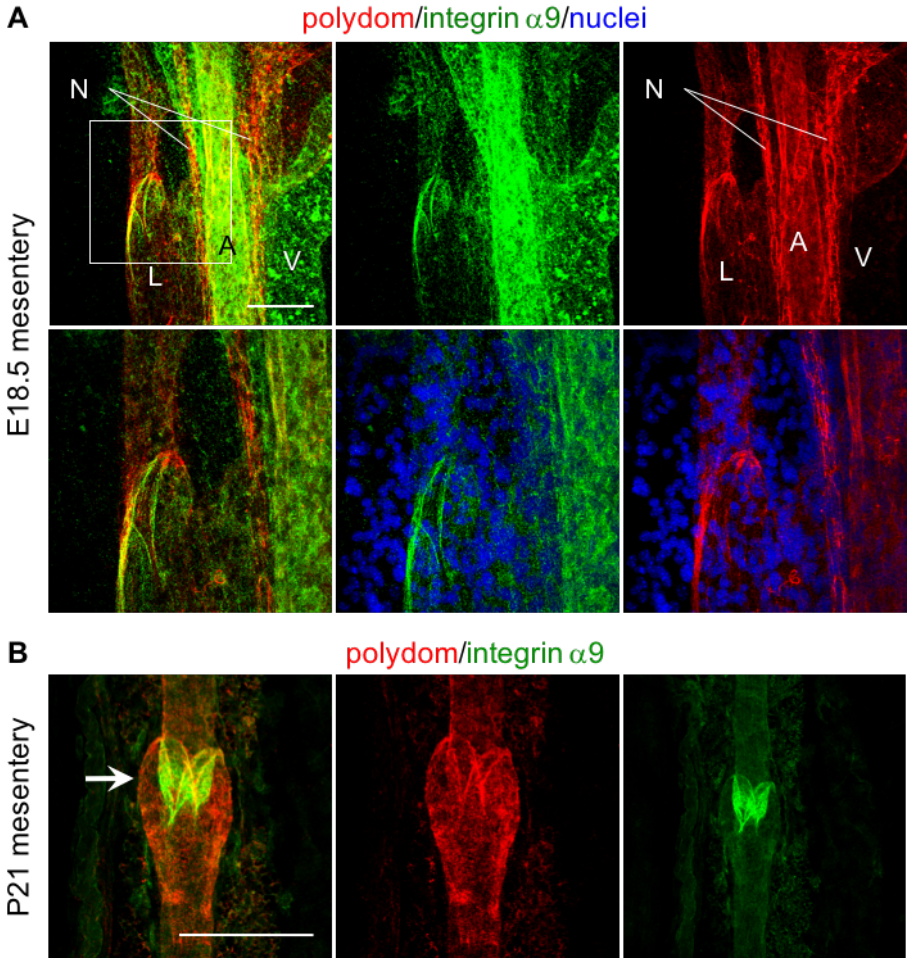

Figure 30. Polydom is colocalized with integrin α9 at luminal valves. Whole-mount immunofluorescence staining for polydom (red) and integrin α9 (green) in wild-type mesentery at E18.5 (**A**) and P21 (**B**). Nuclei were stained with Hoechst 33342 (blue). Boxed area in **A** is enlarged on the *bottom* panels. A, artery; L, lymphatic vessel; N, nerve; V, vein. Bar, 100 μm.

Next, I investigated morphology of lymphatic vessels in *Itga9*$^{-/-}$ mice (previously generated in our laboratory, see Materials and Methods). In agreement with previous studies (Bazigou et al., 2009; Danussi et al., 2013), the tortuous structure of the lymphatic plexus in the skin as well as the remodeling defects were not found in *Itga9*$^{-/-}$ mice (Figure 31), even though the delay of the mesh-like structure formation was detected in E15.5 mesentery.

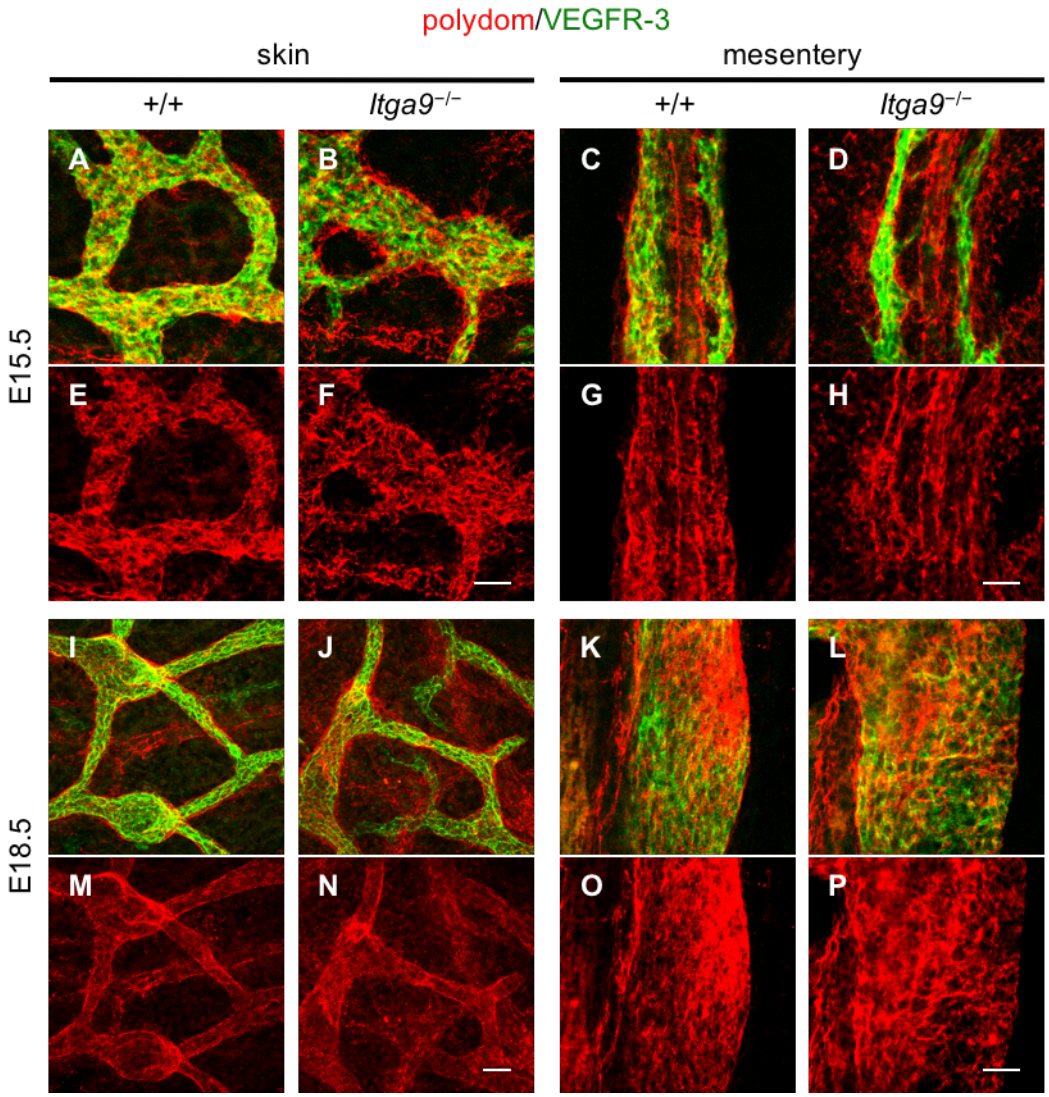

Figure 31. Collecting vessel formation and polydom expression in *Itga9*$^{-/-}$ embryos. Whole-mount immunofluorescence staining for polydom (red) and VEGFR-3 (green) in *Itga9*$^{-/-}$ or wild-type (+/+) skin and mesentery at E15.5 and E18.5. Bars, 50 μm.

In addition, the expression of Foxc2 in *Itga9*$^{-/-}$ mesenteric lymphatic vessels was comparable to that in wild-type (Figure 32), which suggests that integrin α9β1 is not necessary for Foxc2 upregulation. Furthermore, polydom distribution on lymphatic vessels in *Itga9*$^{-/-}$ mice was comparable to that in wild-type (Figure 33), which implies that integrin α9β1 is not involved in deposition of polydom on lymphatic vessels. These results led us to conclude that the interaction between polydom and integrin α9β1 is not necessary for Foxc2 mediated lymphatic vessel remodeling. Notably, however, polydom may contribute to lymphatic valve formation in mice as an integrin α9β1 ligand. Depletion of polydom after E15.5 did not compromise formation of collecting lymphatic vessels, but did result in failure of luminal valve formation (Figure 33).

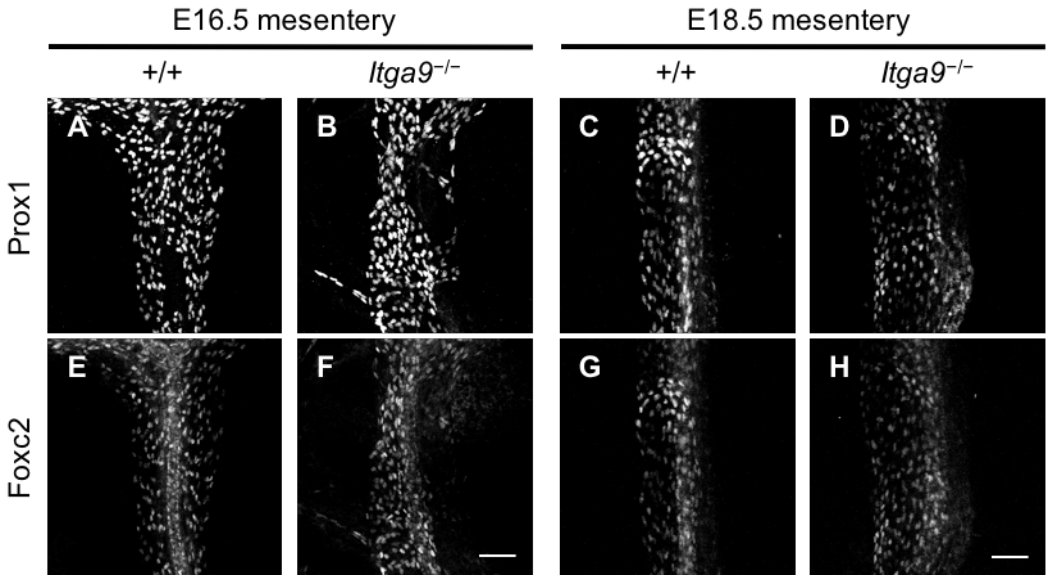

Figure 32. Foxc2 Expression is comparable between wild-type and *Itga9*$^{-/-}$ embryos. Whole-mount immunofluorescence staining for Prox1 (**A**–**D**) and Foxc2 (**E**–**H**) in *Itga9*$^{-/-}$ or wild-type (+/+) mesentery at E16.5 and E18.5. Bars, 100 μm.

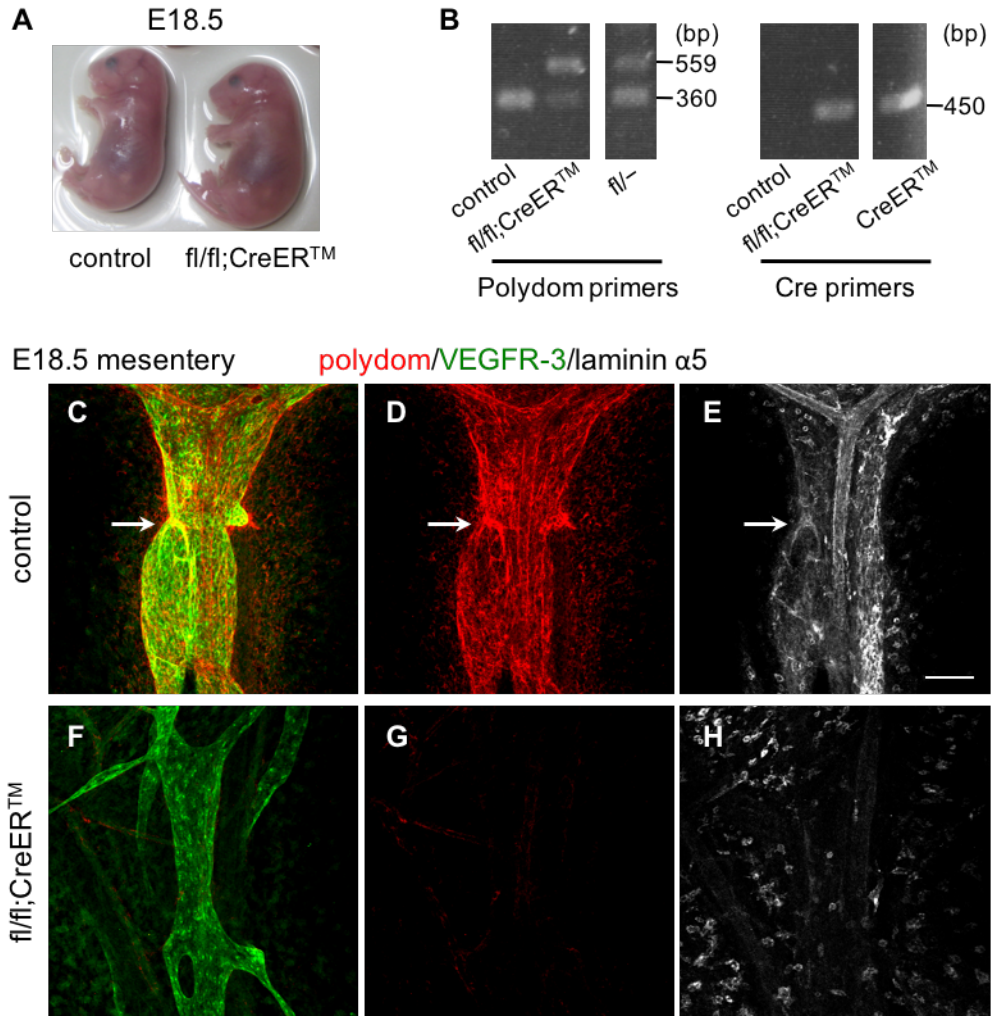

Figure 33. Deletion of *Polydom* after E15.5 rescues collecting vessel formation, but causes a defect in valve formation. (**A**) Lateral views of E18.5 *Polydom*$^{fl/fl}$ (control) and *Polydom*$^{fl/fl}$;CreER^{TM} (fl/fl;CreER^{TM}) embryos exposed to TM at E15.5. Note that TM-induced *Polydom* deletion causes mild edema. (**B**) PCR genotyping with polydom primers (F1, F2, and R1; *left*) and Cre primers (Cre-F and Cre-R; *right*). (**C**) Whole-mount immunofluorescence staining for polydom (red), VEGFR-3 (green), and laminin α5 (white) in the mesentery of E18.5 *Polydom*$^{fl/fl}$ (control) and *Polydom*$^{fl/fl}$;CreER^{TM} (fl/fl;CreER^{TM}) embryos exposed to TM at E15.5. *Arrows* indicate laminin α5^{+} lymphatic valves. Bar, 100 μm.

Ang-2 Binds to Polydom and Potentiates Foxc2 Expression in LECs

Next, I investigated the interactions of polydom with a panel of growth factors involved in lymphatic development, including VEGF-C and Ang-2, using solid-phase binding assays. Recombinant integrin α9β1 and type I collagen were used as positive and negative controls, respectively, in the assays. Polydom did not show any significant binding to VEGF-C, but was capable

of binding to Ang-1 and Ang-2 (Figure 34). When human dermal lymphatic endothelial cells (HDLECs) were cultured in the presence of Ang-1 or Ang-2, only Ang-2 enhanced FOXC2 expression in HDLECs (Figure 35), which suggests that polydom exerts its effect on Foxc2 expression through interaction with Ang-2.

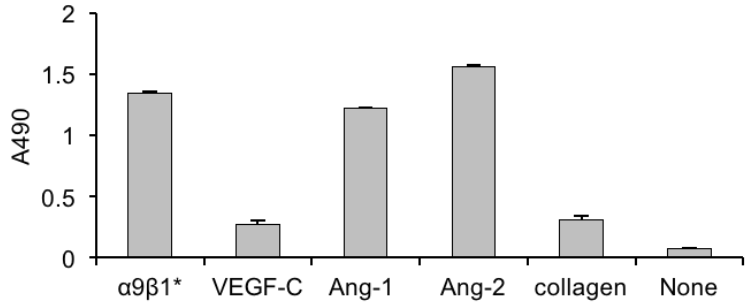

Figure 34. Polydom binds to Ang-1 and Ang-2. (**A**) Binding of polydom to lymphangiogenic growth factors was assessed by solid-phase binding assays. Integrin α9β1 (in the presence of 1 mmol/L $MnCl_2$, *asterisk*) and type I collagen was used as a positive and negative control, respectively. Data are means ± SEM of triplicate determinations. Representative data of three independent experiments are shown. Data were obtained by Dr. Ryoko Sato-Nishiuchi.

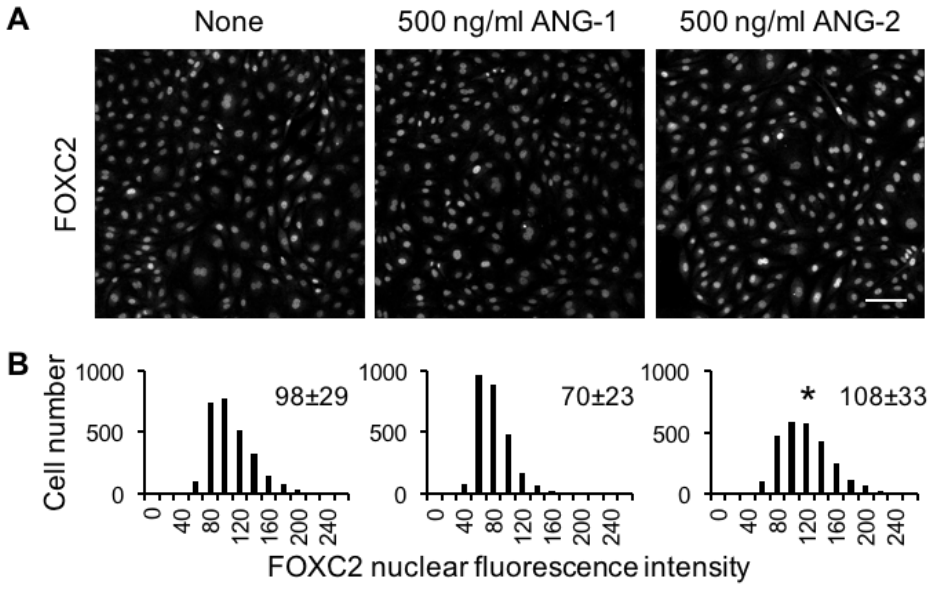

Figure 35. ANG-2 potentiates FOXC2 expression in LECs. (**A**) Immunofluorescence staining of FOXC2 in HDLECs. HDLECs were cultured with or without ANG-1 and ANG-2 (500 ng/ml) for 12 h after 1 h of starvation, and then stained with an anti-FOXC2 antibody. Bar, 100 μm. (**B**) Quantification of fluorescence intensity of nuclear FOXC2. Numbers in the graphs are means ± SEM. **P*<0.05 versus untreated control.

Tie Receptor Expression Is Decreased in *polydom*$^{-/-}$ Mice

Ang-2 has been shown to act as an agonist/antagonist for Tie receptors in a context-dependent manner (Thurston and Daly, 2012). To investigate whether Polydom affects the expressions of Tie1 and Tie2 receptors, I compared expression of *Tie1* and *Tie2* transcripts in dermal LECs from wild-type and *Polydom*$^{-/-}$ mice by quantitative RT-PCR. Transcripts for both *Tie1* and *Tie2* were significantly reduced in *Polydom*$^{-/-}$ mice (Figure 36A). Consistent with the results, immunofluorescence of Tie1 was reduced in *Polydom*$^{-/-}$ lymphatic vessels (Figure 36B, C). Tie2 immunofluorescence was also decreased (although to a lesser extent) in *Polydom*$^{-/-}$ mice. These results suggest that signaling events downstream of Tie receptors are compromised in *Polydom*$^{-/-}$ mice due to reduced Tie1/Tie2 expression.

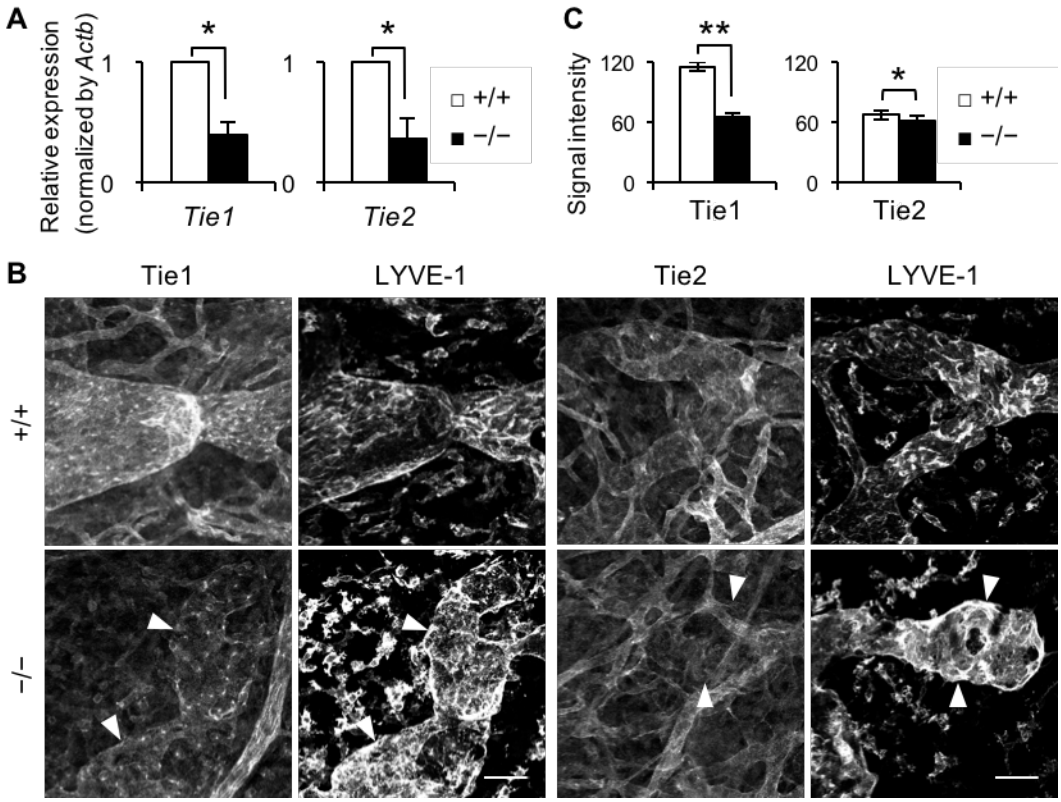

Figure 36. Expression of Tie receptors is reduced in polydom-deficient mice. (**A**) Quantitative RT-PCR analysis of *Tie1* and *Tie2* expression in LECs isolated from the *Polydom*$^{-/-}$ or wild-type (+/+) skin at E18.5. *Actb* was used as a control. Data represents means ± SEM of three independent experiments. **P*<0.05. (**B**) Whole-mount immunofluorescence staining for Tie1 and Tie2 with LYVE-1 in *Polydom*$^{-/-}$ or wild-type (+/+) embryos at E16.5. Expression of Tie1 and Tie2 is significantly less in *Polydom*$^{-/-}$ dermal lymphatic vessels (*arrowheads* in **B**; quantified in **C**). Bars, 50 μm. (**C**) Quantification of immunofluorescence signal intensity for Tie1 and Tie2 in *Polydom*$^{-/-}$ or wild-type (+/+) embryos at E16.5. Data are means ± SEM (Tie1: wild-type (+/+), *n*=4 panels; homozygous (−/−), *n*=5 panels. Tie2: wild-type (+/+), *n*=3 panels; homozygous (−/−), *n*=3 panels). **P*<0.05; ***P*<0.001.

Discussion

The lymphatic vasculature develops through a series of events including formation of lymph sacs, sprouting of lymphatic vessels, and remodeling and maturation of the primitive lymphatic plexus. These events are regulated by factors secreted by either mesodermal/mesenchymal cells or LECs, including VEGF-C (Karkkainen et al., 2004), CCBE1 (Bos et al., 2011; Hagerling et al., 2013; Hogan et al., 2009), FN-EIIIA (Bazigou et al., 2009), and EMILIN1 (Danussi et al., 2008). Here, I provide evidence that polydom, an ECM protein that acts as a high-affinity ligand for integrin α9β1 (Sato-Nishiuchi et al., 2012), is involved in lymphatic development, particularly in the remodeling and maturation process. Polydom-deficient mice developed severe edema and died immediately after birth because of respiratory failure. The primitive lymphatic plexus failed to remodel into collecting lymphatic vessels with luminal valves in *Polydom*$^{-/-}$ mice.

Polydom Upregulates Remodeling Factor Foxc2

Our results showed that the expression of Foxc2 was significantly reduced in *Polydom*$^{-/-}$ mice. The involvement of Foxc2 in lymphatic remodeling has been demonstrated by Petrova et al. (Norrmen et al., 2009; Petrova et al., 2004). Mouse embryos deficient in Foxc2 expression exhibit irregular lymphatic vasculature patterning and a failure to form the collecting trunk, both of which are phenotypic features reminiscent to those of *Polydom*$^{-/-}$ embryos. In lymphatic vascular development, upregulation of Foxc2 precedes the morphological changes and is followed by downregulation of Prox1 and LYVE-1 expression. The lymphatic vessels in *Polydom*$^{-/-}$ embryos failed to downregulate Prox1 and LYVE-1 expression, consistent with the phenotypes of Foxc2-deficient mice (Norrmen et al., 2009).

Furthermore, *Polydom*$^{-/-}$ mice showed increased recruitment of pericytes/SMCs in dermal lymphatic capillaries, similar to the case for *Foxc2*$^{-/-}$ mice (Norrmen et al., 2009; Petrova et al., 2004). *Pdgfb* expression is irregularly upregulated in *Foxc2*$^{-/-}$ dermal lymphatic capillaries (Petrova et al., 2004), which means Foxc2 is required for the establishment of the pericyte/SMC-free lymphatic capillary network through the suppression of *Pdgfb* expression in lymphatic vessels. Contrary to our

expectation, *Pdgfb* expression was decreased in isolated LECs from *Polydom*$^{-/-}$ skin. The reason for this might be that the isolated dermal LECs included both *Pdgfb*$^{+}$ collecting LECs and *Pdgfb*$^{-}$ capillary LECs, and the results were mainly affected by the failure of collecting lymphatic formation in *Polydom*$^{-/-}$ mice. It should also be noted that the number of irregular pericyte/SMC recruitment was less than five sites in *Polydom*$^{-/-}$ whole backskin, whereas all dermal lymphatic capillaries were associated with pericytes/SMCs in *Foxc2*$^{-/-}$ mice (Petrova et al., 2004). These results raise the possibility that expression of *Pdgfb* in *Polydom*$^{-/-}$ mice is increased lesser than that in *Foxc2*$^{-/-}$ mice. Foxc2 has been reported to downregulate type IV collagen expression in cultured LECs (Petrova et al., 2004); consistent with this, type IV collagen expression was increased in *Polydom*$^{-/-}$ skin capillaries similar to *Foxc2*$^{-/-}$ vessels. *Polydom*$^{-/-}$ mice also showed overexpression of *Ang2* in LECs, similar to the case for *Foxc2*$^{-/-}$ mice (Norrmen et al., 2009; Petrova et al., 2004). Taken together, these phenotypic similarities between *Polydom*$^{-/-}$ and *Foxc2*$^{-/-}$ mice suggest that the downregulation of Foxc2 is responsible for the lymphatic defects in *Polydom*$^{-/-}$ mice.

Polydom Regulates Foxc2 via Ang-2 Mediated Signaling

Polydom-Integrin α9β1 Interaction Is Not Necessary for Lymphatic Vessel Remodeling

Because polydom is a high-affinity ligand for integrin α9β1 (Sato-Nishiuchi et al., 2012), the interaction with integrin α9β1 may lead to the upregulation of Foxc2 expression. The involvement of integrin α9β1 in lymphatic development, particularly in lymphatic valve formation, has been documented (Bazigou et al., 2009). However, the phenotype of *Itga9*$^{-/-}$ mice is less severe than that of *Polydom*$^{-/-}$ mice, given that *Itga9*$^{-/-}$ mice survive for 6–12 days after birth (Huang et al., 2000) while *Polydom*$^{-/-}$ neonates die within 30 min. The tortuous structure of the lymphatic plexus in the skin as well as the remodeling defects observed in the mesenteric vessels in *Polydom*$^{-/-}$ mice were not found in *Itga9*$^{-/-}$ mice (Bazigou et al., 2009; Danussi et al., 2013). These discrepancies between the phenotypes of *Itga9*$^{-/-}$ and *Polydom*$^{-/-}$ mice raise the possibility that integrin α9β1 is not the putative polydom receptor responsible for the sprouting of new capillaries and formation of collecting lymphatic vessels. In agreement with the possibility, Foxc2 expression in *Itga9*$^{-/-}$ collecting trunk was

comparable to that in wild-type, which suggests that integrin α9 is not involved in the regulation of Foxc2 expression. Furthermore, polydom deposition around lymphatic vessels was not impaired in *Itga9*$^{-/-}$ mice, suggesting that integrin α9 is not necessary for deposition of polydom on lymphatic vessels.

It should be noted, however, that polydom may contribute to lymphatic valve formation in mice as an integrin α9β1 ligand, because depletion of polydom after E15.5 did not compromise the formation of collecting lymphatic vessels, but did result in failure of luminal valve formation. For lymphatic valve formation, the interaction between integrin α9 and FN-EIIIA has been suggested to play a role in the assembly of an ECM core within developing valve leaflets (Bazigou et al., 2009). However, Dannusi et al showed that the valves appear normal and functional in FN-EIIIA$^{-/-}$ mice (Danussi et al., 2013). It has been reported that EMILIN1, another ligand for integrin α9β1, plays a fundamental role in luminal valve formation and maintenance. In the absence of EMILIN1, mice exhibit defects in lymphatic valve structure and in lymph flow (Danussi et al., 2013). However, defects in *Itga9*$^{-/-}$ mice cannot fully be explained by the mere lack of EMILIN1–integrin α9β1 interaction because *Emilin1*$^{-/-}$ mice show only mild edema in contrast to the fatal bilateral chylothorax in *Itga9*$^{-/-}$ mice. Polydom is expressed in the valve region along with integrin α9 at least from mid-gestation to postnatal day 21, which implies that polydom compensates the absence of EMILIN1–integrin α9β1 engagement in *Emilin1*$^{-/-}$ mice.

Polydom Interacts with Ang-2 and Facilitates its Signaling

Accumulating evidence indicates that ECM proteins bind to growth factors, and thereby regulate their distribution, activation, and presentation to cognate receptors on cells (Hynes, 2009; Rozario and DeSimone, 2010). Although VEGF-C–VEGFR-3 signaling is a well-known pathway involved in lymphangiogenesis, our solid-phase binding assays failed to demonstrate any significant interaction between polydom and VEGF-C. We tried to express recombinant CCBE1 (Roukens et al., 2015) in human 293 cells but the yield of the recombinant protein was very low and we could not obtain enough amount of CCBE1 for solid-phase assays. Disruption of VEGF-C or VEGFR-3 causes early lymphatic defects in pTD formation as well as primitive plexus formation (Karkkainen et al., 2004;

Zhang et al., 2010). These results lead us to conclude that polydom does not contribute to the VEGF-C/VEGFR-3 pathway that is essential for early stage lymphangiogenesis.

Ang-2 is a lymphangiogenic factor involved in remodeling and maturation of the lymphatic vasculature (Dellinger et al., 2008; Gale et al., 2002; Zheng et al., 2014). Ang-2 deficiency leads to failure of lymphatic remodeling from a primitive plexus into collecting vessels as well as impaired recruitment of pericytes/SMCs to the lymphatic capirallies (Dellinger et al., 2008; Gale et al., 2002; Shimoda et al., 2007), being phenotypes reminiscent of *Foxc2*$^{-/-}$ and *Polydom*$^{-/-}$ mice. Our results showed that polydom bound to Ang-1 and Ang-2, but only Ang-2 could enhance Foxc2 expression in HDLECs, raising the possibility that polydom exerts its effect on Foxc2 expression in LECs by potentiating Ang-2. Consistent with this possibility, Dellinger et al. showed that *Ang2*$^{-/-}$; *Foxc2*$^{+/-}$ compound mutant mice die during embryonic and neonatal development despite the viability of individual *Ang2*$^{-/-}$ and *Foxc2*$^{+/-}$ mice (Dellinger et al., 2008), suggesting the genetic interaction between *Ang2* and *Foxc2*. Furthermore, inhibition of Ang-2 in mouse embryos by treatment with an Ang-2-blocking antibody led to downregulation of Foxc2 in lymphatic vessels (Zheng et al., 2014).

Angiopoietins regulate vascular development through interaction with Tie receptors (Augustin et al., 2009; Eklund et al., 2017). Several lines of evidence indicate that Tie1 is involved in lymphatic development: Tie1 deficiency in mice leads to edema (D'Amico et al., 2010; Sato et al., 1995), and remodeling defects in lymphatic vessels (Qu et al., 2010; Shen et al., 2014). Conditional deletion of *Tie1* with *Nfatc1Cre* leads to the defects in lymphatic valve formation and collecting vessel remodeling and is associated with lower *Foxc2* expression (Qu et al., 2015). Our results show that Tie1 expression is significantly reduced in *Polydom*$^{-/-}$ mice, which implies that the reduced Tie1 expression downregulates signaling events downstream of the Angiopoietin–Tie system, thereby resulting in reduced Foxc2 expression. This supposition is supported by the common phenotypical features—including severe edema and defects in lymphatic remodeling—seen in mice deficient in expression of polydom, Ang-2, Tie1, or Foxc2 (Dellinger et al., 2008; Gale et al., 2002; Norrmen et al., 2009; Petrova et al., 2004; Qu et al., 2010; Shen et al., 2014), although how polydom regulates Tie1 expression is not yet clear. Ang-2 was recently reported to induce Tie1 expression in tracheal blood vessels (Korhonen et al., 2016), which raises the possibility that polydom regulates Tie1 expression by

facilitating Ang-2 activity.

Schematic Model for Lymphatic Remodeling

Based on these findings, I propose a model for lymphatic vessel development in which polydom regulates lymphatic remodeling through upregulation of the transcription factor Foxc2 (Figure 37). Polydom is secreted by mesenchymal cells and becomes deposited around lymphatic vessels. Polydom binds to Ang-2 secreted by LECs, and thereby facilitates the interaction of Ang-2 with the receptor tyrosine kinases Tie1/Tie2 on LECs, leading to lymphatic remodeling to form the mature lymphatic vascular network through upregulation of Foxc2 expression. The mechanism by which polydom potentiates the interaction of Ang-2 with Tie1/Tie2 receptors and subsequent signaling events remains to be explored.

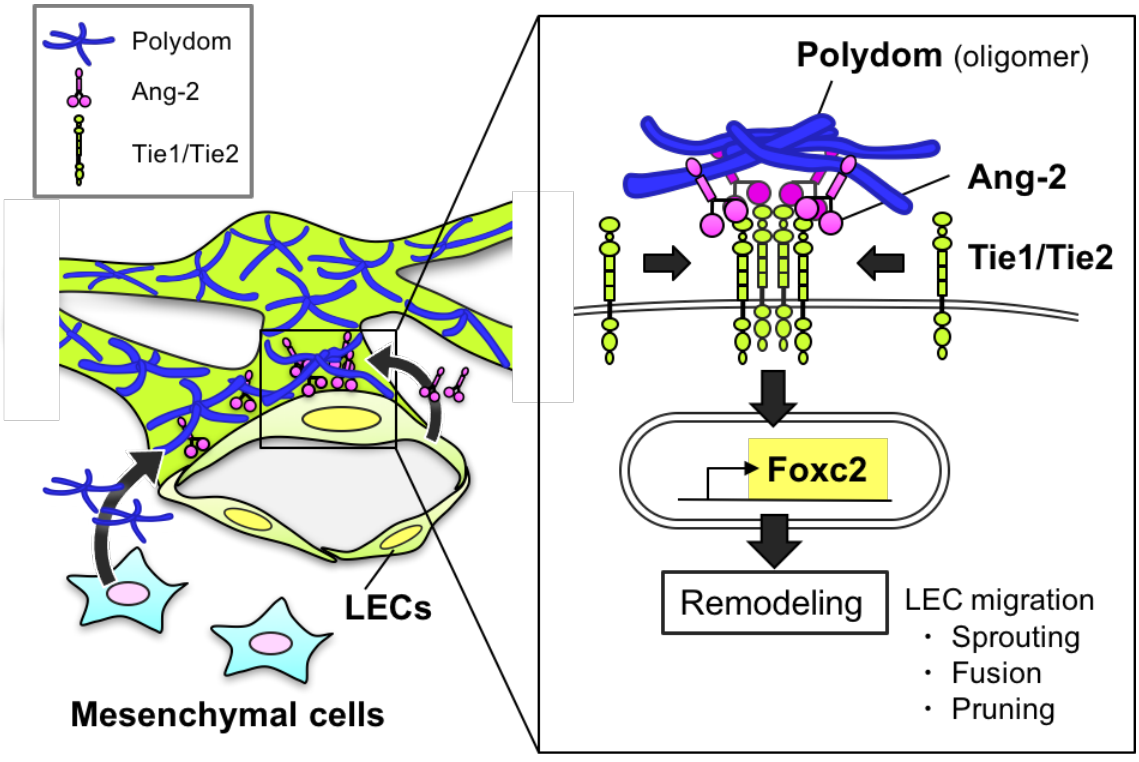

Figure 37. Schematic model of lymphatic remodeling. Polydom secreted from mesenchymal cells is deposited around lymphatic vessels in a fibrillar meshwork and tethers Ang-2 to present it to Tie1/Tie2 receptors in an oligomeric state, thereby potentiating signaling events downstream of Tie1/Tie2 receptors. Activation of Tie1/Tie2 receptors leads to upregulation of *Foxc2* transcription, which promotes sprouting of new capillaries and fusion or pruning of primitive lymphatic vessels.

1. Whether Polydom Induces Tie Receptor Activation or Not?

If polydom mediates signals into LECs through Tie1/Tie2, the receptors should be activated by polydom bound Ang-2. Activation of Tie2 requires receptor clustering facilitated by the multimeric Ang-1. Angiopoietin monomers are dimerized by its coiled-coil domain and further multimerized by N-terminal super-clustering domain. Tetramers are the minimal size required for activating endothelial Tie2 (Figure 38A, B) (Barton et al., 2014; Davis et al., 2003). Ang-2, on the other hand, is considered to act as an antagonist of Tie2. Ang-2 is not able to activate Tie2 in spite of having similar structures of C-terminal fibrinogen-like domain and similar Tie2 binding affinity compared to Ang-1 (Barton et al., 2005; Maisonpierre, 1997). Ang-2 mainly forms dimers, whereas Ang-1 forms variably sized multimers (Kim et al., 2005). Ang-2 permits Tie1/Tie2 heterodimerization and thereby inhibits Tie2 clustering (Figure 38C) (Seegar et al., 2010; Yu et al., 2013). However, Ang-2 antagonistic/agonistic activity is context dependent. Ang-2 agonistic activity has been reported in the lymphatic vessel, tumor vasculature, stressed endothelial cells that have reduced Ang-1–Tie2–Akt signaling, and endothelial cells in which Tie1–Tie2 interaction was disrupted (Figure 38D) (Daly et al., 2013; Daly et al., 2006; Gale et al., 2002; Kim et al., 2006; Seegar et al., 2010; Song et al., 2012; Yuan et al., 2009). Recently, Han et al. generated an Ang-2 antibody that can activate Tie2 by cross-linking Ang-2 dimers to form an Ang-2 multicomplex (Figure 38D) (Han et al., 2016). These findings suggest that Ang-2 can activate Tie2 possibly by changing the structure of ligand-receptor complex. Given that polydom readily produces oligomers (Sato-Nishiuchi et al., 2012), polydom may serve as a scaffold that binds Ang-2 and presents it to Tie2 receptors in an oligomeric state to induce downstream signaling events (Figure 38E).

Another possibility is that polydom induces Tie1 signaling mediated by Ang-2. However, little is known about Tie1 signaling because Tie1 does not associate with any of the angiopoietins (Ang-1 to Ang-4) or other proteins. Although Tie1 has been considered an orphan receptor, the results from Tie1 deficient mice suggest that Tie1 positively regulates lymphatic remodeling. Phenotypic similarities among *Polydom*$^{-/-}$mice, *Foxc2*$^{-/-}$ mice, and *Tie1* deficient mice let us consider that polydom could change Ang-2 conformation and facilitates its binding to Tie1 to induce signaling events downstream of Tie1 (Figure 38F).

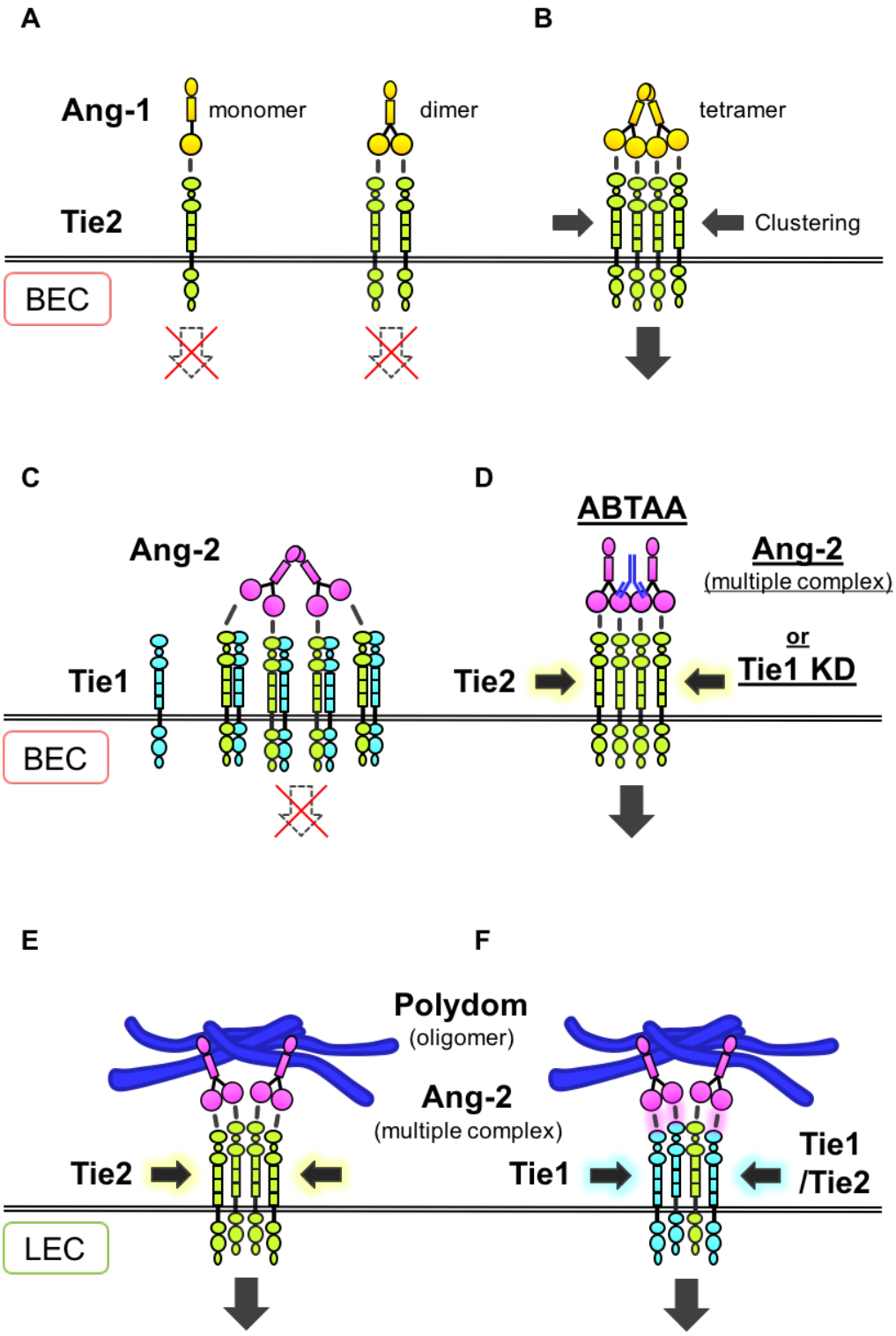

Figure 38. Schematic models of Tie receptor activation. (**A**) Monomeric and dimeric Ang-1 bind to Tie2 but cannot activate Tie2 receptors in blood endothelial cells (BECs). (**B**) Tetrameric Ang1 binds to and clusters Tie2, leading to its activation in BECs. (**C**) Ang-2 can bind to Tie2 in a same manner of Ang-1 but cannot induce clustering of Tie2 because it permits Tie1/Tie2 heterodimerization. (**D**) Ang-2 can activate Tie2 clustering with ABTAA, an antibody that facilitates Ang-2 multimer formation (Han et al., 2016), or by knock-down of Tie1 expression in BECs. (**E**) Upon binding to Ang-2, polydom may trigger Ang-2 clustering, resulting in clustering and activation of Tie2 in LECs. (**F**) Polydom may facilitate binding of Ang-2 to Tie1 and leads Tie1 activation.

2. How Does Polydom Regulate Tie Receptor Expression?

Reduction of Tie receptor expression in *Polydom*$^{-/-}$ mice suggests that polydom regulates the expression of Tie receptors. *Polydom*$^{-/-}$ mice showed reduction of *Tie1* and *Tie2* mRNA, indicating that polydom upregulates the expression of Tie receptors at the transcriptional level. It should be investigated whether Ang-2 is involved in this regulation. Recent study by Korhonen et al. demonstrated that overexpression of Ang-2 induces *Tie1* expression in mice (Korhonen et al., 2016). Consistent with this, my preliminary data showed that the expression of Tie1 protein was high in Ang-2 stimulated HDLECs compared to non-stimulated controls. Alternatively, polydom may contribute to stabilization of Tie receptors on cell surface. Tie1 is known to undergo ectodomain processing by membrane bound metalloproteinase in endothelial cells (Marron et al., 2007; Yabkowitz et al., 1999). In mouse lungs, Tie1 is rapidly cleaved within 30 minutes of LPS challenge, but Ang-1 pretreatment reduced LPS-induced Tie1 cleavage (Korhonen et al., 2016), which suggests that Ang-1 could prevent Tie1 from shedding. These results raise the possibility that the polydom–Ang-2 complex suppresses Tie receptor processing and stabilizes angiopoietin–Tie signaling.

3. What Is the Downstream Signaling Events of Tie Receptors?

Numerous studies have demonstrated that Tie2 stimulates PI3K pathway in endothelial cells in the presence of cell-cell contact (Fukuhara et al., 2008; Kim et al., 2000; Saharinen et al., 2008). In the absence of cell-cell contacts, Ang-1 promotes ERK and Dok2 activation (Fukuhara et al., 2008; Saharinen et al., 2008). The idea that polydom–Ang-2 complex regulates the Tie2 signaling in LECs should be tested. Recently, Chu et al. demonstrated that Tie2 is required for vein specification via regulating COUP-TFII (Chu et al., 2016). When *Tie2* is deleted in mice during embryogenesis, both venous and lymphatic vessel formation is disrupted (Chu et al., 2016) similar to *Polydom*$^{-/-}$ mice, suggesting that polydom might regulate venous specification through Tie2 signaling. In contrast to Tie2, Tie1 signaling has been elucidated yet due to the lack of known ligands. However, several reports showed that Tie1 has potential to be phosphorylated and/or mediates intracellular PI3K–Akt signaling (Kontos et al., 2002; Saharinen et al., 2005; Yuan et al., 2007). Alternatively, Tie1 might act through interacting with a non-angiopoietin ligand. Because activation of endogenous Tie receptors in endothelial cells is a complex process (presumably because of co-expression of co-receptors or

co-regulators), the involvement of the polydom–Ang-2 complex in Tie signaling needs to be investigated further using appropriate cells such as LECs.

Mechanism of Polydom Expression and Deposition

Despite the localized deposition of polydom on lymphatic vessels, our results showed that polydom was predominantly expressed in mesenchymal cells, but not in LECs. Imaging of the β-galactosidase activity in *Polydom-lacZ* reporter mice demonstrated that polydom-expressing cells were scattered in the dermis, residing beneath lymphatic vessels. The results indicate that the mesenchymal cells residing near the primitive lymphatic plexus express and secrete polydom, which is deposited on LECs to facilitate the remodeling of lymphatic vessels. In support of this possibility, significant polydom expression was detected in cells that express PDGFR-α and PDGFR-β. It is yet unclear how scattered mesenchymal cells deposit polydom on lymphatic vessels; polydom may be secreted into the extracellular fluid and diffuse toward lymphatic vessels, or mesenchymal cells attach to lymphatic vessels temporarily and deposit polydom, or mesenchymal cells extend protrusion towards LECs to secret polydom at the site. It should also be elucidated what is the cell surface molecule that connects polydom to LEC, as well as whether LECs and polydom-expressing mesenchymal cells affect each other.

LEC Migration in Lymphatic Vessel Remodeling

The remodeling of blood vessels in embryos proceeds in two steps, i.e., endothelial cell migration and subsequent fusion of neighboring vessels, resulting in a decrease in vascular complexity and an increase in vessel diameter (Korn and Augustin, 2015; Udan et al., 2013). Similar to blood vessel remodeling, LEC migration is considered to initiate the lymphatic vessel remodeling, followed by fusion or pruning of the vessels. Thus, the impaired remodeling in *Polydom*$^{-/-}$ mice may result from defects in LEC migration, ending in the incomplete fusion or pruning of lymphatic vessels, as typically observed in the mesenteric collecting trunk in *Polydom*$^{-/-}$ mice. Consistent with this scenario, new sprouts from the primitive lymphatic plexus were significantly reduced in the *Polydom*$^{-/-}$ skin and intestinal tube. The elongation of lymphatic capillaries was also impaired in the heart of *Polydom*$^{-/-}$

mice. These results obtained for polydom-deficient mice lend support for the possibility that polydom is involved in the migration of LECs through the upregulation of Foxc2, thereby facilitating the remodeling of the primitive lymphatic plexus into a hierarchical vascular tree.

ECM Function in Lymphatic Vascular Development

Comprehensive ECM analysis in embryonic skin showed that several ECM proteins other than polydom also associate with lymphatic vessels. Basement membrane proteins, such as laminin α4, β1, β2, γ1, type IV collagen, perlecan, nidgens, were expressed in lymphangion of collecting trunk, suggesting that heterotrimers of laminin 411 (α4β1γ1) and/or laminin 421 (α4β2γ1) are associated with LECs and thereby facilitate the assembly of other basement membrane proteins onto LEC surface. The same expression profile has been reported for human adult skin (Vainionpaa et al., 2007). On the other hand, laminin α5 and laminin β2 were prominently expressed in luminal valves, which indicates that laminin 521 (α5β2γ1) is mainly used as a substrate for endothelial cells of the valve leaflets. Laminin isoforms have been reported to be used properly in different tissues and developmental stages (Miner, 2008). In blood vessels, laminin α4 is ubiquitously expressed from the early stages of tube formation (Frieser et al., 1997), whereas laminin α5 appears postnatally when the vessel maturation occurs and its distribution varies with vessel type (Di Russo et al., 2017a; Sorokin et al., 1997; Yousif et al., 2013). Vascular SMCs express laminin β1 chain in developing vessels, but supplement laminin β2 chain in the mature vasculature (Glukhova et al., 1993). Our results suggest that LECs in lymphangion and LECs in luminal valves use different ECM components to constitute customized environments or niches for themselves.

Laminin α4-containing isoforms are considered to provide looser basement membrane compared with laminin α5-containing isoforms, because of the lack of N-terminal LN domain in α4 chain, which is involved in self-assembly of laminins. In addition, laminin 411 is less potent in integrin binding affinity and endothelial cell-adhesive activity than laminin 511/521 (Fujiwara et al., 2004; Nishiuchi et al., 2006). Furthermore, laminin α5 stabilizes VE-cadherin at cell-cell junction of arterial endothelial cells so that artery might have resistance to shear stress (Di Russo et al., 2017b). Laminin

α5 expression suggests that lymphatic valves need stronger cell-cell and cell-matrix interaction to resist continuous stimuli of lymph flow.

There are five types of laminin binding integrins, α3β1, α6β1, α6β4, α7X1β1, and α7X2β1. Among these, laminin α4-containing isoforms bind to α6β1 and α7X1β1 integrins, whereas laminin α5-containing isoforms bind to all of them (Nishiuchi et al., 2006). Several microarray analyses showed that LECs express some of these integrins (Hirakawa et al., 2003; Petrova et al., 2002; Podgrabinska et al., 2002); however, it is unknown whether LECs in lymphangion and in valve region use different types of integrins. Since α3β1 and/or α7X2β1 integrins show higher binding affinity to laminin 521 than laminin 511 (Taniguchi et al., 2009), endothelial cells of the valve leaflets is expected to use α3β1 and/or α7X2β1 integrins rather than α6β1, α6β4, α7X1β1 integrins. Further investigation on lymphatic ECMs and their receptors will provide insight into the mechanism of lymphatic valve formation and the homeostasis of lymphatic vessels.

Conclusion

There is accumulating evidence that extracellular factors secreted by mesenchymal cells play essential roles in lymphatic vascular development. VEGF-C and CCBE1, which are both secreted by mesodermal/mesenchymal cells, have been shown to act in the initial stage of lymphatic development, i.e., sprouting of lymphangioblasts from the venous endothelium (Bos et al., 2011; Hogan et al., 2009; Karkkainen et al., 2004). However, the roles of mesenchymal factors in lymphatic remodeling and maturation have been poorly understood. Our results showed, for the first time, that polydom is a mesenchymal factor involved in lymphatic remodeling. Although it remains to be elucidated how polydom facilitates the remodeling and maturation of the lymphatic vasculature, further investigations into the mechanisms by which polydom acts on the primitive lymphatic plexus to upregulate Foxc2 expression should provide insights into the interplay between LECs and the surrounding mesenchymal cells that ensures the development of the lymphatic vasculature and maintenance of the fluid homeostasis in the body.

Impairment of lymphatic transport capacity causes lymphedema, usually a progressive and lifelong condition for which curative treatments are not available at present. Fluid accumulation results in a persistent inflammatory response, leading to fibrosis, impaired immune responses. Lymphedema is classified into primary (congenital) lymphedema and secondary (acquired) lymphedema. The primary lymphedema caused by mutation in human *Polydom* (*SVEP1*) gene has not been reported yet (Aspelund et al., 2016), but further analysis of congenital lymphatic malformation should be needed. Secondary lymphedema, which is caused by filariasis or breast cancer surgery, is typically due to damage to the collecting vessels. The treatment of lymphedema is currently based on physiotherapy, compression garments, liposuction, and occasional surgery such as lymphaticovenular anastomosis and lymphatic vessel/lymph node transplantation (Alitalo, 2011; Tammela and Alitalo, 2010), but the reconstitution of functional collecting vessels with SMCs and vasa vasorum are rarely successful. The discovery of lymphatic remodeling factors and studies of their signaling pathways will provide new possibilities for the clinical treatment of lymphatic vasculature disease.

References

Abtahian, F., Guerriero, A., Sebzda, E., Lu, M. M., Zhou, R., Mocsai, A., Myers, E. E., Huang, B., Jackson, D. G., Ferrari, V. A., et al. (2003). Regulation of blood and lymphatic vascular separation by signaling proteins SLP-76 and Syk. *Science* **299**, 247-251.

Alberts, B. (2002). *Molecular biology of the cell* (4th edn). New York: Garland Science.

Alitalo, K. (2011). The lymphatic vasculature in disease. *Nature medicine* **17**, 1371-1380.

Alitalo, K., Tammela, T. and Petrova, T. V. (2005). Lymphangiogenesis in development and human disease. *Nature* **438**, 946-953.

Aspelund, A., Robciuc, M. R., Karaman, S., Makinen, T. and Alitalo, K. (2016). Lymphatic System in Cardiovascular Medicine. *Circulation research* **118**, 515-530.

Augustin, H. G., Koh, G. Y., Thurston, G. and Alitalo, K. (2009). Control of vascular morphogenesis and homeostasis through the angiopoietin-Tie system. *Nature reviews. Molecular cell biology* **10**, 165-177.

Baluk, P., Fuxe, J., Hashizume, H., Romano, T., Lashnits, E., Butz, S., Vestweber, D., Corada, M., Molendini, C., Dejana, E., et al. (2007). Functionally specialized junctions between endothelial cells of lymphatic vessels. *The Journal of experimental medicine* **204**, 2349-2362.

Barton, W. A., Dalton, A. C., Seegar, T. C., Himanen, J. P. and Nikolov, D. B. (2014). Tie2 and Eph receptor tyrosine kinase activation and signaling. *Cold Spring Harbor perspectives in biology* **6**.

Barton, W. A., Tzvetkova, D. and Nikolov, D. B. (2005). Structure of the angiopoietin-2 receptor binding domain and identification of surfaces involved in Tie2 recognition. *Structure* **13**, 825-832.

Bazigou, E., Xie, S., Chen, C., Weston, A., Miura, N., Sorokin, L., Adams, R., Muro, A. F., Sheppard, D. and Makinen, T. (2009). Integrin-alpha9 is required for fibronectin matrix assembly during lymphatic valve morphogenesis. *Developmental cell* **17**, 175-186.

Bertozzi, C. C., Schmaier, A. A., Mericko, P., Hess, P. R., Zou, Z., Chen, M., Chen, C. Y., Xu, B., Lu, M. M., Zhou, D., et al. (2010). Platelets regulate lymphatic vascular development through CLEC-2-SLP-76 signaling. *Blood* **116**, 661-670.

Bos, F. L., Caunt, M., Peterson-Maduro, J., Planas-Paz, L., Kowalski, J., Karpanen, T., van Impel, A., Tong, R., Ernst, J. A., Korving, J., et al. (2011). CCBE1 is essential for mammalian lymphatic vascular development and enhances the lymphangiogenic effect of vascular endothelial growth factor-C in vivo. *Circulation research* **109**, 486-491.

Bouvree, K., Brunet, I., Del Toro, R., Gordon, E., Prahst, C., Cristofaro, B., Mathivet, T., Xu, Y., Soueid, J., Fortuna, V., et al. (2012). Semaphorin3A, Neuropilin-1, and PlexinA1 are required for lymphatic valve formation. *Circulation research* **111**, 437-445.

Charbonneau, N. L., Dzamba, B. J., Ono, R. N., Keene, D. R., Corson, G. M., Reinhardt, D. P. and Sakai, L. Y. (2003). Fibrillins can co-assemble in fibrils, but fibrillin fibril composition displays cell-specific differences. *The Journal of biological chemistry* **278**, 2740-2749.

Chu, M., Li, T., Shen, B., Cao, X., Zhong, H., Zhang, L., Zhou, F., Ma, W., Jiang, H., Xie, P., et al. (2016). Angiopoietin receptor Tie2 is required for vein specification and maintenance via regulating COUP-TFII. *Elife* **5**.

Coso, S., Bovay, E. and Petrova, T. V. (2014). Pressing the right buttons: signaling in lymphangiogenesis. *Blood* **123**, 2614-2624.

D'Amico, G., Korhonen, E. A., Waltari, M., Saharinen, P., Laakkonen, P. and Alitalo, K. (2010). Loss of endothelial Tie1 receptor impairs lymphatic vessel development-brief report. *Arteriosclerosis, thrombosis, and vascular biology* **30**, 207-209.

Daly, C., Eichten, A., Castanaro, C., Pasnikowski, E., Adler, A., Lalani, A. S., Papadopoulos, N., Kyle, A. H., Minchinton, A. I., Yancopoulos, G. D., et al. (2013). Angiopoietin-2 functions as a Tie2 agonist in tumor models, where it limits the effects of VEGF inhibition. *Cancer research* **73**, 108-118.

Daly, C., Pasnikowski, E., Burova, E., Wong, V., Aldrich, T. H., Griffiths, J., Ioffe, E., Daly, T. J., Fandl, J. P., Papadopoulos, N., et al. (2006). Angiopoietin-2 functions as an autocrine

protective factor in stressed endothelial cells. *Proceedings of the National Academy of Sciences of the United States of America* **103**, 15491-15496.

Danussi, C., Del Bel Belluz, L., Pivetta, E., Modica, T. M., Muro, A., Wassermann, B., Doliana, R., Sabatelli, P., Colombatti, A. and Spessotto, P. (2013). EMILIN1/alpha9beta1 integrin interaction is crucial in lymphatic valve formation and maintenance. *Molecular and cellular biology* **33**, 4381-4394.

Danussi, C., Spessotto, P., Petrucco, A., Wassermann, B., Sabatelli, P., Montesi, M., Doliana, R., Bressan, G. M. and Colombatti, A. (2008). Emilin1 deficiency causes structural and functional defects of lymphatic vasculature. *Molecular and cellular biology* **28**, 4026-4039.

Davis, S., Papadopoulos, N., Aldrich, T. H., Maisonpierre, P. C., Huang, T., Kovac, L., Xu, A., Leidich, R., Radziejewska, E., Rafique, A., et al. (2003). Angiopoietins have distinct modular domains essential for receptor binding, dimerization and superclustering. *Nat Struct Biol* **10**, 38-44.

Dellinger, M., Hunter, R., Bernas, M., Gale, N., Yancopoulos, G., Erickson, R. and Witte, M. (2008). Defective remodeling and maturation of the lymphatic vasculature in Angiopoietin-2 deficient mice. *Developmental biology* **319**, 309-320.

Di Russo, J., Hannocks, M. J., Luik, A. L., Song, J., Zhang, X., Yousif, L., Aspite, G., Hallmann, R. and Sorokin, L. (2017a). Vascular laminins in physiology and pathology. *Matrix biology : journal of the International Society for Matrix Biology* **57-58**, 140-148.

Di Russo, J., Luik, A. L., Yousif, L., Budny, S., Oberleithner, H., Hofschroer, V., Klingauf, J., van Bavel, E., Bakker, E. N., Hellstrand, P., et al. (2017b). Endothelial basement membrane laminin 511 is essential for shear stress response. *The EMBO journal* **36**, 183-201.

Eklund, L., Kangas, J. and Saharinen, P. (2017). Angiopoietin-Tie signalling in the cardiovascular and lymphatic systems. *Clin Sci (Lond)* **131**, 87-103.

Forsberg, E., Hirsch, E., Frohlich, L., Meyer, M., Ekblom, P., Aszodi, A., Werner, S. and Fassler, R. (1996). Skin wounds and severed nerves heal normally in mice lacking tenascin-C. *Proceedings of the National Academy of Sciences of the United States of America* **93**, 6594-6599.

Francois, M., Caprini, A., Hosking, B., Orsenigo, F., Wilhelm, D., Browne, C., Paavonen, K., Karnezis, T., Shayan, R., Downes, M., et al. (2008). Sox18 induces development of the lymphatic vasculature in mice. *Nature* **456**, 643-647.

Frieser, M., Nockel, H., Pausch, F., Roder, C., Hahn, A., Deutzmann, R. and Sorokin, L. M. (1997). Cloning of the mouse laminin alpha 4 cDNA. Expression in a subset of endothelium. *European journal of biochemistry / FEBS* **246**, 727-735.

Fujiwara, H., Gu, J. and Sekiguchi, K. (2004). Rac regulates integrin-mediated endothelial cell adhesion and migration on laminin-8. *Experimental cell research* **292**, 67-77.

Fukamauchi, F., Mataga, N., Wang, Y. J., Sato, S., Youshiki, A. and Kusakabe, M. (1996). Abnormal behavior and neurotransmissions of tenascin gene knockout mouse. *Biochemical and biophysical research communications* **221**, 151-156.

Fukuhara, S., Sako, K., Minami, T., Noda, K., Kim, H. Z., Kodama, T., Shibuya, M., Takakura, N., Koh, G. Y. and Mochizuki, N. (2008). Differential function of Tie2 at cell-cell contacts and cell-substratum contacts regulated by angiopoietin-1. *Nature cell biology* **10**, 513-526.

Gale, N. W., Thurston, G., Hackett, S. F., Renard, R., Wang, Q., McClain, J., Martin, C., Witte, C., Witte, M. H., Jackson, D., et al. (2002). Angiopoietin-2 is required for postnatal angiogenesis and lymphatic patterning, and only the latter role is rescued by Angiopoietin-1. *Developmental cell* **3**, 411-423.

Gerli, R., Ibba, L. and Fruschelli, C. (1990). A fibrillar elastic apparatus around human lymph capillaries. *Anat Embryol (Berl)* **181**, 281-286.

Gerli, R., Solito, R., Weber, E. and Agliano, M. (2000). Specific adhesion molecules bind anchoring filaments and endothelial cells in human skin initial lymphatics. *Lymphology* **33**, 148-157.

Gilges, D., Vinit, M. A., Callebaut, I., Coulombel, L., Cacheux, V., Romeo, P. H. and Vigon, I. (2000). Polydom: a secreted protein with pentraxin, complement control protein, epidermal growth factor and von Willebrand factor A domains. *The Biochemical journal* **352 Pt 1**, 49-59.

Glukhova, M., Koteliansky, V., Fondacci, C., Marotte, F. and Rappaport, L. (1993). Laminin variants and integrin laminin receptors in developing and adult human smooth muscle.

Developmental biology **157**, 437-447.

Hagerling, R., Pollmann, C., Andreas, M., Schmidt, C., Nurmi, H., Adams, R. H., Alitalo, K., Andresen, V., Schulte-Merker, S. and Kiefer, F. (2013). A novel multistep mechanism for initial lymphangiogenesis in mouse embryos based on ultramicroscopy. *The EMBO journal* **32**, 629-644.

Han, S., Lee, S. J., Kim, K. E., Lee, H. S., Oh, N., Park, I., Ko, E., Oh, S. J., Lee, Y. S., Kim, D., et al. (2016). Amelioration of sepsis by TIE2 activation-induced vascular protection. *Sci Transl Med* **8**, 335ra355.

Hayashi, S. and McMahon, A. P. (2002). Efficient recombination in diverse tissues by a tamoxifen-inducible form of Cre: a tool for temporally regulated gene activation/inactivation in the mouse. *Developmental biology* **244**, 305-318.

Hellstrom, M., Kalen, M., Lindahl, P., Abramsson, A. and Betsholtz, C. (1999). Role of PDGF-B and PDGFR-beta in recruitment of vascular smooth muscle cells and pericytes during embryonic blood vessel formation in the mouse. *Development* **126**, 3047-3055.

Hirakawa, S., Hong, Y.-K., Harvey, N., Schacht, V., Matsuda, K., Libermann, T. and Detmar, M. (2003). Identification of Vascular Lineage-Specific Genes by Transcriptional Profiling of Isolated Blood Vascular and Lymphatic Endothelial Cells. *The American journal of pathology* **162**, 575-586.

Hirashima, M., Sano, K., Morisada, T., Murakami, K., Rossant, J. and Suda, T. (2008). Lymphatic vessel assembly is impaired in Aspp1-deficient mouse embryos. *Developmental biology* **316**, 149-159.

Hogan, B. M., Bos, F. L., Bussmann, J., Witte, M., Chi, N. C., Duckers, H. J. and Schulte-Merker, S. (2009). Ccbe1 is required for embryonic lymphangiogenesis and venous sprouting. *Nature genetics* **41**, 396-398.

Huang, X. Z., Wu, J. F., Ferrando, R., Lee, J. H., Wang, Y. L., Farese, R. V., Jr. and Sheppard, D. (2000). Fatal bilateral chylothorax in mice lacking the integrin alpha9beta1. *Molecular and cellular biology* **20**, 5208-5215.

Hynes, R. O. (2009). The extracellular matrix: not just pretty fibrils. *Science* **326**, 1216-1219.

Hynes, R. O. and Naba, A. (2012). Overview of the matrisome--an inventory of extracellular matrix constituents and functions. *Cold Spring Harbor perspectives in biology* **4**, a004903.

Ichise, H., Ichise, T., Ohtani, O. and Yoshida, N. (2009). Phospholipase Cgamma2 is necessary for separation of blood and lymphatic vasculature in mice. *Development* **136**, 191-195.

Jeltsch, M., Jha, S. K., Tvorogov, D., Anisimov, A., Leppanen, V. M., Holopainen, T., Kivela, R., Ortega, S., Karpanen, T. and Alitalo, K. (2014). CCBE1 enhances lymphangiogenesis via A disintegrin and metalloprotease with thrombospondin motifs-3-mediated vascular endothelial growth factor-C activation. *Circulation* **129**, 1962-1971.

Jeltsch, M., Tammela, T., Alitalo, K. and Wilting, J. (2003). Genesis and pathogenesis of lymphatic vessels. *Cell and tissue research* **314**, 69-84.

Jurisic, G., Maby-El Hajjami, H., Karaman, S., Ochsenbein, A. M., Alitalo, A., Siddiqui, S. S., Ochoa Pereira, C., Petrova, T. V. and Detmar, M. (2012). An unexpected role of semaphorin3a-neuropilin-1 signaling in lymphatic vessel maturation and valve formation. *Circulation research* **111**, 426-436.

Kampmeier, O. F. (1969). *Evolution and Comparative Morphology of the Lymphatic System*: Charles C. Thomas.

Kanki, H., Suzuki, H. and Itohara, S. (2006). High-efficiency CAG-FLPe deleter mice in C57BL/6J background. *Exp Anim* **55**, 137-141.

Karkkainen, M. J., Haiko, P., Sainio, K., Partanen, J., Taipale, J., Petrova, T. V., Jeltsch, M., Jackson, D. G., Talikka, M., Rauvala, H., et al. (2004). Vascular endothelial growth factor C is required for sprouting of the first lymphatic vessels from embryonic veins. *Nature immunology* **5**, 74-80.

Kazenwadel, J., Secker, G. A., Betterman, K. L. and Harvey, N. L. (2012). In vitro assays using primary embryonic mouse lymphatic endothelial cells uncover key roles for FGFR1 signalling in lymphangiogenesis. *PloS one* **7**, e40497.

Kim, I., Kim, H. G., So, J. N., Kim, J. H., Kwak, H. J. and Koh, G. Y. (2000). Angiopoietin-1 regulates endothelial cell survival through the phosphatidylinositol 3'-Kinase/Akt signal

transduction pathway. *Circulation research* **86**, 24-29.

Kim, K. E., Sung, H. K. and Koh, G. Y. (2007). Lymphatic development in mouse small intestine. *Developmental dynamics : an official publication of the American Association of Anatomists* **236**, 2020-2025.

Kim, K. L., Shin, I. S., Kim, J. M., Choi, J. H., Byun, J., Jeon, E. S., Suh, W. and Kim, D. K. (2006). Interaction between Tie receptors modulates angiogenic activity of angiopoietin2 in endothelial progenitor cells. *Cardiovasc Res* **72**, 394-402.

Kim, K. T., Choi, H. H., Steinmetz, M. O., Maco, B., Kammerer, R. A., Ahn, S. Y., Kim, H. Z., Lee, G. M. and Koh, G. Y. (2005). Oligomerization and multimerization are critical for angiopoietin-1 to bind and phosphorylate Tie2. *The Journal of biological chemistry* **280**, 20126-20131.

Kisanuki, Y. Y., Hammer, R. E., Miyazaki, J., Williams, S. C., Richardson, J. A. and Yanagisawa, M. (2001). Tie2-Cre transgenic mice: a new model for endothelial cell-lineage analysis in vivo. *Developmental biology* **230**, 230-242.

Klotz, L., Norman, S., Vieira, J. M., Masters, M., Rohling, M., Dube, K. N., Bollini, S., Matsuzaki, F., Carr, C. A. and Riley, P. R. (2015). Cardiac lymphatics are heterogeneous in origin and respond to injury. *Nature* **522**, 62-67.

Kontos, C. D., Cha, E. H., York, J. D. and Peters, K. G. (2002). The Endothelial Receptor Tyrosine Kinase Tie1 Activates Phosphatidylinositol 3-Kinase and Akt To Inhibit Apoptosis. *Molecular and cellular biology* **22**, 1704-1713.

Korhonen, E. A., Lampinen, A., Giri, H., Anisimov, A., Kim, M., Allen, B., Fang, S., D'Amico, G., Sipila, T. J., Lohela, M., et al. (2016). Tie1 controls angiopoietin function in vascular remodeling and inflammation. *The Journal of clinical investigation* **126**, 3495-3510.

Korn, C. and Augustin, H. G. (2015). Mechanisms of Vessel Pruning and Regression. *Developmental cell* **34**, 5-17.

Kuchler, A. M., Gjini, E., Peterson-Maduro, J., Cancilla, B., Wolburg, H. and Schulte-Merker, S. (2006). Development of the zebrafish lymphatic system requires VEGFC signaling. *Current biology : CB* **16**, 1244-1248.

Lauweryns, J. M. and Boussauw, L. (1973). The ultrastructure of lymphatic valves in the adult rabbit lung. *Z Zellforsch Mikrosk Anat* **143**, 149-168.

Leak, L. V. and Burke, J. F. (1968). Ultrastructural studies on the lymphatic anchoring filaments. *The Journal of cell biology* **36**, 129-149.

Liaw, L., Birk, D. E., Ballas, C. B., Whitsitt, J. S., Davidson, J. M. and Hogan, B. L. (1998). Altered wound healing in mice lacking a functional osteopontin gene (spp1). *The Journal of clinical investigation* **101**, 1468-1478.

Lindahl, P. (1997). Pericyte Loss and Microaneurysm Formation in PDGF-B-Deficient Mice. *Science* **277**, 242-245.

Maisonpierre, P. C. (1997). Angiopoietin-2, a Natural Antagonist for Tie2 That Disrupts in vivo Angiogenesis. *Science* **277**, 55-60.

Makinen, T., Adams, R. H., Bailey, J., Lu, Q., Ziemiecki, A., Alitalo, K., Klein, R. and Wilkinson, G. A. (2005). PDZ interaction site in ephrinB2 is required for the remodeling of lymphatic vasculature. *Genes & development* **19**, 397-410.

Manabe, R., Ohe, N., Maeda, T., Fukuda, T. and Sekiguchi, K. (1997). Modulation of cell-adhesive activity of fibronectin by the alternatively spliced EDA segment. *The Journal of cell biology* **139**, 295-307.

Manabe, R., Tsutsui, K., Yamada, T., Kimura, M., Nakano, I., Shimono, C., Sanzen, N., Furutani, Y., Fukuda, T., Oguri, Y., et al. (2008). Transcriptome-based systematic identification of extracellular matrix proteins. *Proceedings of the National Academy of Sciences of the United States of America* **105**, 12849-12854.

Marron, M. B., Singh, H., Tahir, T. A., Kavumkal, J., Kim, H. Z., Koh, G. Y. and Brindle, N. P. (2007). Regulated proteolytic processing of Tie1 modulates ligand responsiveness of the receptor-tyrosine kinase Tie2. *The Journal of biological chemistry* **282**, 30509-30517.

Matsumura, H., Hasuwa, H., Inoue, N., Ikawa, M. and Okabe, M. (2004). Lineage-specific cell disruption in living mice by Cre-mediated expression of diphtheria toxin A chain. *Biochemical and biophysical research communications* **321**, 275-279.

Miner, J. H. (2008). Laminins and their roles in mammals. *Microscopy research and technique* **71**, 349-356.

Murtomaki, A., Uh, M. K., Kitajewski, C., Zhao, J., Nagasaki, T., Shawber, C. J. and Kitajewski, J. (2014). Notch signaling functions in lymphatic valve formation. *Development* **141**, 2446-2451.

Naba, A., Clauser, K. R., Hoersch, S., Liu, H., Carr, S. A. and Hynes, R. O. (2012). The matrisome: in silico definition and in vivo characterization by proteomics of normal and tumor extracellular matrices. *Mol Cell Proteomics* **11**, M111 014647.

Nishiuchi, R., Takagi, J., Hayashi, M., Ido, H., Yagi, Y., Sanzen, N., Tsuji, T., Yamada, M. and Sekiguchi, K. (2006). Ligand-binding specificities of laminin-binding integrins: a comprehensive survey of laminin-integrin interactions using recombinant alpha3beta1, alpha6beta1, alpha7beta1 and alpha6beta4 integrins. *Matrix biology : journal of the International Society for Matrix Biology* **25**, 189-197.

Norrmen, C., Ivanov, K. I., Cheng, J., Zangger, N., Delorenzi, M., Jaquet, M., Miura, N., Puolakkainen, P., Horsley, V., Hu, J., et al. (2009). FOXC2 controls formation and maturation of lymphatic collecting vessels through cooperation with NFATc1. *The Journal of cell biology* **185**, 439-457.

Oliver, G. (2004). Lymphatic vasculature development. *Nature reviews. Immunology* **4**, 35-45.

Petrova, T. V., Karpanen, T., Norrmen, C., Mellor, R., Tamakoshi, T., Finegold, D., Ferrell, R., Kerjaschki, D., Mortimer, P., Yla-Herttuala, S., et al. (2004). Defective valves and abnormal mural cell recruitment underlie lymphatic vascular failure in lymphedema distichiasis. *Nature medicine* **10**, 974-981.

Petrova, T. V., Makinen, T., Makela, T. P., Saarela, J., Virtanen, I., Ferrell, R. E., Finegold, D. N., Kerjaschki, D., Yla-Herttuala, S. and Alitalo, K. (2002). Lymphatic endothelial reprogramming of vascular endothelial cells by the Prox-1 homeobox transcription factor. *The EMBO journal* **21**, 4593-4599.

Podgrabinska, S., Braun, P., Velasco, P., Kloos, B., Pepper, M. S. and Skobe, M. (2002). Molecular characterization of lymphatic endothelial cells. *Proceedings of the National Academy of Sciences of the United States of America* **99**, 16069-16074.

Qu, X., Tompkins, K., Batts, L. E., Puri, M. and Baldwin, H. S. (2010). Abnormal embryonic lymphatic vessel development in Tie1 hypomorphic mice. *Development* **137**, 1285-1295.

Qu, X., Zhou, B. and Scott Baldwin, H. (2015). Tie1 is required for lymphatic valve and collecting vessel development. *Developmental biology* **399**, 117-128.

Roukens, M. G., Peterson-Maduro, J., Padberg, Y., Jeltsch, M., Leppanen, V. M., Bos, F. L., Alitalo, K., Schulte-Merker, S. and Schulte, D. (2015). Functional Dissection of the CCBE1 Protein: A Crucial Requirement for the Collagen Repeat Domain. *Circulation research* **116**, 1660-1669.

Rozario, T. and DeSimone, D. W. (2010). The extracellular matrix in development and morphogenesis: a dynamic view. *Developmental biology* **341**, 126-140.

Sabine, A., Agalarov, Y., Maby-El Hajjami, H., Jaquet, M., Hagerling, R., Pollmann, C., Bebber, D., Pfenniger, A., Miura, N., Dormond, O., et al. (2012). Mechanotransduction, PROX1, and FOXC2 cooperate to control connexin37 and calcineurin during lymphatic-valve formation. *Developmental cell* **22**, 430-445.

Saharinen, P., Eklund, L., Miettinen, J., Wirkkala, R., Anisimov, A., Winderlich, M., Nottebaum, A., Vestweber, D., Deutsch, U., Koh, G. Y., et al. (2008). Angiopoietins assemble distinct Tie2 signalling complexes in endothelial cell-cell and cell-matrix contacts. *Nature cell biology* **10**, 527-537.

Saharinen, P., Kerkela, K., Ekman, N., Marron, M., Brindle, N., Lee, G. M., Augustin, H., Koh, G. Y. and Alitalo, K. (2005). Multiple angiopoietin recombinant proteins activate the Tie1 receptor tyrosine kinase and promote its interaction with Tie2. *The Journal of cell biology* **169**, 239-243.

Sato, T. N., Tozawa, Y., Deutsch, U., Wolburg-Buchholz, K., Fujiwara, Y., Gendron-Maguire, M., Gridley, T., Wolburg, H., Risau, W. and Qin, Y. (1995). Distinct roles of the receptor tyrosine kinases Tie-1 and Tie-2 in blood vessel formation. *Nature* **376**, 70-74.

Sato-Nishiuchi, R., Nakano, I., Ozawa, A., Sato, Y., Takeichi, M., Kiyozumi, D., Yamazaki, K.,

Yasunaga, T., Futaki, S. and Sekiguchi, K. (2012). Polydom/SVEP1 is a ligand for integrin alpha9beta1. *The Journal of biological chemistry* **287**, 25615-25630.

Schulte-Merker, S., Sabine, A. and Petrova, T. V. (2011). Lymphatic vascular morphogenesis in development, physiology, and disease. *The Journal of cell biology* **193**, 607-618.

Schwarz, R. S., Bosch, T. C. and Cadavid, L. F. (2008). Evolution of polydom-like molecules: identification and characterization of cnidarian polydom (Cnpolydom) in the basal metazoan Hydractinia. *Developmental and comparative immunology* **32**, 1192-1210.

Seegar, T. C., Eller, B., Tzvetkova-Robev, D., Kolev, M. V., Henderson, S. C., Nikolov, D. B. and Barton, W. A. (2010). Tie1-Tie2 interactions mediate functional differences between angiopoietin ligands. *Mol Cell* **37**, 643-655.

Sevick-Muraca, E. M., Kwon, S. and Rasmussen, J. C. (2014). Emerging lymphatic imaging technologies for mouse and man. *The Journal of clinical investigation* **124**, 905-914.

Shen, B., Shang, Z., Wang, B., Zhang, L., Zhou, F., Li, T., Chu, M., Jiang, H., Wang, Y., Qiao, T., et al. (2014). Genetic dissection of tie pathway in mouse lymphatic maturation and valve development. *Arteriosclerosis, thrombosis, and vascular biology* **34**, 1221-1230.

Shimoda, H., Bernas, M. J., Witte, M. H., Gale, N. W., Yancopoulos, G. D. and Kato, S. (2007). Abnormal recruitment of periendothelial cells to lymphatic capillaries in digestive organs of angiopoietin-2-deficient mice. *Cell and tissue research* **328**, 329-337.

Shur, I., Socher, R., Hameiri, M., Fried, A. and Benayahu, D. (2006). Molecular and cellular characterization of SEL-OB/SVEP1 in osteogenic cells in vivo and in vitro. *Journal of cellular physiology* **206**, 420-427.

Skarnes, W. C., Rosen, B., West, A. P., Koutsourakis, M., Bushell, W., Iyer, V., Mujica, A. O., Thomas, M., Harrow, J., Cox, T., et al. (2011). A conditional knockout resource for the genome-wide study of mouse gene function. *Nature* **474**, 337-342.

Solito, R., Alessandrini, C., Fruschelli, M., Pucci, A. M. and Gerli, R. (1997). An immunological correlation between the anchoring filaments of initial lymph vessels and the neighboring elastic fibers: a unified morphofunctional concept. *Lymphology* **30**, 194-202.

Song, S. H., Kim, K. L., Lee, K. A. and Suh, W. (2012). Tie1 regulates the Tie2 agonistic role of angiopoietin-2 in human lymphatic endothelial cells. *Biochemical and biophysical research communications* **419**, 281-286.

Sorokin, L. M., Pausch, F., Frieser, M., Kroger, S., Ohage, E. and Deutzmann, R. (1997). Developmental regulation of the laminin alpha5 chain suggests a role in epithelial and endothelial cell maturation. *Developmental biology* **189**, 285-300.

Srinivasan, R. S., Geng, X., Yang, Y., Wang, Y., Mukatira, S., Studer, M., Porto, M. P., Lagutin, O. and Oliver, G. (2010). The nuclear hormone receptor Coup-TFII is required for the initiation and early maintenance of Prox1 expression in lymphatic endothelial cells. *Genes & development* **24**, 696-707.

Srinivasan, R. S. and Oliver, G. (2011). Prox1 dosage controls the number of lymphatic endothelial cell progenitors and the formation of the lymphovenous valves. *Genes & development* **25**, 2187-2197.

Suzuki-Inoue, K., Inoue, O., Ding, G., Nishimura, S., Hokamura, K., Eto, K., Kashiwagi, H., Tomiyama, Y., Yatomi, Y., Umemura, K., et al. (2010). Essential in vivo roles of the C-type lectin receptor CLEC-2: embryonic/neonatal lethality of CLEC-2-deficient mice by blood/lymphatic misconnections and impaired thrombus formation of CLEC-2-deficient platelets. *The Journal of biological chemistry* **285**, 24494-24507.

Tammela, T. and Alitalo, K. (2010). Lymphangiogenesis: Molecular mechanisms and future promise. *Cell* **140**, 460-476.

Taniguchi, Y., Ido, H., Sanzen, N., Hayashi, M., Sato-Nishiuchi, R., Futaki, S. and Sekiguchi, K. (2009). The C-terminal region of laminin beta chains modulates the integrin binding affinities of laminins. *The Journal of biological chemistry* **284**, 7820-7831.

Thurston, G. and Daly, C. (2012). The complex role of angiopoietin-2 in the angiopoietin-tie signaling pathway. *Cold Spring Harbor perspectives in medicine* **2**, a006550.

Udan, R. S., Vadakkan, T. J. and Dickinson, M. E. (2013). Dynamic responses of endothelial cells to changes in blood flow during vascular remodeling of the mouse yolk sac. *Development* **140**, 4041-4050.

Uhrin, P., Zaujec, J., Breuss, J. M., Olcaydu, D., Chrenek, P., Stockinger, H., Fuertbauer, E., Moser, M., Haiko, P., Fassler, R., et al. (2010). Novel function for blood platelets and podoplanin in developmental separation of blood and lymphatic circulation. *Blood* **115**, 3997-4005.

Vainionpaa, N., Butzow, R., Hukkanen, M., Jackson, D. G., Pihlajaniemi, T., Sakai, L. Y. and Virtanen, I. (2007). Basement membrane protein distribution in LYVE-1-immunoreactive lymphatic vessels of normal tissues and ovarian carcinomas. *Cell and tissue research* **328**, 317-328.

Wigle, J. T. and Oliver, G. (1999). Prox1 function is required for the development of the murine lymphatic system. *Cell* **98**, 769-778.

Witte, M. H., Bernas, M. J., Martin, C. P. and Witte, C. L. (2001). Lymphangiogenesis and lymphangiodysplasia: from molecular to clinical lymphology. *Microscopy research and technique* **55**, 122-145.

Xu, Y., Yuan, L., Mak, J., Pardanaud, L., Caunt, M., Kasman, I., Larrivee, B., Del Toro, R., Suchting, S., Medvinsky, A., et al. (2010). Neuropilin-2 mediates VEGF-C-induced lymphatic sprouting together with VEGFR3. *The Journal of cell biology* **188**, 115-130.

Yabkowitz, R., Meyer, S., Black, T., Elliott, G., Merewether, L. A. and Yamane, H. K. (1999). Inflammatory cytokines and vascular endothelial growth factor stimulate the release of soluble tie receptor from human endothelial cells via metalloprotease activation. *Blood* **93**, 1969-1979.

Yamauchi, Y., Abe, K., Mantani, A., Hitoshi, Y., Suzuki, M., Osuzu, F., Kuratani, S. and Yamamura, K. (1999). A novel transgenic technique that allows specific marking of the neural crest cell lineage in mice. *Developmental biology* **212**, 191-203.

Yang, Y. and Oliver, G. (2014). Development of the mammalian lymphatic vasculature. *The Journal of clinical investigation* **124**, 888-897.

Yaniv, K., Isogai, S., Castranova, D., Dye, L., Hitomi, J. and Weinstein, B. M. (2006). Live imaging of lymphatic development in the zebrafish. *Nature medicine* **12**, 711-716.

Yousif, L. F., Di Russo, J. and Sorokin, L. (2013). Laminin isoforms in endothelial and perivascular basement membranes. *Cell Adh Migr* **7**, 101-110.

Yu, X., Seegar, T. C., Dalton, A. C., Tzvetkova-Robev, D., Goldgur, Y., Rajashankar, K. R., Nikolov, D. B. and Barton, W. A. (2013). Structural basis for angiopoietin-1-mediated signaling initiation. *Proceedings of the National Academy of Sciences of the United States of America* **110**, 7205-7210.

Yuan, H. T., Khankin, E. V., Karumanchi, S. A. and Parikh, S. M. (2009). Angiopoietin 2 is a partial agonist/antagonist of Tie2 signaling in the endothelium. *Molecular and cellular biology* **29**, 2011-2022.

Yuan, H. T., Venkatesha, S., Chan, B., Deutsch, U., Mammoto, T., Sukhatme, V. P., Woolf, A. S. and Karumanchi, S. A. (2007). Activation of the orphan endothelial receptor Tie1 modifies Tie2-mediated intracellular signaling and cell survival. *FASEB journal : official publication of the Federation of American Societies for Experimental Biology* **21**, 3171-3183.

Yuan, L., Moyon, D., Pardanaud, L., Breant, C., Karkkainen, M. J., Alitalo, K. and Eichmann, A. (2002). Abnormal lymphatic vessel development in neuropilin 2 mutant mice. *Development* **129**, 4797-4806.

Zhang, L., Zhou, F., Han, W., Shen, B., Luo, J., Shibuya, M. and He, Y. (2010). VEGFR-3 ligand-binding and kinase activity are required for lymphangiogenesis but not for angiogenesis. *Cell research* **20**, 1319-1331.

Zheng, W., Nurmi, H., Appak, S., Sabine, A., Bovay, E., Korhonen, E. A., Orsenigo, F., Lohela, M., D'Amico, G., Holopainen, T., et al. (2014). Angiopoietin 2 regulates the transformation and integrity of lymphatic endothelial cell junctions. *Genes & development* **28**, 1592-1603.

List of Publications

1. **Morooka N, Futaki S, Sato-Nishiuchi R, Nishino M, Totani Y, Shimono C, Nakano I, Nakajima H, Mochizuki N, Sekiguchi K.** (2017). Polydom is an Extracellular Matrix Protein Involved in Lymphatic Vessel Remodeling. *Circulation Research* **120**, 1276-1288.

2. **Kärpanen T, Padberg Y, van de Pavert SA, Dierkes C, Morooka N, Peterson-Maduro J, van de Hoek G, Adrian M, Mochizuki N, Sekiguchi K, Kiefer F, Schulte D, Schulte-Merker S.** (2017). An Evolutionarily Conserved Role for Polydom/Svep1 During Lymphatic Vessel Formation. *Circulation Research* **120**, 1263-1275.

Acknowledgements

The work which thesis is based upon was mainly carried out at the Laboratory of Extracellular Matrix Biochemistry, now Division of Matrixome Research and Application, Institute for Protein Research, Osaka University (2011-2017).

I would like to thank everyone who positively influenced the progression of this thesis. First, I would like to express my gratitude to my supervisor, Prof. Kiyotoshi Sekiguchi. He has always fought me with real swords in science, so I have desperately tried to catch up with him. I learned how to think and write logically in science. I would like to thank my excellent mentors, Dr. Sugiko Futaki, Dr. Ryoko Sato-Nishiuchi, and Dr. Daiji Kiyozumi for training, discussing, encouraging, and fighting our boss together. I would like to thank all of my co-workers for supporting my research and helpful discussions, especially Mr. Masafumi Nishino and Dr. Hiroyuki Nakajima (NCVC) for fish work of the *Circ Res.* paper, Mr. Yuta Totani for mice work, Dr. Chisei Shimono for molecular work, and Ms. Itsuko Nakano for preparing beautiful cross sections.

I would like express my gratitude to Prof. Naoki Mochizuki, National Cerebral and Cardiovascular Center Research Institute. He has kindly helped me with my study by introducing a lot of great vascular biologists. I learned an importance of communication and collaboration with other scientists. Among those vascular biologists, I would like to thank Prof. Tetsuro Watabe and Dr. Yasuhiro Yoshimatsu (Tokyo Medical and Dental University), and Prof. Satoshi Hirakawa (Hamamatsu University School of Medicine) for protocols and kind suggestions in lymphatic vascular research. I would like also express my gratitude to Prof. Stefan Schulte-Merker, WWU Münster, for kindly sharing unpublished polydom/svep1 results and helpful discussion and suggestion.

I would like to express my gratitude to Prof. Takahisa Furukawa, Prof. Masato Okada, Prof. Hiroaki Miki for reviewing my thesis.

I would like to express extra special thanks to my friends, former teachers, STS scientists, and those who have been bathed in the “cyalume” light. Thank to them, I found my dream to become a top scientist and I could keep my motivation for science.

Finally, I am grateful to my father, who made an opportunity to enter a scientific world, and my mother, who is a role model of my life, for a good long time support and never ending encouragement.

Nanami Morooka

Osaka, August 2017